AUG 8 1968
OCT 1 4 1986

THEORETICAL PERFORMANCE OF THE EXPANSION TUNNEL OPERATING IN THE HIGH DENSITY TEST REGIME

Glenn D. Norfleet

ARO, Inc.

July 1968

VON KÁRMÁN GAS DYNAMICS FACILITY
ARNOLD ENGINEERING DEVELOPMENT CENTER
AIR FORCE SYSTEMS COMMAND
ARNOLD AIR FORCE STATION, TENNESSEE

NOTICES

THEORETICAL PERFORMANCE OF
THE EXPANSION TUNNEL OPERATING IN
THE HIGH DENSITY TEST REGIME

Glenn D. Norfleet

ARO, Inc.

This document has been approved for public release
and sale; its distribution is unlimited.

FOREWORD

The work reported herein was sponsored by Headquarters, Arnold Engineering Development Center (AEDC), Air Force Systems Command (AFSC), under Program Element 6241003F, Project 7778, Task 777807.

The results of research presented were obtained by ARO, Inc. (a subsidiary of Sverdrup & Parcel and Associates, Inc.), contract operator of AEDC, AFSC, Arnold Air Force Station, Tennessee, under Contract F40600-69-C-0001. The research was conducted from September 1967 to January 1968 under ARO Project No. VW3824, and the manuscript was submitted for publication on April 16, 1968.

This technical report has been reviewed and is approved.

Elmer E. Goins
Captain, USAF
Technical Facility
  Development Division
Directorate of Plans
  and Technology

Edward R. Feicht
Colonel, USAF
Director of Plans
  and Technology

ABSTRACT

Theoretical real gas performance calculations have been made for the expansion tunnel operating in a high density regime at modest velocity. Both Mach number-Reynolds number simulation and flow duplication were considered. Typical results and detailed working graphs are presented. To illustrate the potential of the expansion tunnel, the performance was calculated for the case of a 1000°K, 5000-atm helium driver. This example illustrates that the expansion tunnel does show promise for testing in the high density regime at modest velocity.

CONTENTS

APPENDIXES

I. ILLUSTRATIONS

Figure

NOMENCLATURE

A	Cross-sectional area of tube
a	Acoustic speed
d	Tube inside diameter
h	Enthalpy
ℓ	Length
ℓ_1, ℓ_4, ℓ_8	Tube length
ℓ_t	Test gas slug length at time of secondary diaphragm rupture
M	Mach number
M_s	Shock Mach number
p	Pressure
Re	Reynolds number
T	Temperature
Δt_2	Run time in region ②, i.e., time required for the test gas in the ② region to flow past the secondary diaphragm station
Δt_r	Ideal expansion tunnel run time (assumes nozzle loss time = 0)
U	Velocity
U_s	Shock velocity
x	Axial distance along tube
μ	Viscosity
ρ	Density

SUBSCRIPTS

1, 2, 3, 6A, etc.	Denote various flow regions (see Fig. 2)
vis	Viscous

SECTION I
INTRODUCTION

Consideration of low altitude reentry trajectories has generated interest in very high density, hypersonic test facilities. There is interest both in Mach number-Reynolds number simulation and in flow duplication at conditions existing in low altitude, hypersonic flight.

The two major limitations involved in obtaining high density flows in conventional wind tunnels are excessive reservoir pressure and/or excessive flow energy. These limitations suggest the use of an expansion tube, or some modification thereof, for high density aerodynamic testing. The expansion tube offers two distinct advantages over stagnated reservoir, steady expansion-type wind tunnels:

1. Since the flow is not stagnated in the reservoir and since the isentropic stagnation pressure is increased by the unsteady expansion, the isentropic stagnation pressure in the test section is many times the maximum pressure that must be contained anywhere in the system. This helps to alleviate the reservoir pressure limitation. *

2. The unsteady expansion is an energy multiplier (or concentrator) and this alleviates to some degree the flow energy problem.

The experimental expansion tube studies (Refs. 1, 2, 3, and 4) have shown that the experimental performance, i.e., velocity at a given altitude, is in reasonable agreement with theoretical predictions; however, the basic problem has been in the quality of the test flow. There is some indication (Ref. 3) that the flow quality problem is associated with the proximity of the test gas to the secondary diaphragm at the time of rupture. This problem may become less severe as the test gas slug is lengthened, since, if the test gas slug is long enough, the gas used late in the run is not in close proximity to the secondary diaphragm at the time of rupture.

As was demonstrated in Ref. 5 (see Fig. 1, Appendix I) the test gas slug length, ℓ_t, varies inversely with free-stream velocity. This

---

*Shock-tube driver pressure may be a limitation, but was not investigated or reported herein.

raises the possibility that the quality of expansion tunnel flow might be acceptable for modest velocities, say from 5000 to 10,000 ft/sec. In addition, it might be possible to achieve quite high density at these velocities since, for a given shock-tube driver, the expansion tunnel allows a trade-off between velocity and density.

It appears, then, that the expansion tube/tunnel might be a useful device for high density aerodynamic testing at modest velocities. The purpose of this investigation is to theoretically assess the performance of the expansion tube/tunnel for hypersonic high Reynolds number simulation and low altitude flow duplication.

SECTION II
CALCULATIONS

The calculations were made in part by an existing machine program and in part by hand. Basic flow calculations and tube length calculations were made using the machine program which was formulated for the study described in Ref. 5. The following were not included in the program and were calculated by hand:

1. test flow Reynolds number, Re,

2. acceleration tube charge-to-test pressure ratio, P_8/P_{6A},

3. acceleration tube shock strength, M_{s_8},

4. test gas slug length ratio, ℓ_t/ℓ_8,

5. effects of mass loss in the boundary layer.

The machine program starts with the free-stream, ⑥Ⓐ|, conditions and works backward through the steady isentropic expansion, the unsteady isentropic expansion, and crosses the normal shock to give the initial conditions in the driven tube. In addition, it calculates the run time per unit length of acceleration tube and the acceleration-to-driven tube length ratio. The test gas (air) is assumed to be in thermodynamic and chemical equilibrium throughout. The thermodynamic properties of air were taken from Refs. 6, 7, and 8. Standard atmospheric properties as a function of altitude were taken from Ref. 9. The expansion tunnel computer program is described in detail in Ref. 5, and input and output data are shown in Table I, Appendix IV.

To assess the Mach number-Reynolds number simulation regime, it is necessary to put some limit on the minimum allowable free-stream temperature, T_{6A}. For these calculations, T_{6A} was chosen to be 100°K. For very high density, this is approximately the lique-faction temperature; for lower density the liquefaction temperature is somewhat less, and, in addition, some supersaturation might be tolerated. However, this is a conservative choice since the perform-ance in terms of Mach number-Reynolds number could be increased by allowing lower free-stream temperatures.

Previously, either the altitude (for altitude duplication) or the free-stream pressure and entropy were inputs to the computer pro-gram and the machine determined the other free-stream thermody-namic properties by interpolation of tabulated air data (Refs. 6, 7, and 8). The lowest temperature in the tabulated air data is 100°K. To avoid interpolation problems the program was modified to accept all free-stream thermodynamic properties as input data. No other modi-fications were required to permit use of the existing program for the Mach number-Reynolds number simulation cases.

The hand calculations were all straightforward. The unit Reynolds number was calculated from:

$$Re_{6A} = \frac{\rho_{6A} U_{6A}}{\mu_{6A}}$$

where

ρ_{6A} and U_{6A} are input values

and

$\mu_{6A} = 14.5 \times 10^{-8}$ slugs/ft-sec

from Sutherland's equation at

$T_{6A} = 100°K.$

The acceleration tube charge-to-test gas pressure ratio, P_8/P_{6A}, and test gas slug length ratio, ℓ_t/ℓ_8, were calculated as described in Ref. 5. The acceleration tube shock strength, M_{S_8}, was determined from $M_S = f(U_2/a_1)$ (Fig. 2e of Ref. 10) where:

$(U_2/a_1)_{Ref. 10} = U_7/a_8 = U_6/a_8$

U_6 was taken from computer output

a_8 is an independent variable

It was assumed that the charge gas in region ⑧ would be room temperature air hence:

$$a_8 = 1130 \text{ ft/sec}$$

As was pointed out previously it is quite likely that the test flow uniformity will depend upon the test gas slug length-to-diameter ratio, ℓ_t/d_8. Since this parameter is directly proportional to the acceleration tube length-to-diameter ratio, ℓ_8/d_8, high ℓ/d acceleration tubes are desirable. However, their use raises the question of test time loss resulting from the mass entrained in the tube boundary layer (the "leaky piston" effect, see Ref. 11).

It is not clear how the mass loss (i. e., mass entrained in the boundary layer) from the shock-heated ⑦ region will affect the run time since it is region ⑥, not ⑦, that is expanded through the nozzle for test purposes. The loss of gas from the ⑦ region will tend to accelerate both the ⑥ - ⑦ interface (the passage of which starts the run) and the tail of the unsteady expansion (the passage of which ends the run). Although this may cause some loss, or gain, in test time, the process is quite complicated and its effects will herein be assumed to be negligible.

The mass loss from the shock heated ② region in the driven tube is another matter, and apparently cannot be neglected. For expansion tunnels operating at modest velocity, the optimum driven tube length is of the same order as the acceleration tube length. The mass loss from the shock heated ② region then can become significant, and loss of run time in the ② region relates directly to loss in tunnel run time. Therefore, for a given tunnel run time, the driven tube must be longer than the value calculated from inviscid considerations in order to prevent premature termination of the run by the wave reflected from the ② - ③ interface (see Fig. 2).

The turbulent theory of Mirels, Ref. 11, was used to calculate the loss in run time in the ② region for values of $\ell_1/d_1^{5/4}$ of 100 and 200 ft$^{-1/4}$ which probably brackets the range of interest. The acceleration-to-driven tube length ratio considering the mass loss from the ② region, ℓ_8/ℓ_1, vis was determined from:

$$\ell_8/\ell_{1,vis} = \frac{\ell_8}{\ell_1} \times \frac{\Delta t_{2,vis}}{\Delta t_2}$$

$\dfrac{\ell_8}{\ell_1}$ is from computer output

$\dfrac{\Delta t_{2,vis}}{\Delta t_2}$ is calculated from the theory of Ref. 11

It is also of interest to look at the run time per unit length of acceleration plus driven tube for the case with mass loss to the boundary layer in the driven tube. This parameter* was calculated using:

$$\frac{\Delta t_r}{(\ell_{1,vis} + \ell_8)} = \frac{\Delta t_r}{\ell_8 \left[\dfrac{\ell_{1,vis}}{\ell_8} + 1\right]} = \frac{\Delta t_r}{\ell_8} \left[\dfrac{1}{\dfrac{1}{\ell_8/\ell_{1,vis}} + 1}\right]$$

where:

$\ell_8/\ell_{1,vis}$ is from above calculations

and

$\dfrac{\Delta t_r}{\ell_8}$ is from computer output

The viscous correction considered herein is a correction only to the driven tube length, ℓ_1. Wherever the viscous correction has been applied to ℓ_1, the subscript (vis) has been added. All parameters without this subscript were calculated assuming inviscid equilibrium flow.

SECTION III
RESULTS

Results of the calculations are presented in the Appendixes. General illustrations are presented in Appendix I. Appendix II deals with the case of Mach number-Reynolds number simulation, and a list of figures in Appendix II is given at the beginning of the Appendix. Appendix III deals with the case of flow duplication, and a list of figures is given at the beginning of the Appendix.

The performance of a given facility depends upon the specific shock-tube driver used. Specifically, the performance depends upon the shock strength, M_{s_1}, that the driver can produce in a given driven tube charge pressure, P_1. To gain some insight into the potential of the expansion tunnel, it would be instructive to consider a case utilizing a potent, but

---

*The run time Δt_r assumes no losses in the nozzle starting and stopping processes. These losses are a direct function of nozzle length, and since sizing of nozzles is beyond the scope of this paper, run time loss was not investigated. A discussion of nozzle loss time in expansion tunnels can be found in Ref. 12.

technically feasible, driver. For this case the driver conditions chosen were:

$$P_4 = 5000 \text{ atm (helium)}$$

$$T_4 = 1000 \text{°K}$$

$$A_4/A_1 = 1$$

Driver performance, $M_{s_1} = f(P_1)$, was taken from Fig. 11 of Ref. 13 and is based on perfect gas, no loss calculations. The driver performance is therefore optimistic, but should serve to illustrate the tunnel performance potential. The working charts of the Appendixes were then used to generate selected tunnel performance data. The area ratio, A_{6A}/A_6, of 20 was chosen since it offers a reasonable compromise between performance and run time (and test gas slug length). In reality some other area ratio might be more advantageous for a specific facility.

The resulting Mach number-Reynolds number simulation line and the flow duplication line for low altitude are shown in Fig. 3. To provide some feeling for existing capabilities, the AEDC-VKF Hotshot Tunnel F (Gas Dynamic Wind Tunnel, Hypersonic (F), operating regime is shown in Fig. 3a.* This comparison should not be taken too literally since it compares the actual performance of Tunnel F with theoretical (no loss) performance of a hypothetical expansion tunnel. Also, the minimum static temperature of Tunnel F is somewhat below the 100°K taken for the expansion tunnel. The comparison does, however, indicate that the expansion tunnel has considerable potential in the area of high Reynolds number testing.

Run time per unit length of driven tube plus acceleration tube is shown in Fig. 4. For a reasonable tube length, say $\ell_8 + \ell_1 = 100$ ft, the run time varies from about 2.7 msec at Mach number 10 to about 0.75 msec at Mach number 20. For the altitude duplication case the run time (for $\ell_1 + \ell_8 = 100$ ft) varies from 1.6 msec at 10,000 ft/sec to about 0.75 msec at 15,000 ft/sec.

The test gas slug length ratio, ℓ_t/ℓ_8, is shown in Fig. 5. Also shown in Fig. 5 is the test gas slug length-to-diameter ratio for the case of

---

*Also shown is the expected performance of Tunnel F with the addition of a larger, "Full Volume", ARC chamber. This modification is scheduled for completion on 15 September 1968.

$\ell_8/d_8 = 150$ (which from past experience might be a reasonable value). This parameter varies from about 7 at low Mach numbers and velocities to about 0.3 at the higher values of Mach number and velocity.

SECTION IV
CONCLUDING REMARKS

Theoretical calculations have been made for the expansion tunnel designed to simulate Reynolds number at hypersonic Mach numbers and for the tunnel designed for flow duplication at low altitudes and modest velocities. The results are presented in the form of working graphs in Appendixes II and III.

A driver condition was arbitrarily chosen so that tunnel performance, run time, and test gas slug length could be illustrated for a specific example. The results indicate that the expansion tunnel does indeed offer considerable potential in the high Reynolds number or low altitude test regime. Further, both the run time and the test gas slug length indicate promise for testing at lower velocities and Mach numbers.

Although the results of these calculations demonstrate that the expansion tunnel has considerable potential for this operating regime, the real utility of the expansion tunnel for this type of testing remains to be shown experimentally.

REFERENCES

1. Jones, J. J. "Some Performance Characteristics of the LRC 3-1/4-Inch Pilot Expansion Tube Using an Unheated Hydrogen Driver." Fourth Hypervelocity Techniques Symposium, Arnold Air Force Station, Tennessee, November 1965, p. 7.

2. Givens, John J., Page, William A., and Reynolds, Robert M. "Evaluation of Flow Properties in a Combustion-Driven Expansion Tube Operating at 7.5 km/sec." Fourth Hypervelocity Techniques Symposium, Arnold Air Force Station, Tennessee, November 1965, p. 27.

3. Norfleet, Glenn D., Lacey, John J., Jr., and Whitfield, Jack D. "Results of an Experimental Investigation of the Performance of an Expansion Tube." Fourth Hypervelocity Techniques Symposium, Arnold Air Force Station, Tennessee, November 1965, p. 49.

4. Spurk, Joseph H. "Design, Operation, and Preliminary Results of the BRL Expansion Tube." Fourth Hypervelocity Techniques Symposium, Arnold Air Force Station, Tennessee, November 1965, p. 111.

5. Norfleet, Glenn D. and Loper, F. C. "A Theoretical Real-Gas Analysis of the Expansion Tunnel." AEDC-TR-66-71 (AD633656), June 1966.

6. Grabau, Martin and Brahinsky, H. S. "Thermodynamic Properties of Air from 300 to 6000°K and from 1 to 1000 Amagats." AEDC-TR-66-247 (AD646172), January 1967.

7. Hilsenrath, J. and Klein, M. "Tables of Thermodynamic Properties of Air in Chemical Equilibrium Including Second Virial Corrections from 1500°K to 15,000 °K. AEDC-TDR-63-161 (AD416040), August 1963.

8. Humphrey, R. L. and Neel, C. A. "Tables of Thermodynamic Properties of Air from 90 to 1500°K. AEDC-TN-61-103 (AD262692), August 1961.

9. U. S. Standard Atmosphere, 1962. U. S. Government Printing Office, Washington, D. C., December 1962.

10. Lewis, Clark H. and Burgess, E. G. "Charts of Normal Shock Wave Properties in Imperfect Air." AEDC-TDR-64-43 (AD433958), March 1964.

11. Mirels, H. "Shock Tube Test Time Limitation Due to Turbulent-Wall Boundary Layer." AIAA Journal, Vol. 2, January 1964, pp. 84-93.

12. Trimpi, Robert L. and Callis, Linwood B. "A Perfect-Gas Analysis of the Expansion Tunnel, A Modification to the Expansion Tube." NASA TR R-223, April 1965.

13. Lam, L. Y. and Clark, K. R. "Electric Internal Heater for the Lockheed 100-Inch Shock Tunnel." Fifth Hypervelocity Techniques Symposium, Denver, Colorado, March 1967, Vol. 1, p. 61.

Fig. 1 Proximity of Test Gas to Secondary Diaphragm
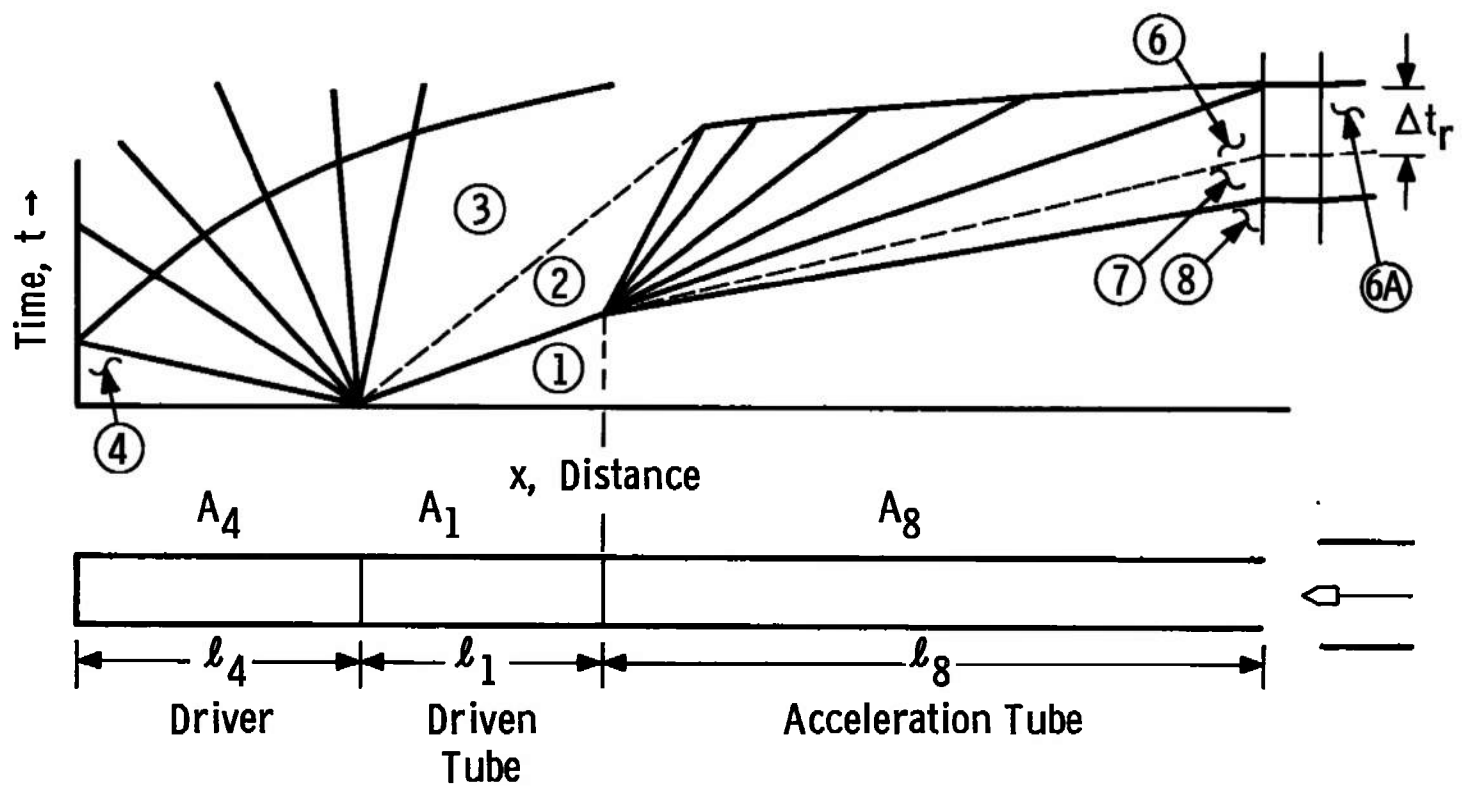
Fig. 2 Basic Wave Diagram

$A_{6A}/A_6 = 20$
$T_\infty = 100^\circ K$
Driver Conditions
$p_4 = 5000$ atm
$T_4 = 1000^\circ K$ (Helium)
Driver Performance Based on
Perfect Gases, No Losses

Expansion Tunnel

AEDC VKF Hotshot Tunnel "F"
Future Capability
Present Capability
(from Ref. 14)

4.5-ft-diam Test Section

9-ft-diam Test Section

Re/ft

M_{6A}

a. Mach Number-Reynolds Number Simulation

Altitude, ft x 10^3

U_{6A} x 10^{-3}, ft/sec
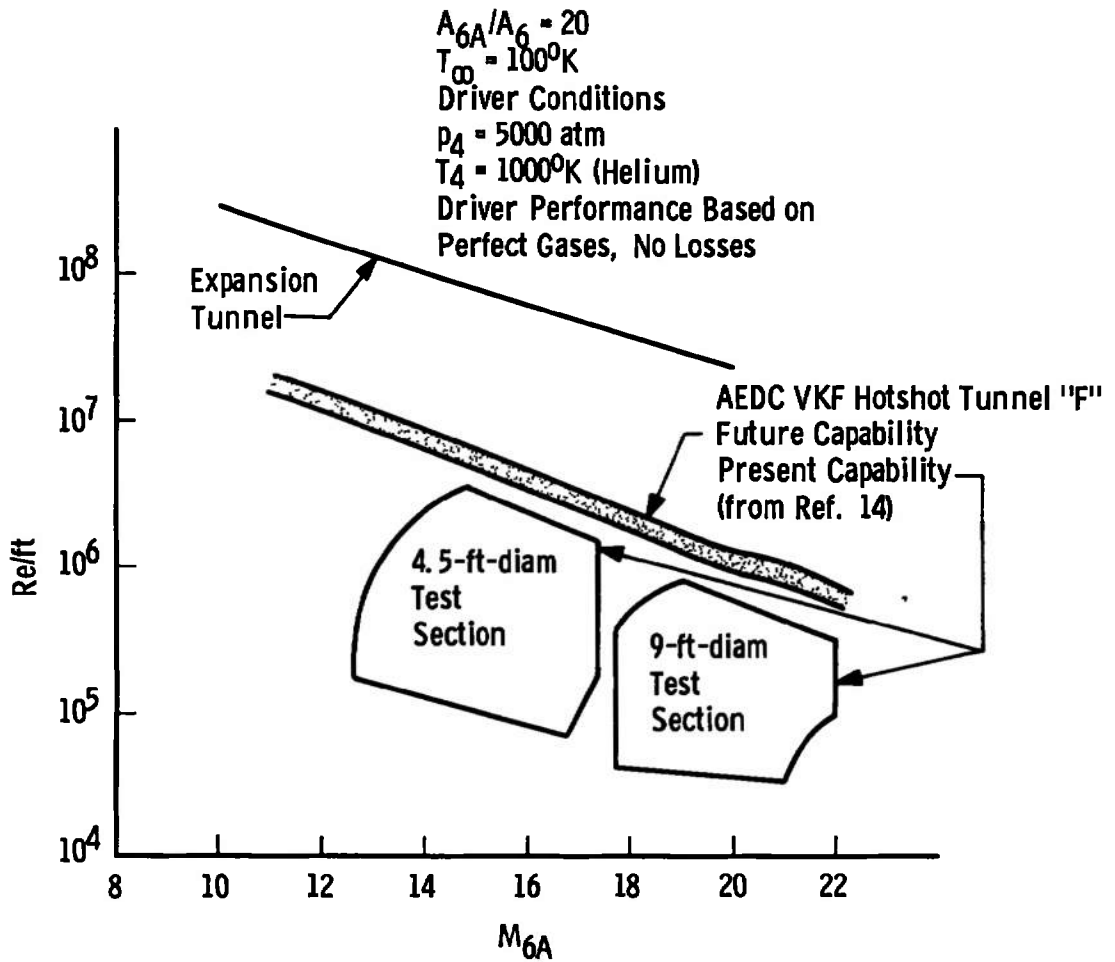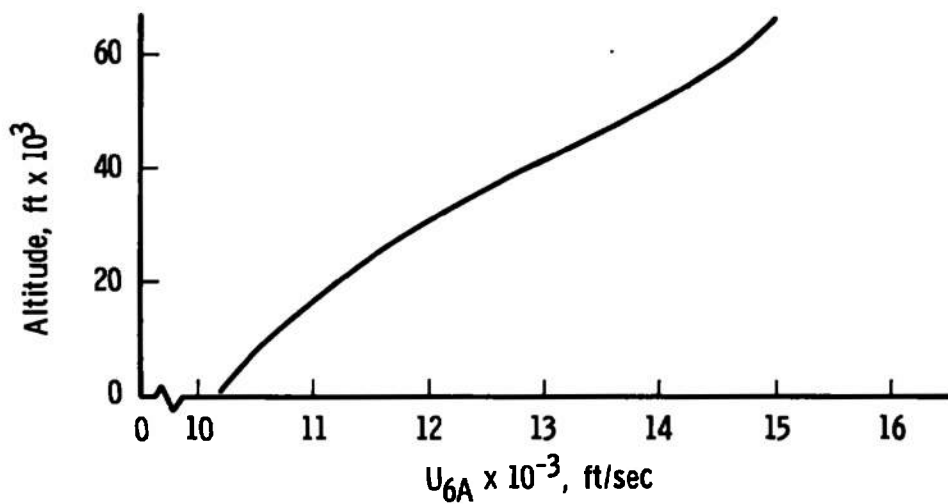
b. Flow Duplication

Fig. 3 Example of Expansion Tunnel Performance
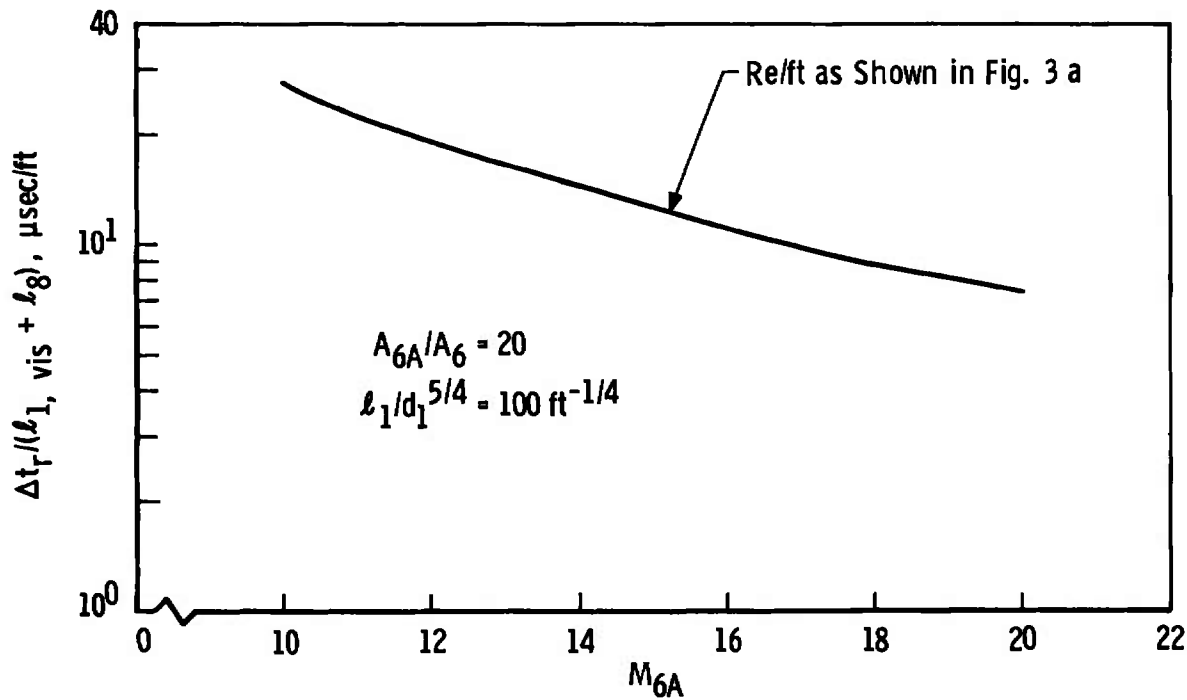
a. Mach Number-Reynolds Number Simulation
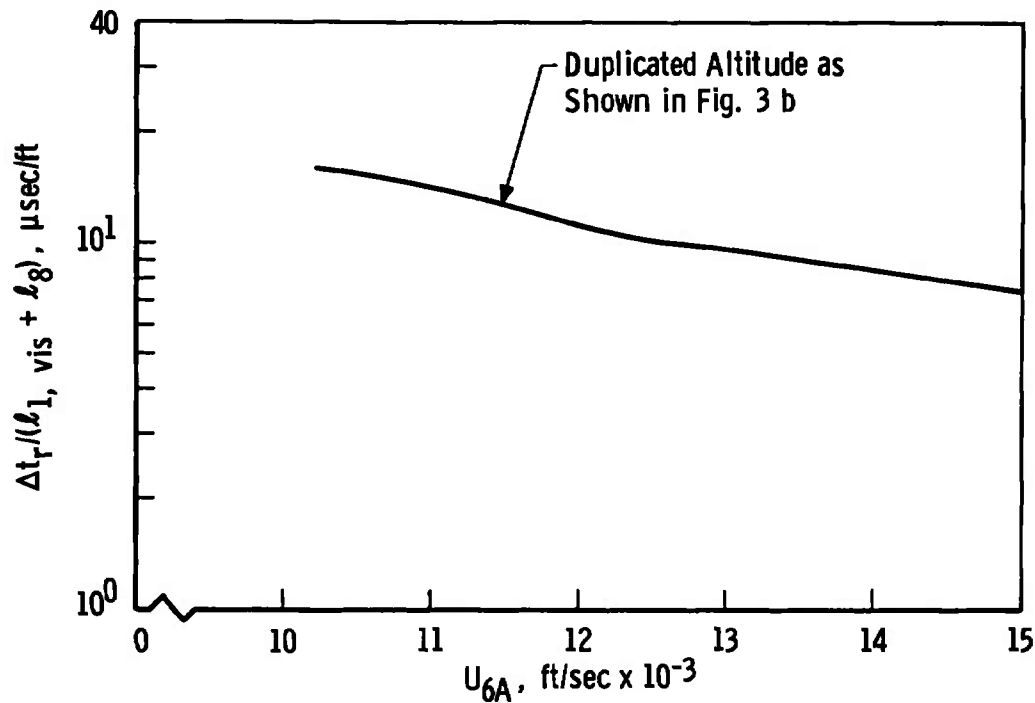
b. Flow Duplication

Fig. 4 Run Time per Unit Tube Length
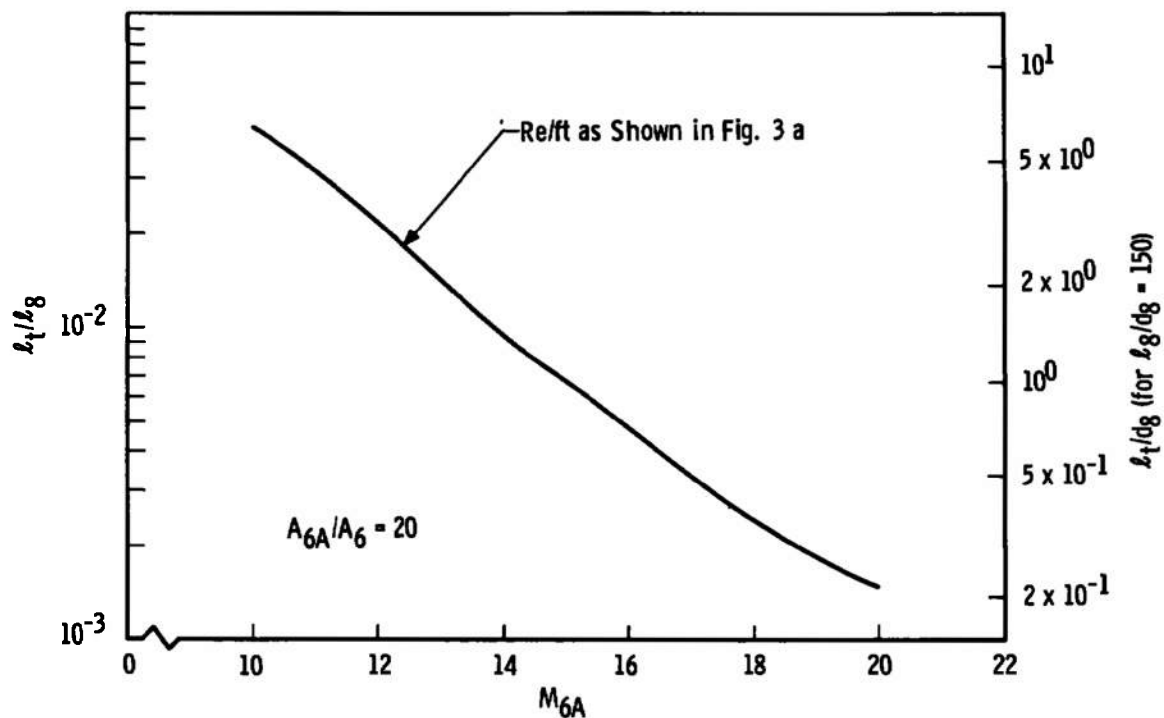
a. Mach Number-Reynolds Number Simulation
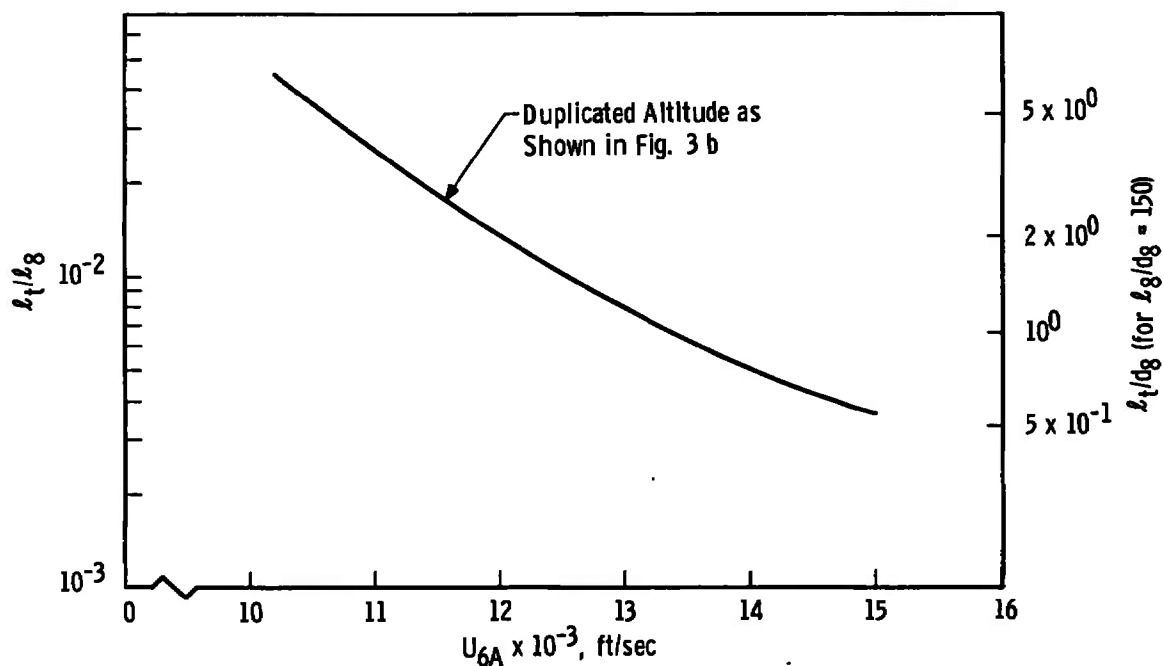
b. Flow Duplication

Fig. 5 Test Gas Slug Length Ratio

APPENDIX II
WORKING GRAPHS FOR MACH NUMBER-REYNOLDS NUMBER SIMULATION

a. $A_{6A}/A_6 = 1$

Fig. II-1 M_{6A} and Re/ft as a Function of M_{s_1} and P_1

b. $A_{6A}/A_6 = 10$

Fig. II-1 Continued
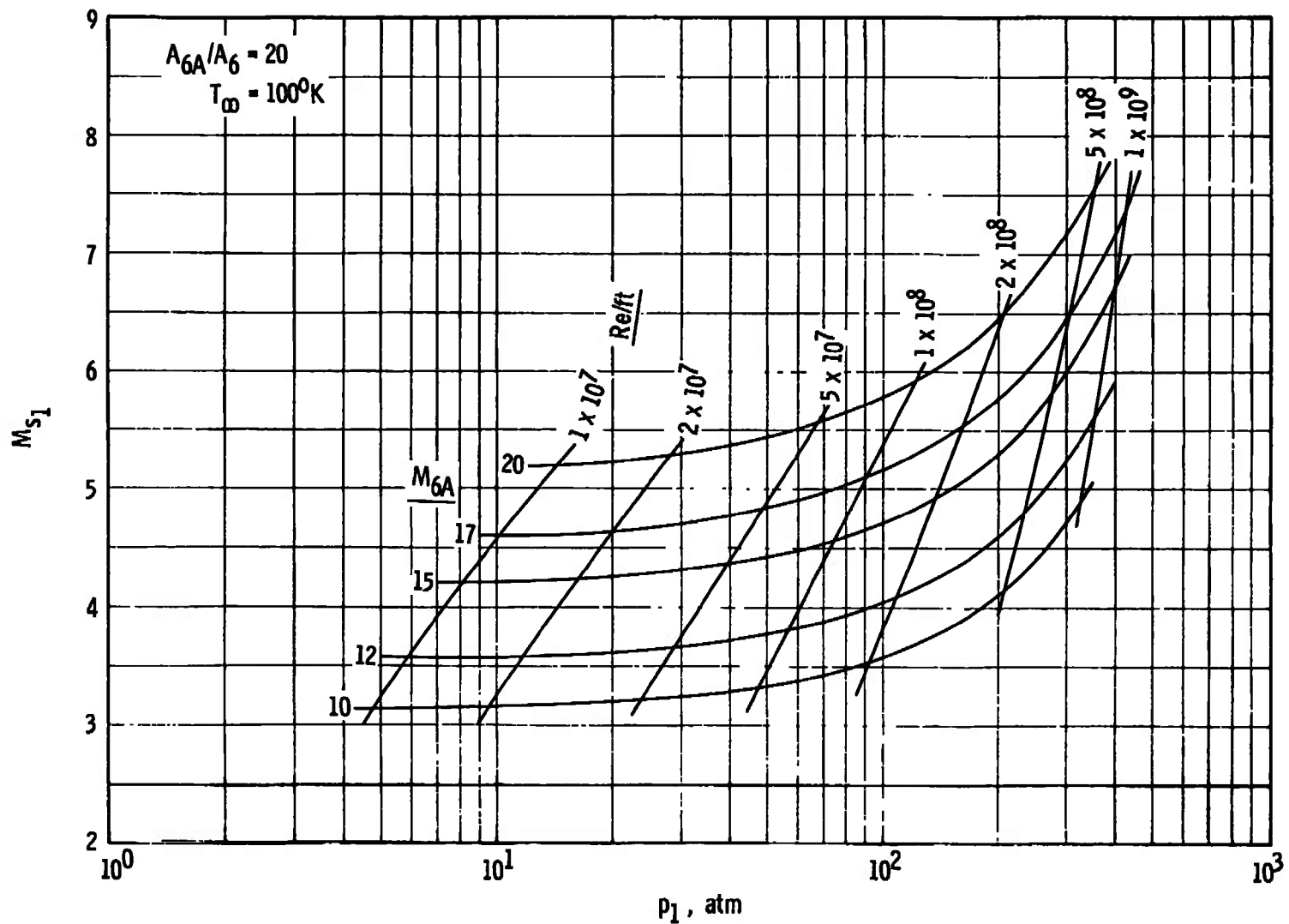
c. $A_{6A}/A_6 = 20$

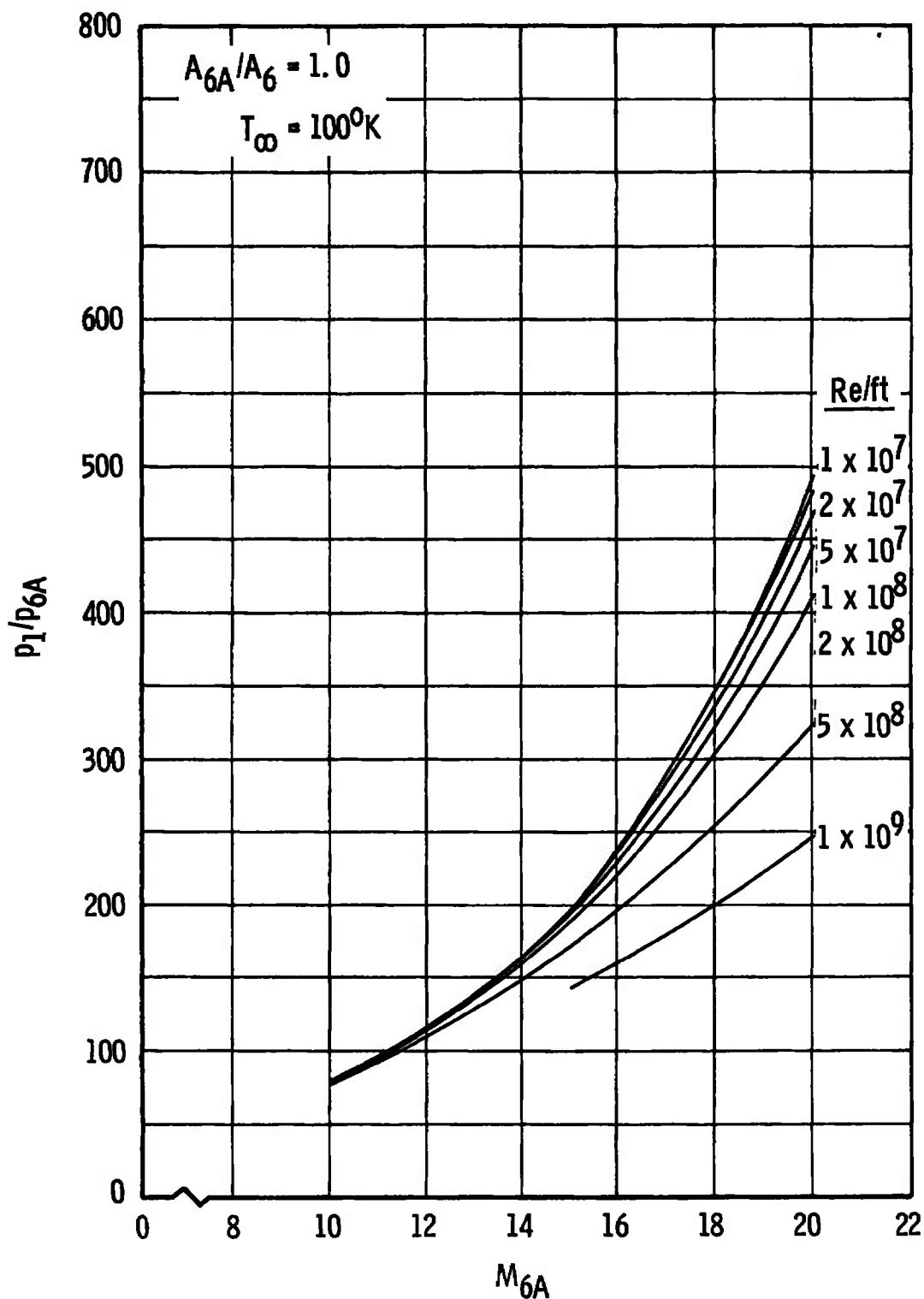Fig. II-1 Continued
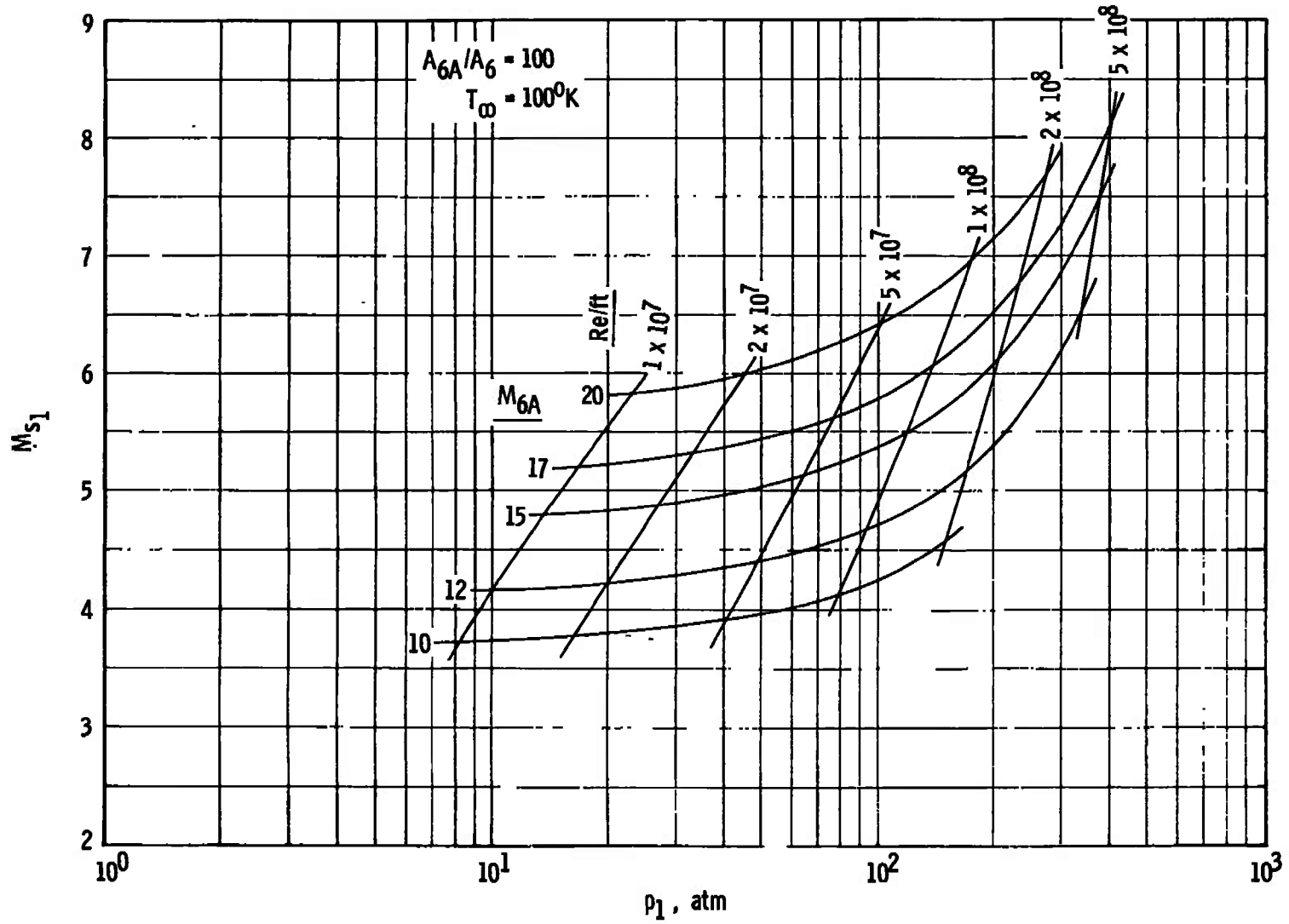
d. $A_{6A}/A_6 = 100$

Fig. II-1 Concluded
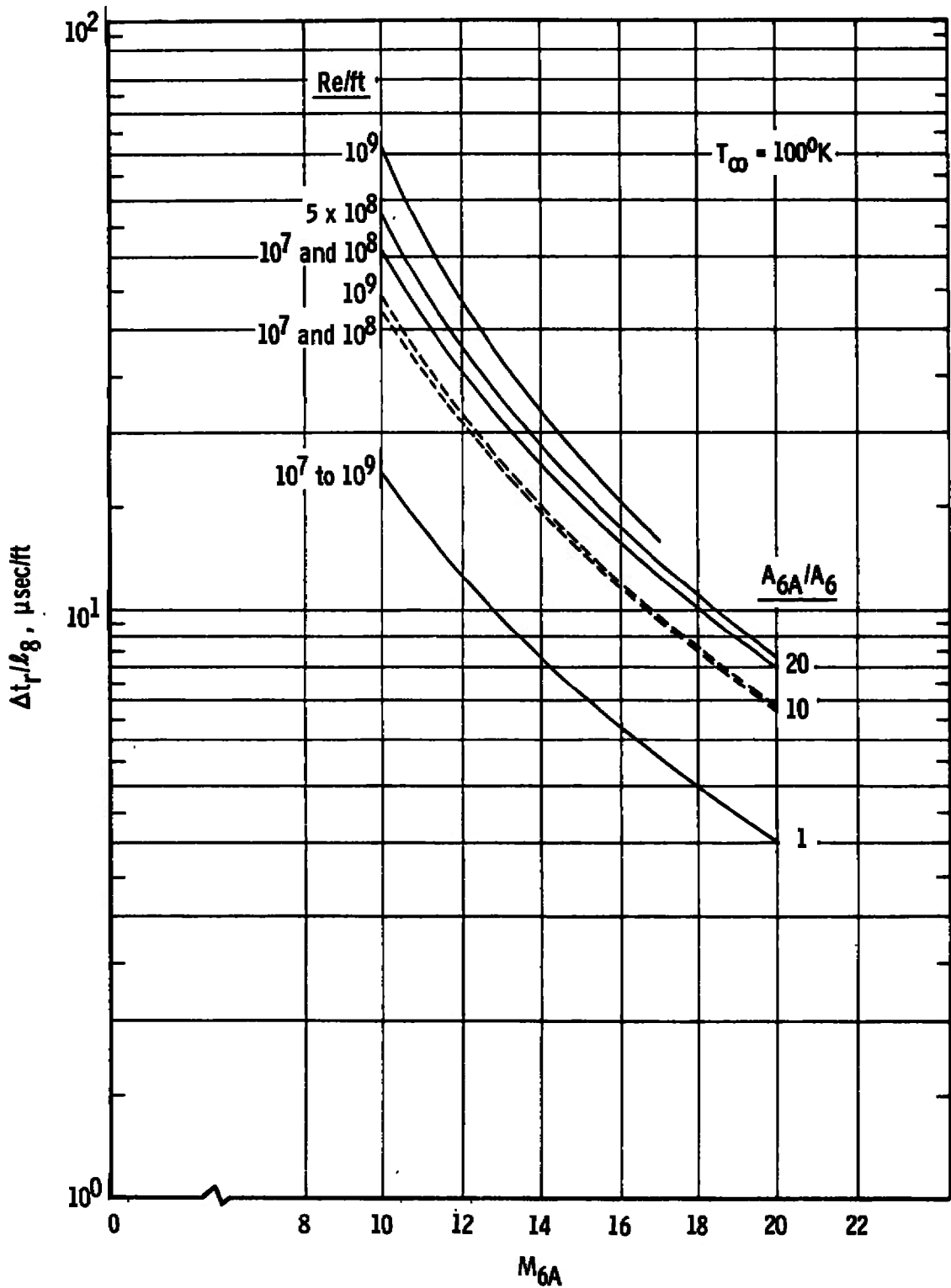
a. A_{6A}/A_6 = 1, 10, and 20

Fig. II-2 Run Time per Unit Length of Acceleration Tube, $\Delta t_r / l_8$, versus M_{6A}
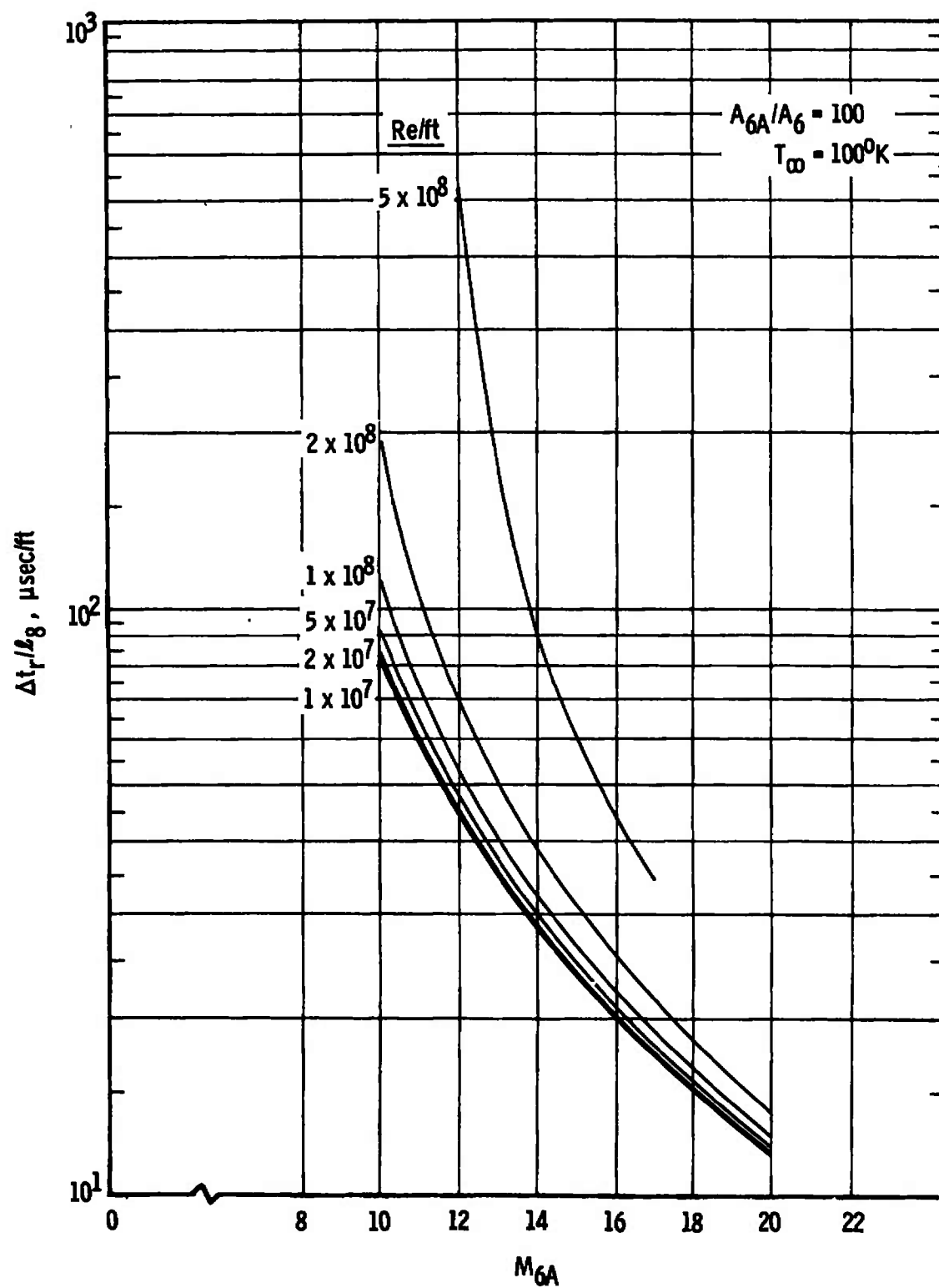
b. $A_{6A}/A_6 = 100$
Fig. II-2 Concluded
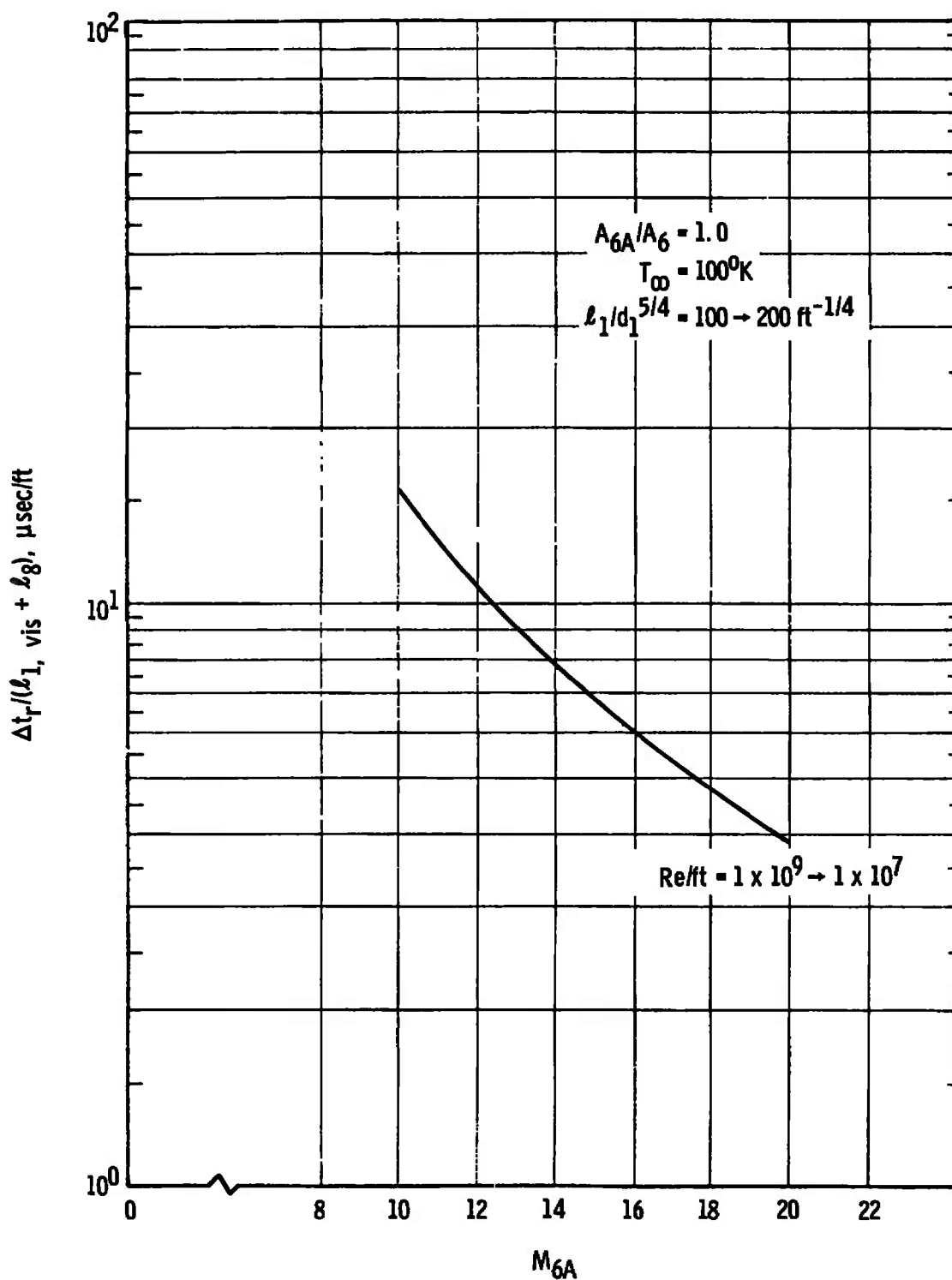
a. $A_{6A}/A_6 = 1$, $\ell_1/d_1^{5/4} = 100$ and 200 ft$^{-1/4}$

Fig. II-3 Run Time per Unit Length of Driven and Acceleration
Tubes, $\Delta t_r / \left(\ell_{1,vis} + \ell_8 \right)$, versus M_{6A}

24
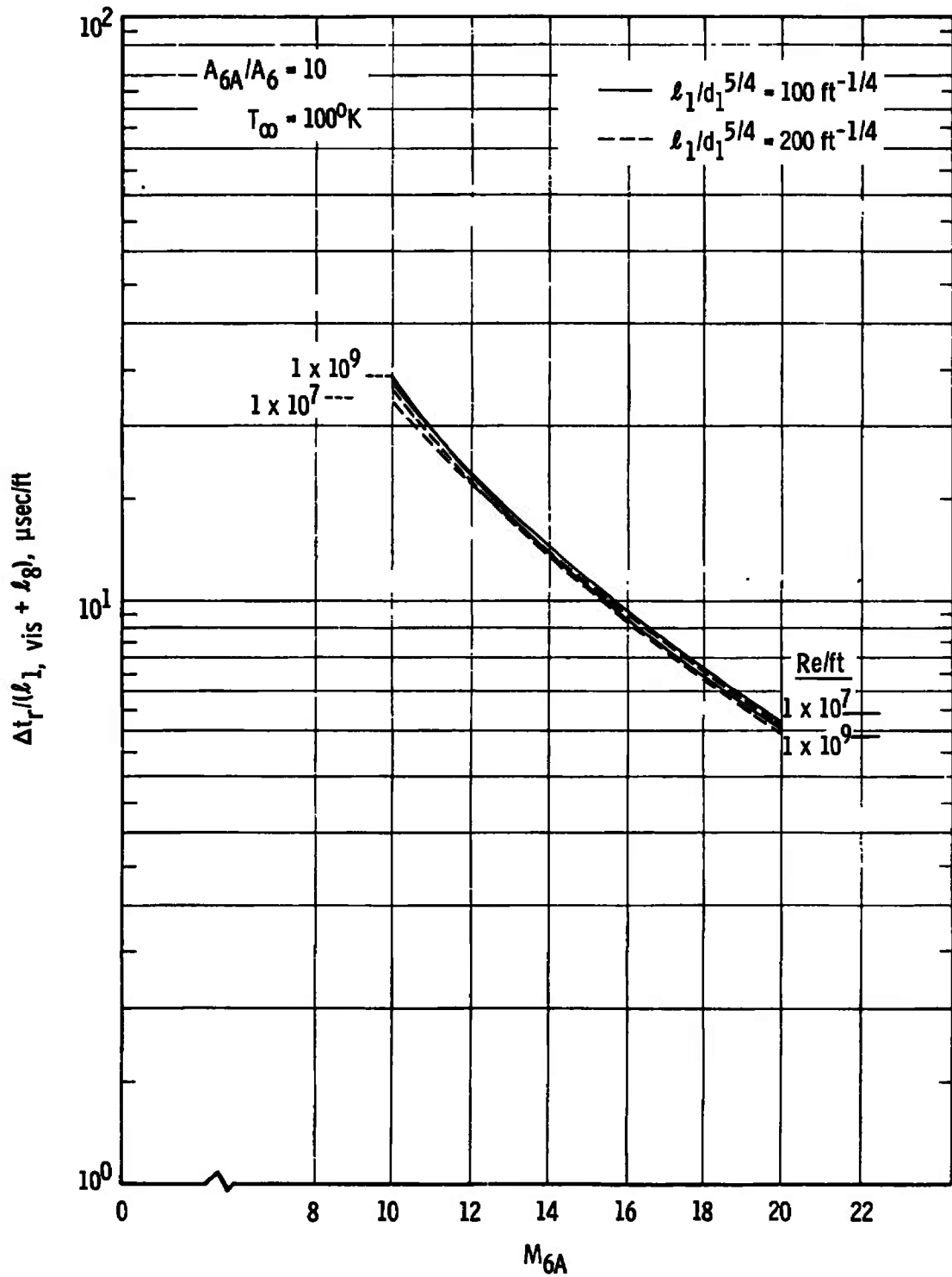
b. $A_{6A}/A_6 = 10$, $\ell_1/d_1^{5/4} = 100$ and 200 ft$^{-1/4}$
Fig. II-3 Continued
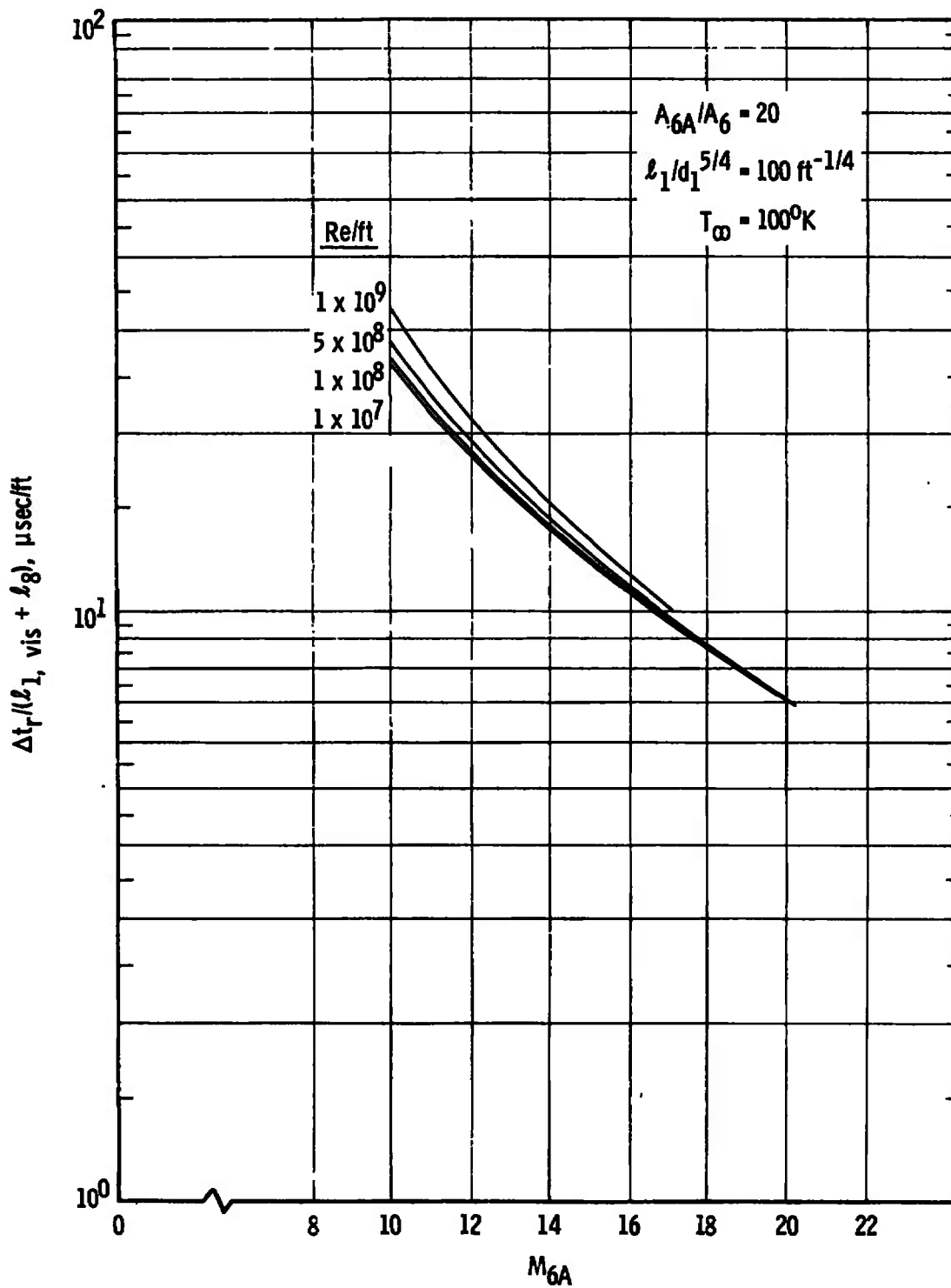
c. $A_{6A}/A_6 = 20$, $\ell_1/d_1^{5/4} = 100$ ft$^{-1/4}$
Fig. II-3 Continued
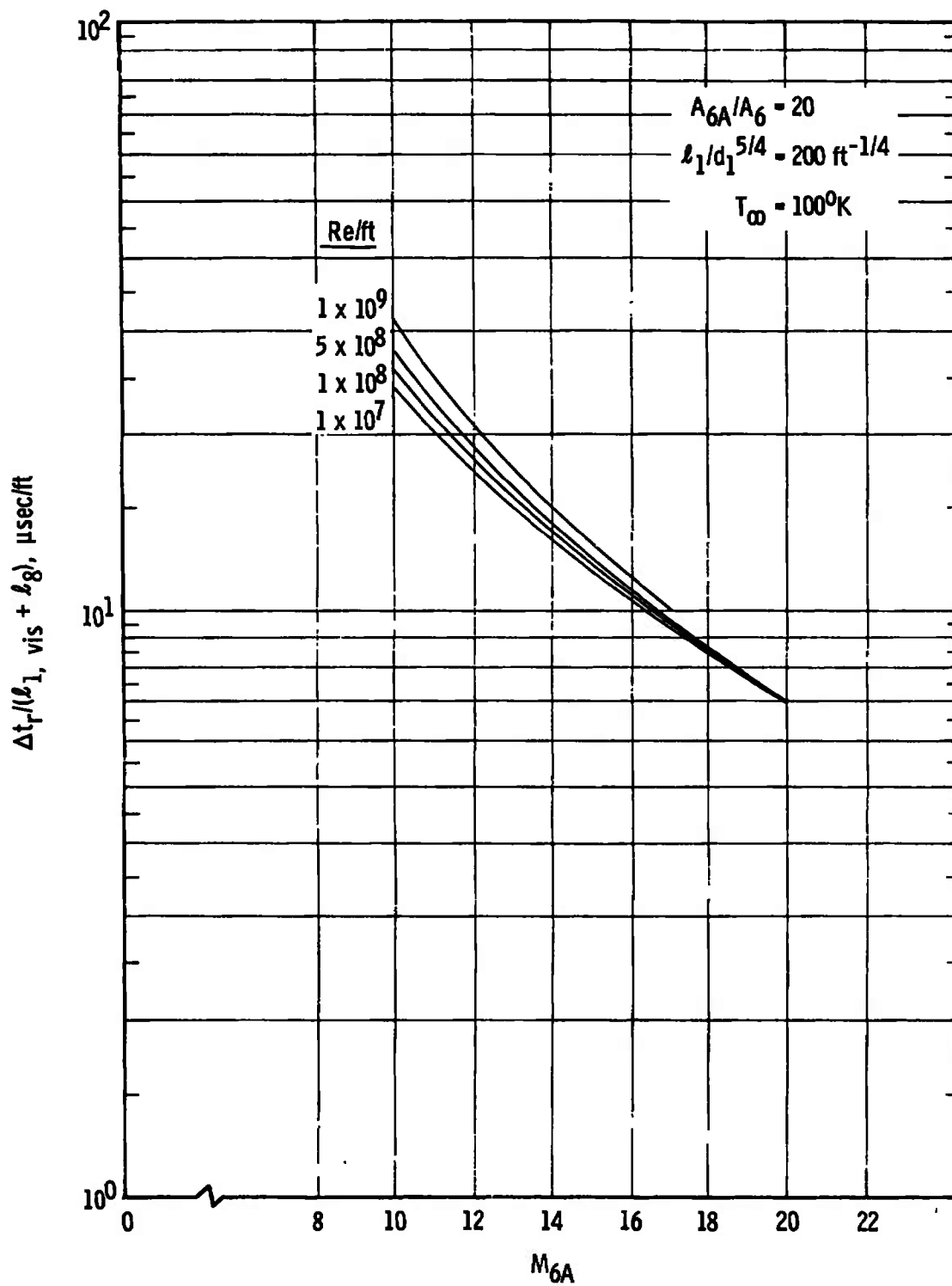
d. $A_{6A}/A_6 = 20$, $\ell_1/d_1^{5/4} = 200$ ft$^{-1/4}$
Fig. II-3 Continued
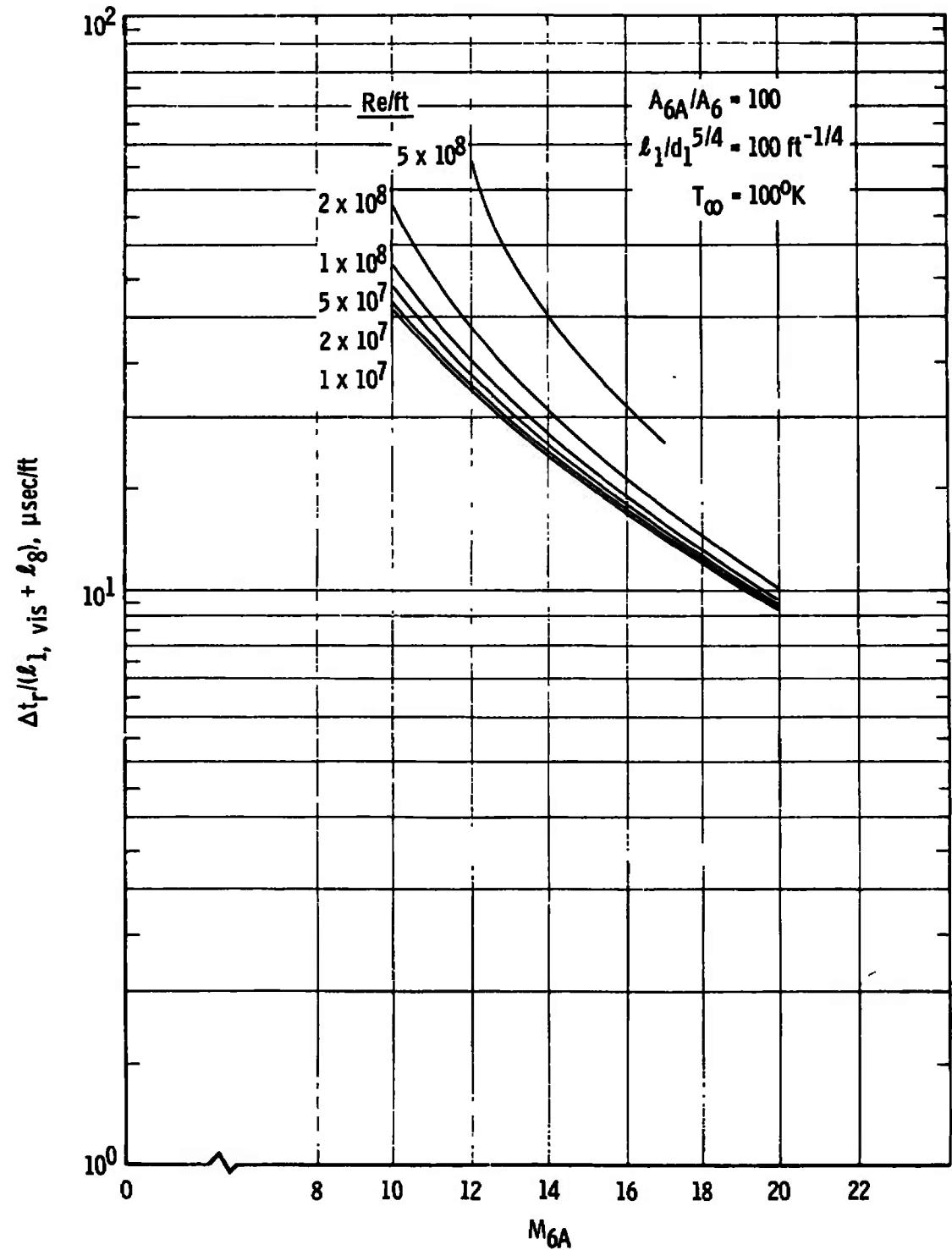
e. $A_{6A}/A_6 = 100$, $\ell_1/d_1^{5/4} = 100$ ft$^{-1/4}$
Fig. II-3 Continued
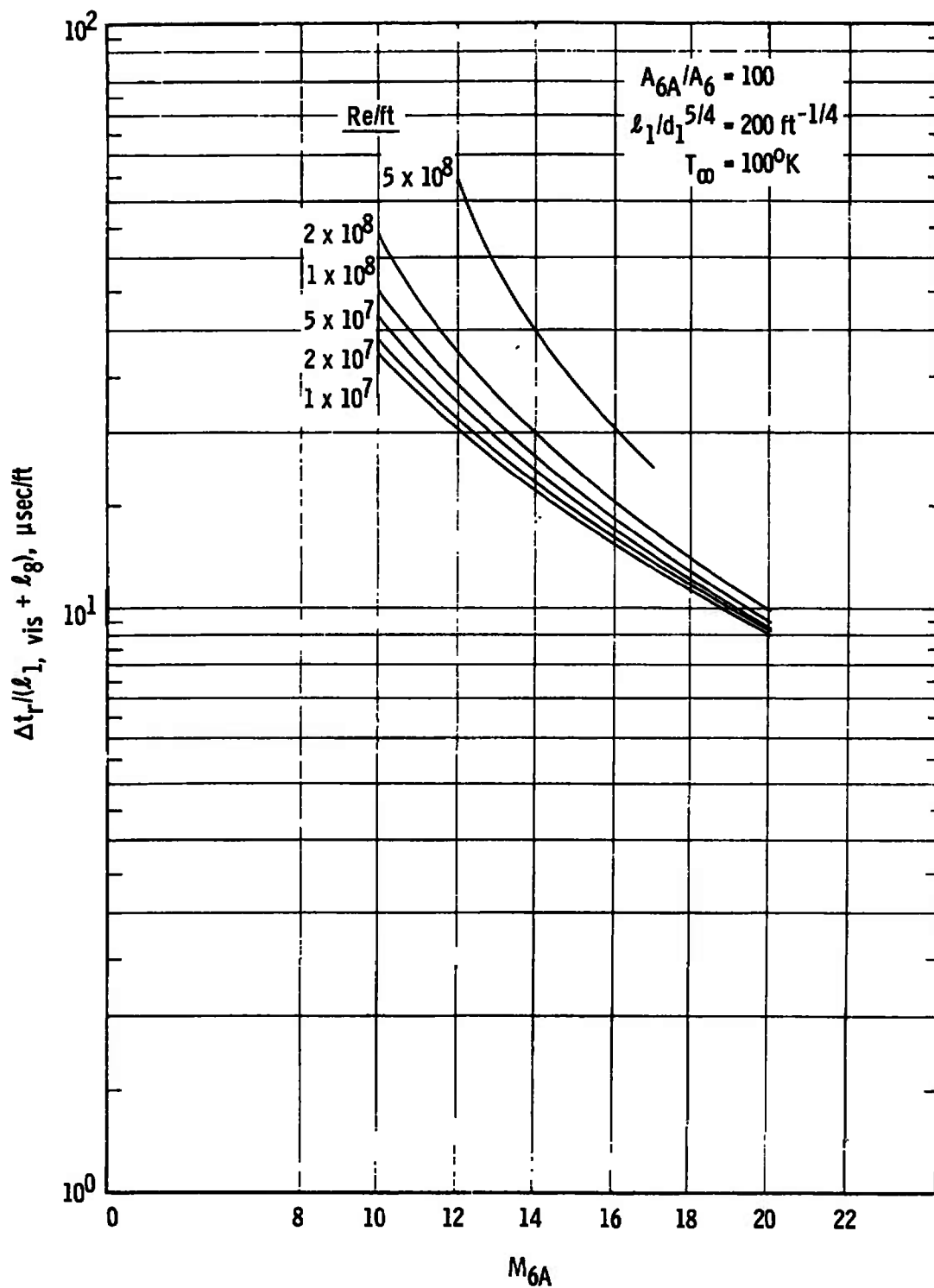
f. $A_{6A}/A_6 = 100$, $\ell_1/d_1^{5/4} = 100 \text{ ft}^{-1/4}$

Fig. II-3 Concluded
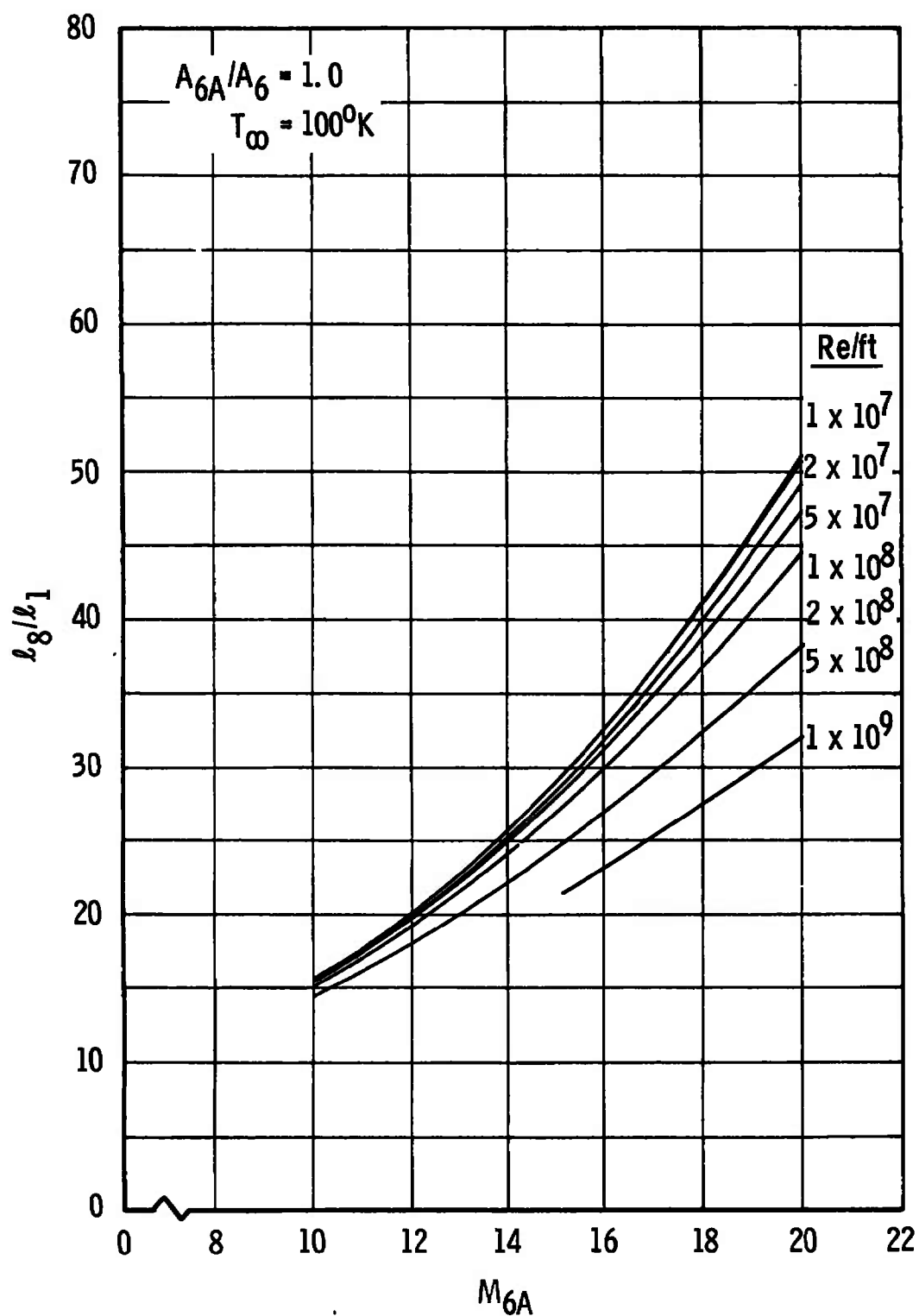
a. $A_{6A}/A_6 = 1$

Fig. II-4 Acceleration-to-Driven Tube Length Ratio (Inviscid), l_8/l_1, versus M_{6A}
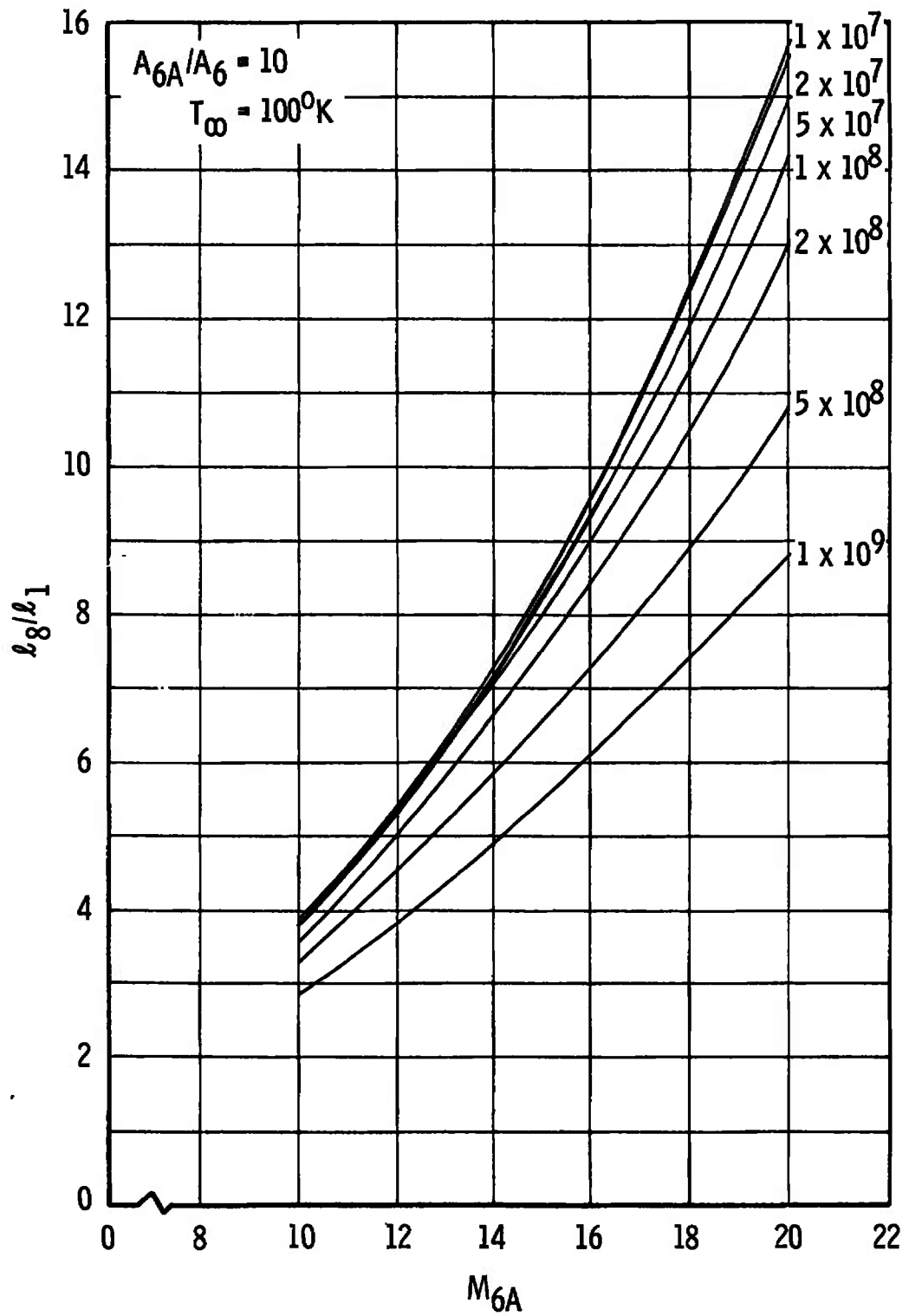
b. $A_{6A}/A_6 = 10$
Fig. II-4 Continued
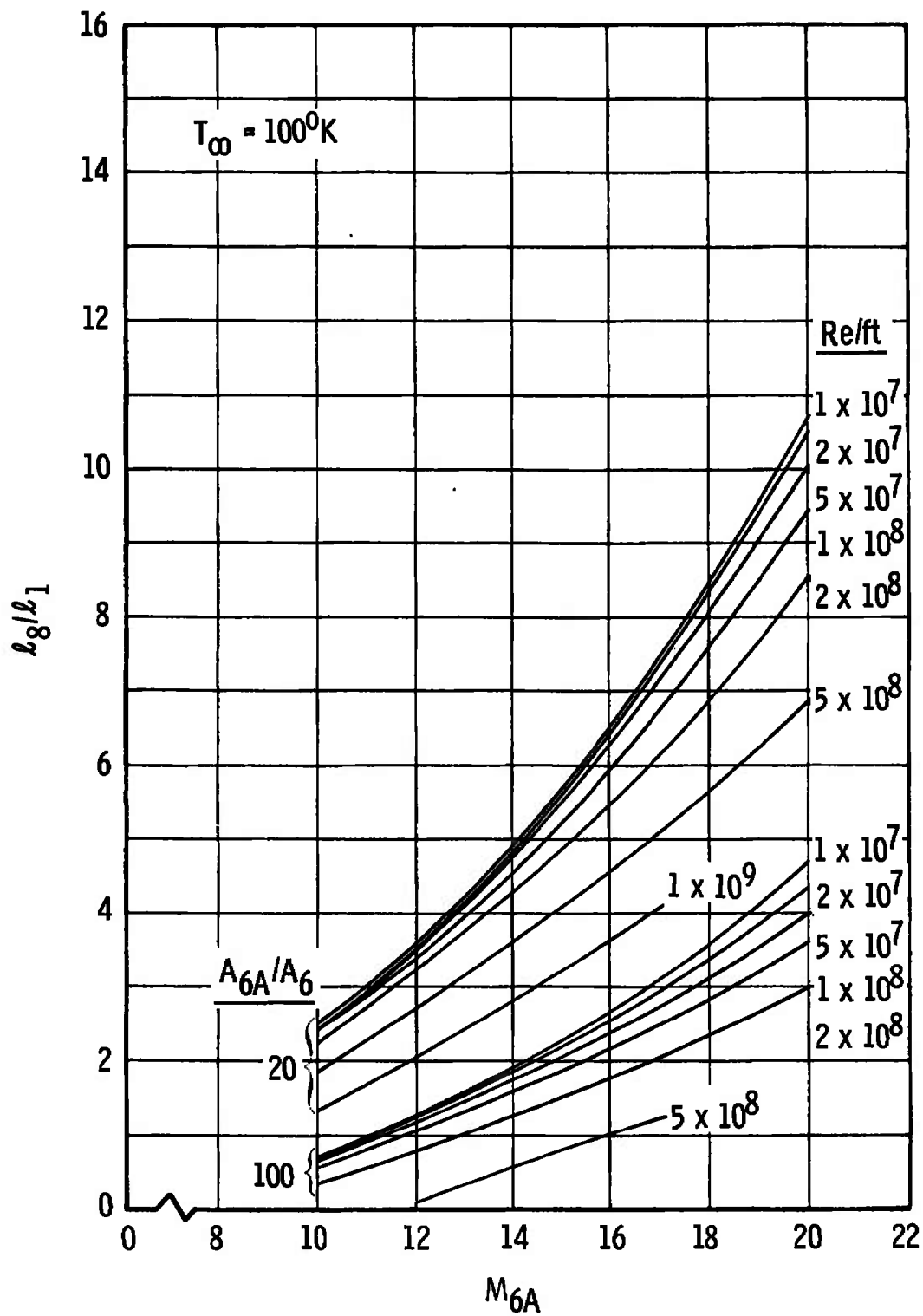
c. $A_{6A}/A_6 = 20$ and 100
Fig. II-4 Concluded
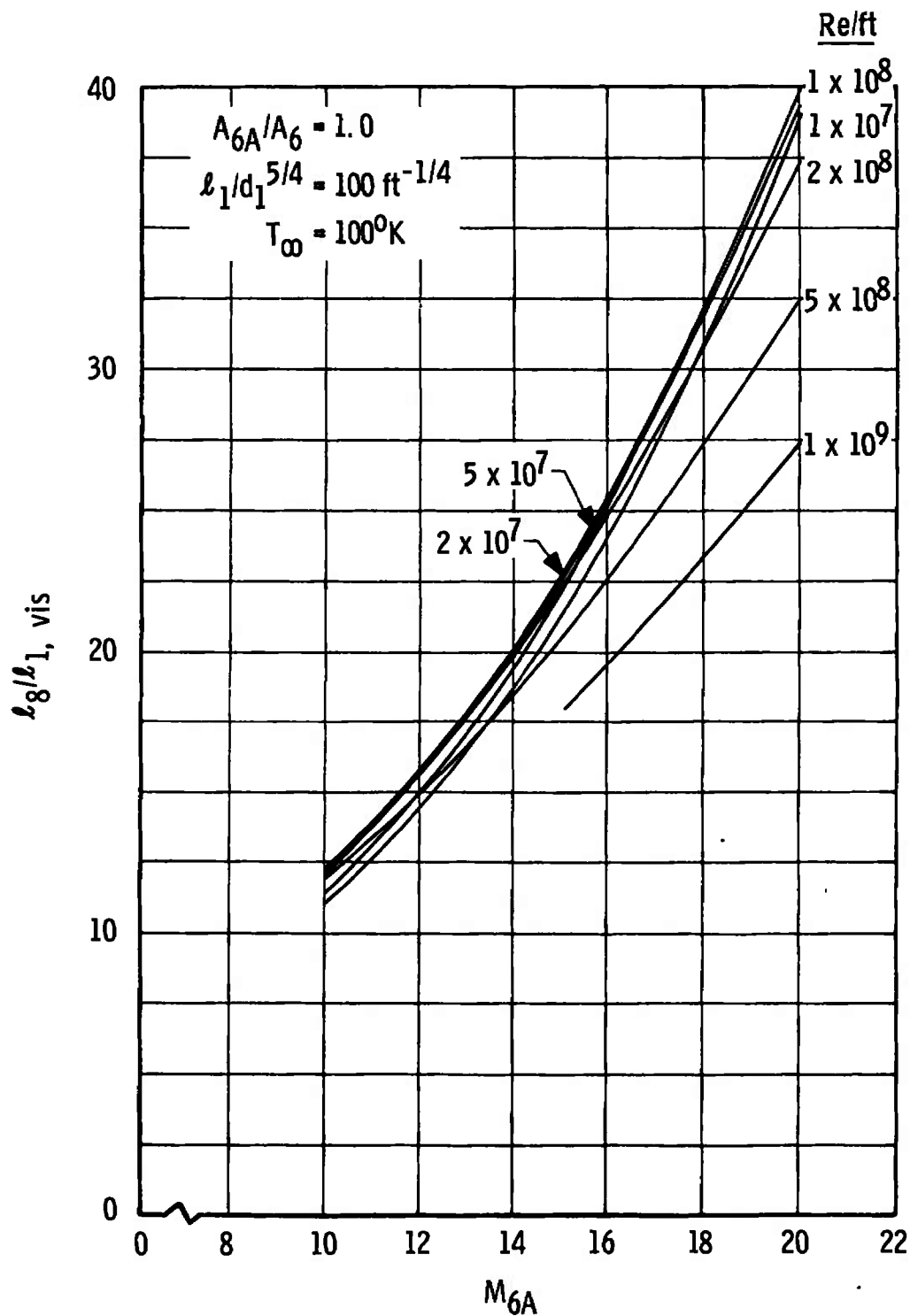
a. $A_{6A}/A_6 = 1$, $\ell_1/d_1^{5/4} = 100$ ft$^{-1/4}$

Fig. II-5 Acceleration-to-Driven Tube Length Ratio (Viscid), ℓ_8/ℓ_1 vis, versus M_{6A}
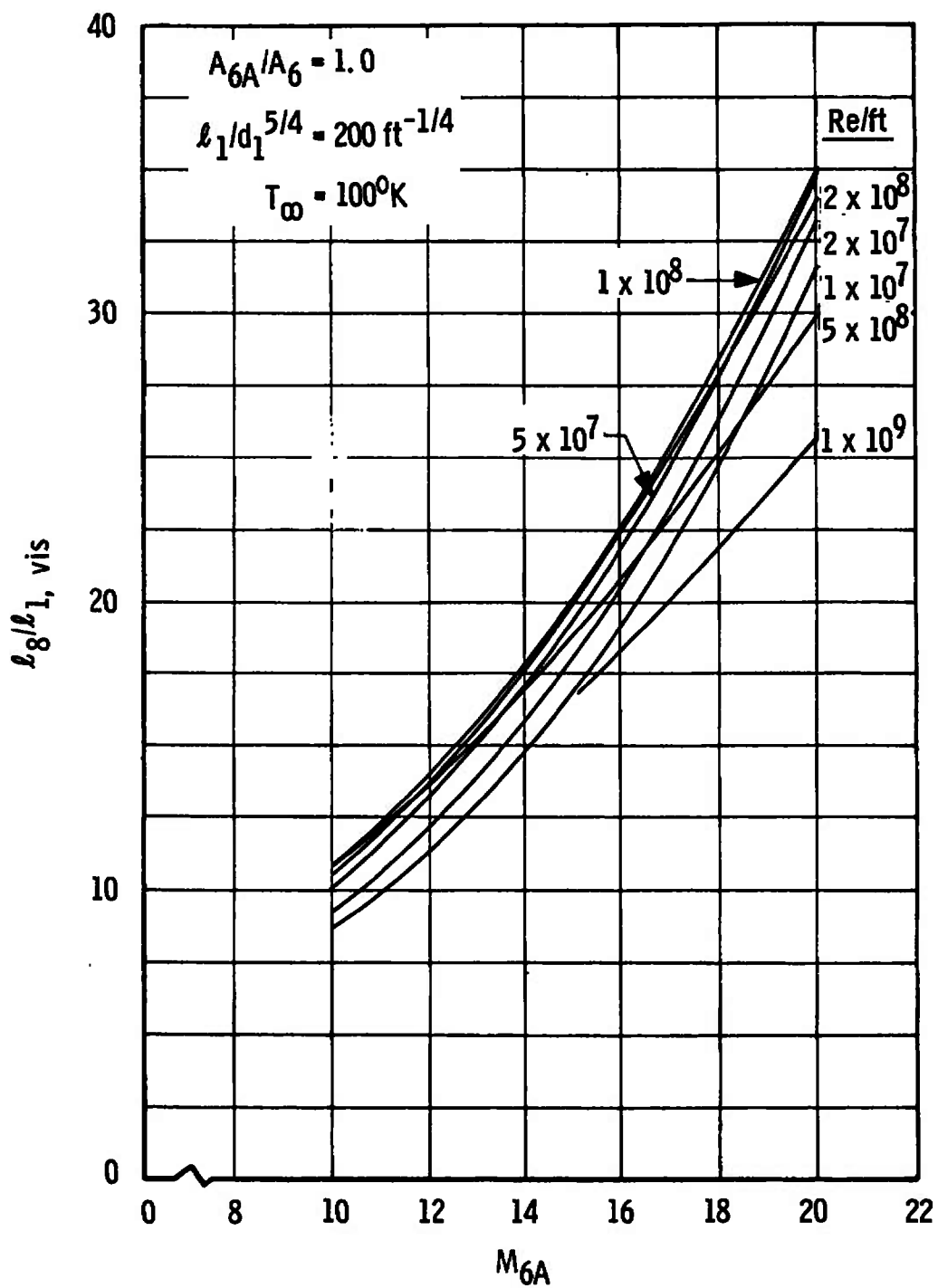
b. $A_{6A}/A_6 = 1$, $\ell_1/d_1^{5/4} = 200$ ft$^{-1/4}$
Fig. II-5 Continued
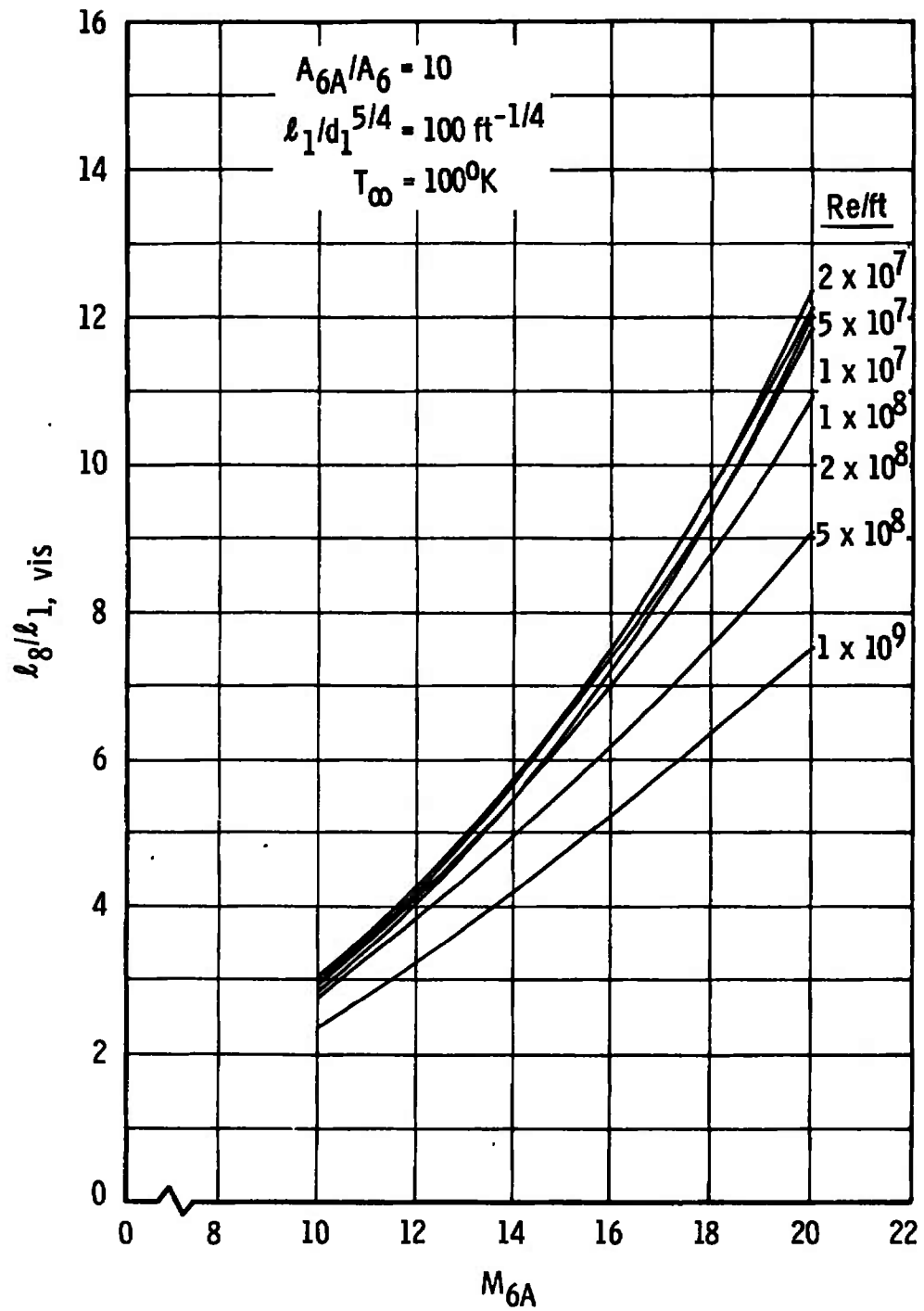
c. $A_{6A}/A_6 = 10$, $\ell_1/d_1^{5/4} = 100 \text{ ft}^{-1/4}$
Fig. II-5 Continued
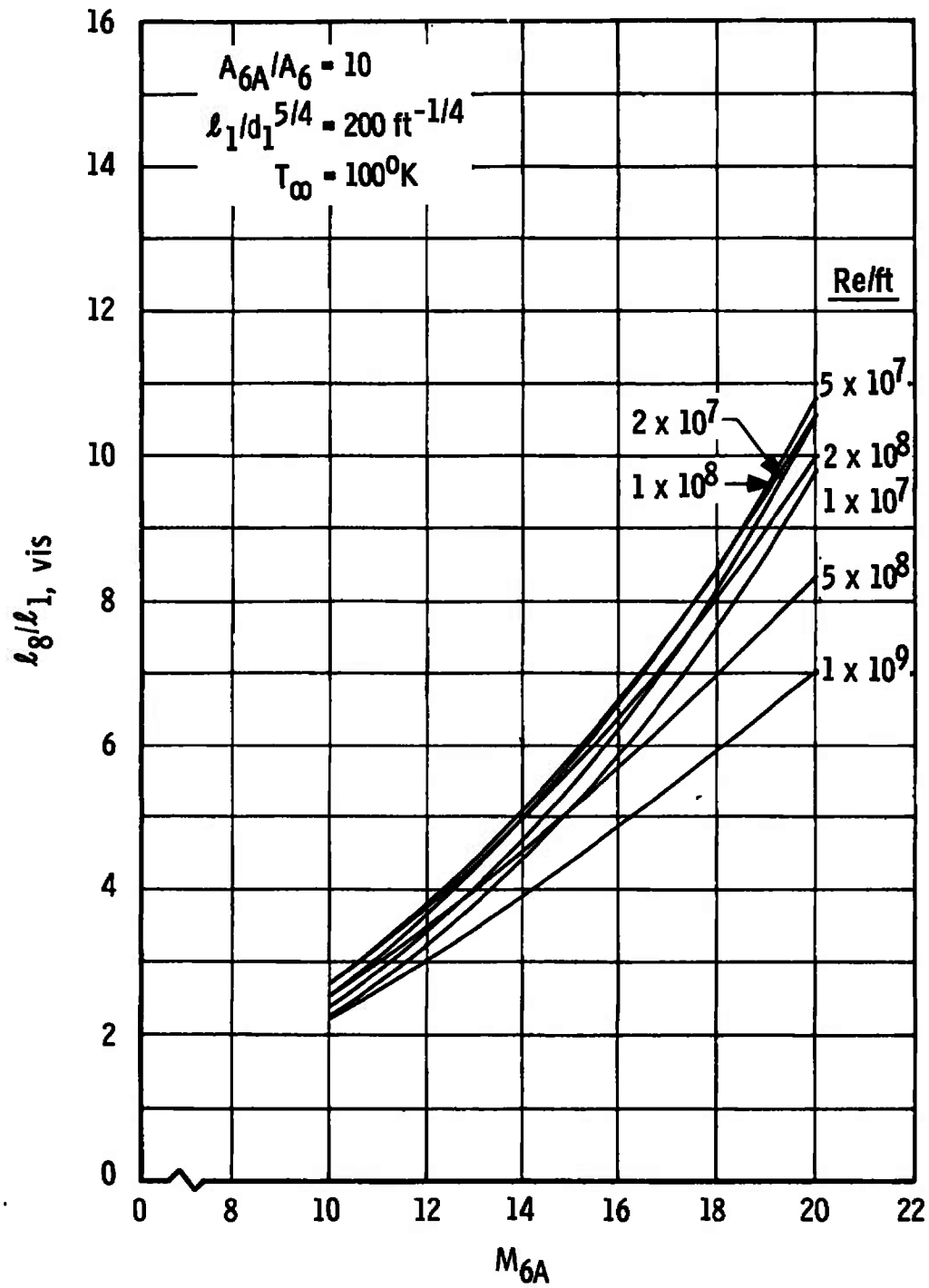
d. $A_{6A}/A_6 = 10$, $l_1/d_1^{5/4} = 200$ ft$^{-1/4}$
Fig. II-5 Continued
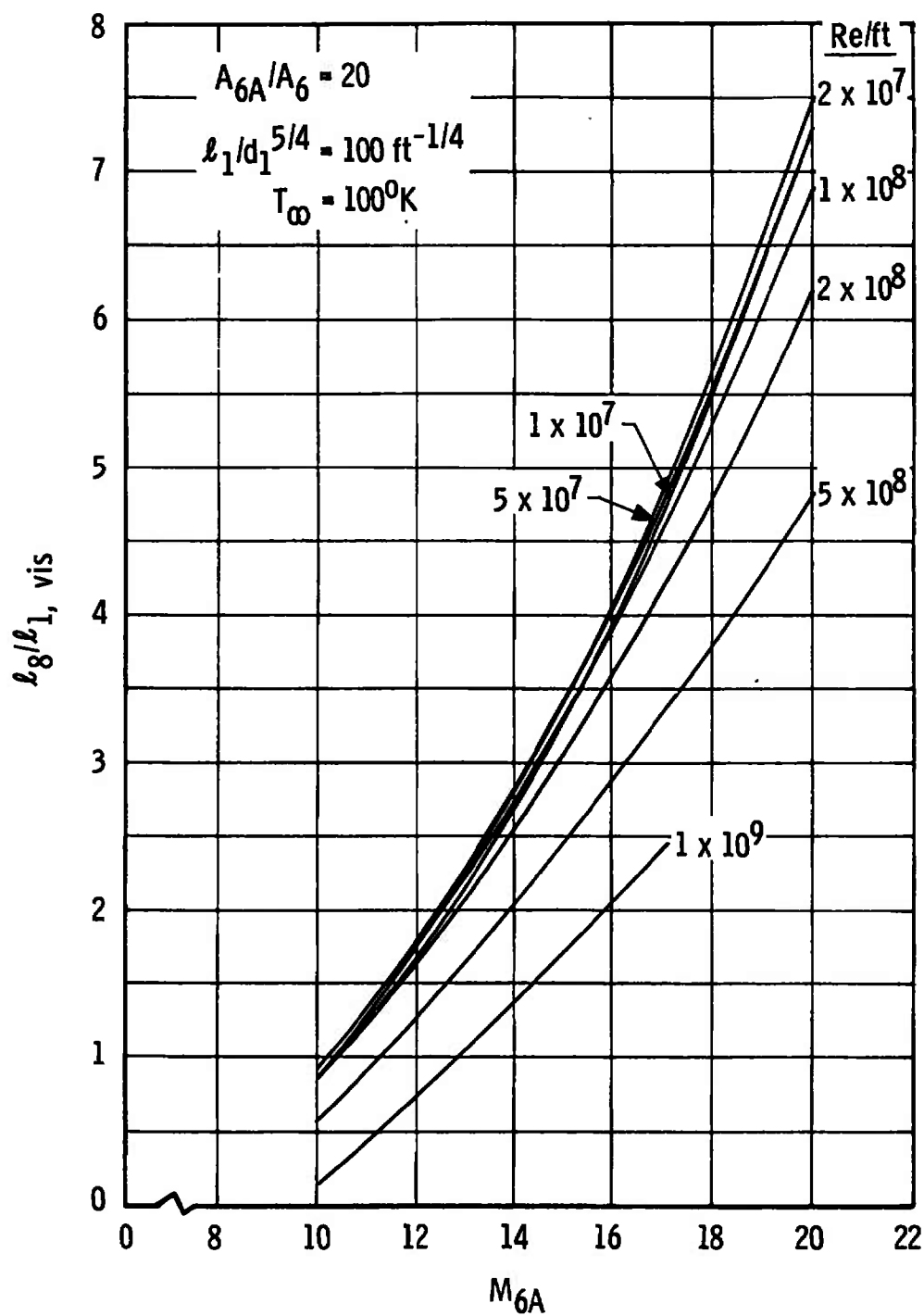
e. $A_{6A}/A_6 = 20$, $\ell_1/d_1^{5/4} = 100$ ft$^{-1/4}$
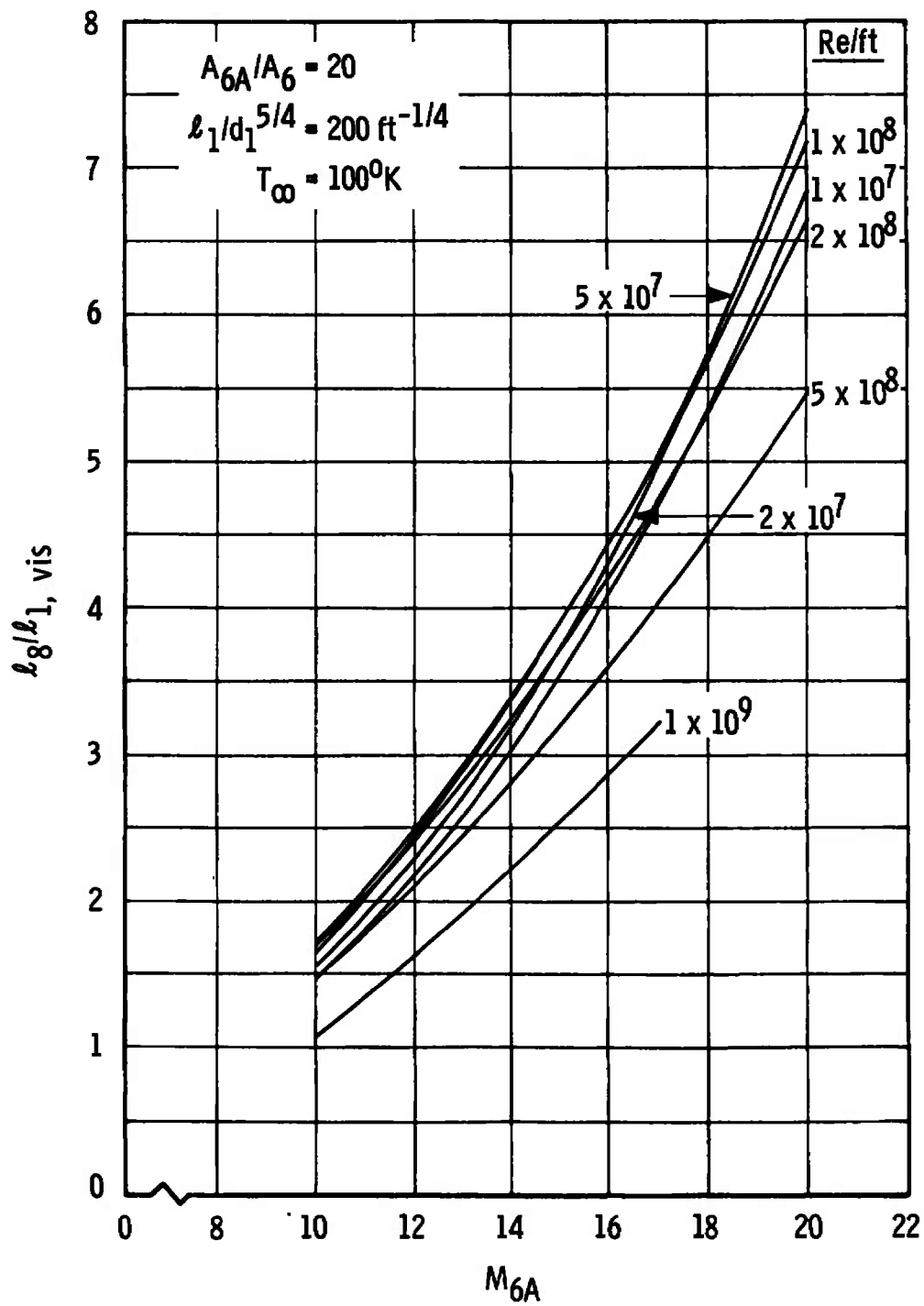
Fig. II-5 Continued

f. $A_{6A}/A_6 = 20$, $\ell_1/d_1^{5/4} = 200$ ft$^{-1/4}$
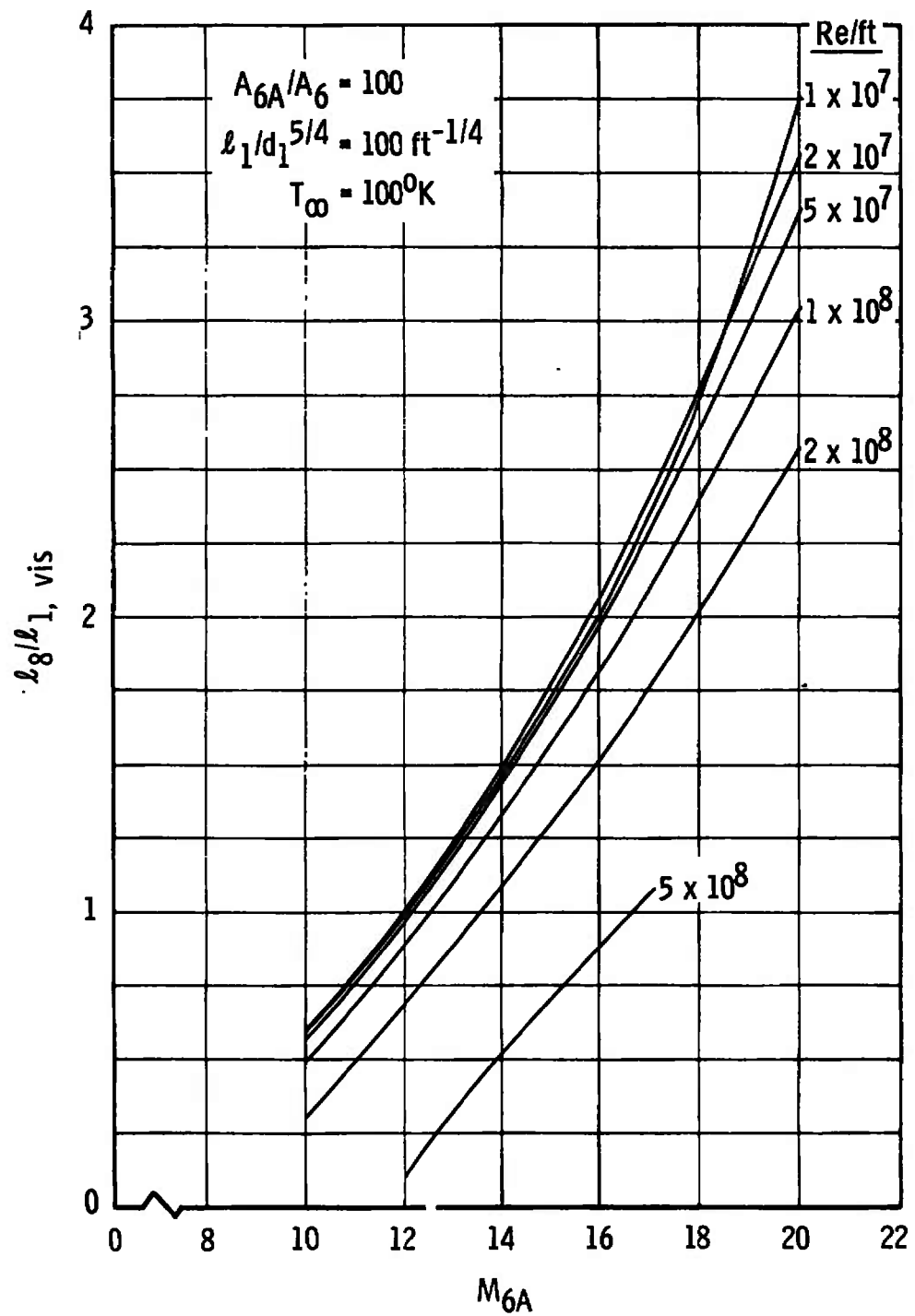
Fig. II-5 Continued

g. $A_{6A}/A_6 = 100$, $\ell_1/d_1^{5/4} \doteq 100 \text{ ft}^{-1/4}$
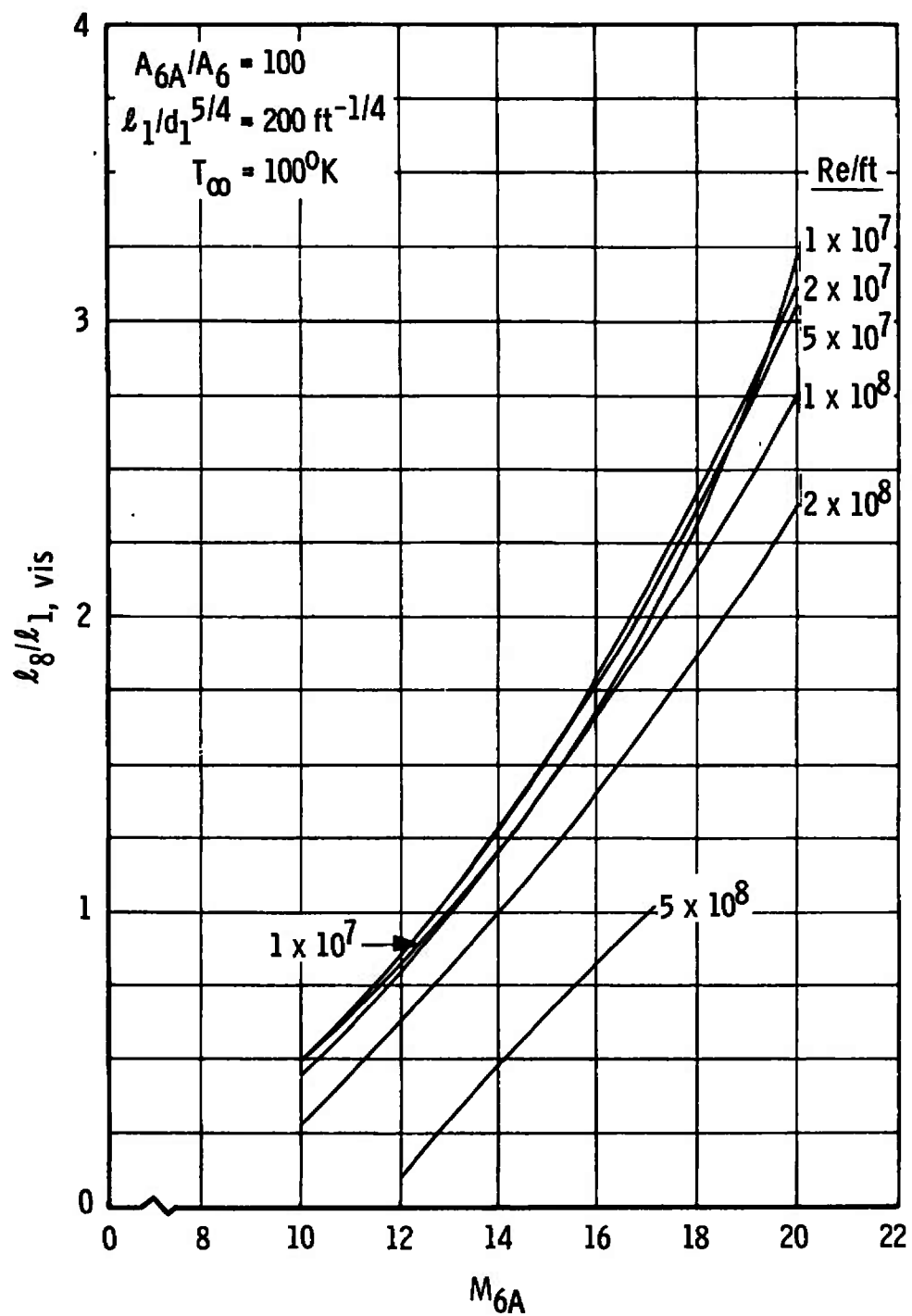
Fig. II-5 Continued

h. $A_{6A}/A_6 = 100$, $\ell_1/d_1^{5/4} = 200 \, \text{ft}^{-1/4}$

Fig. II-5 Concluded
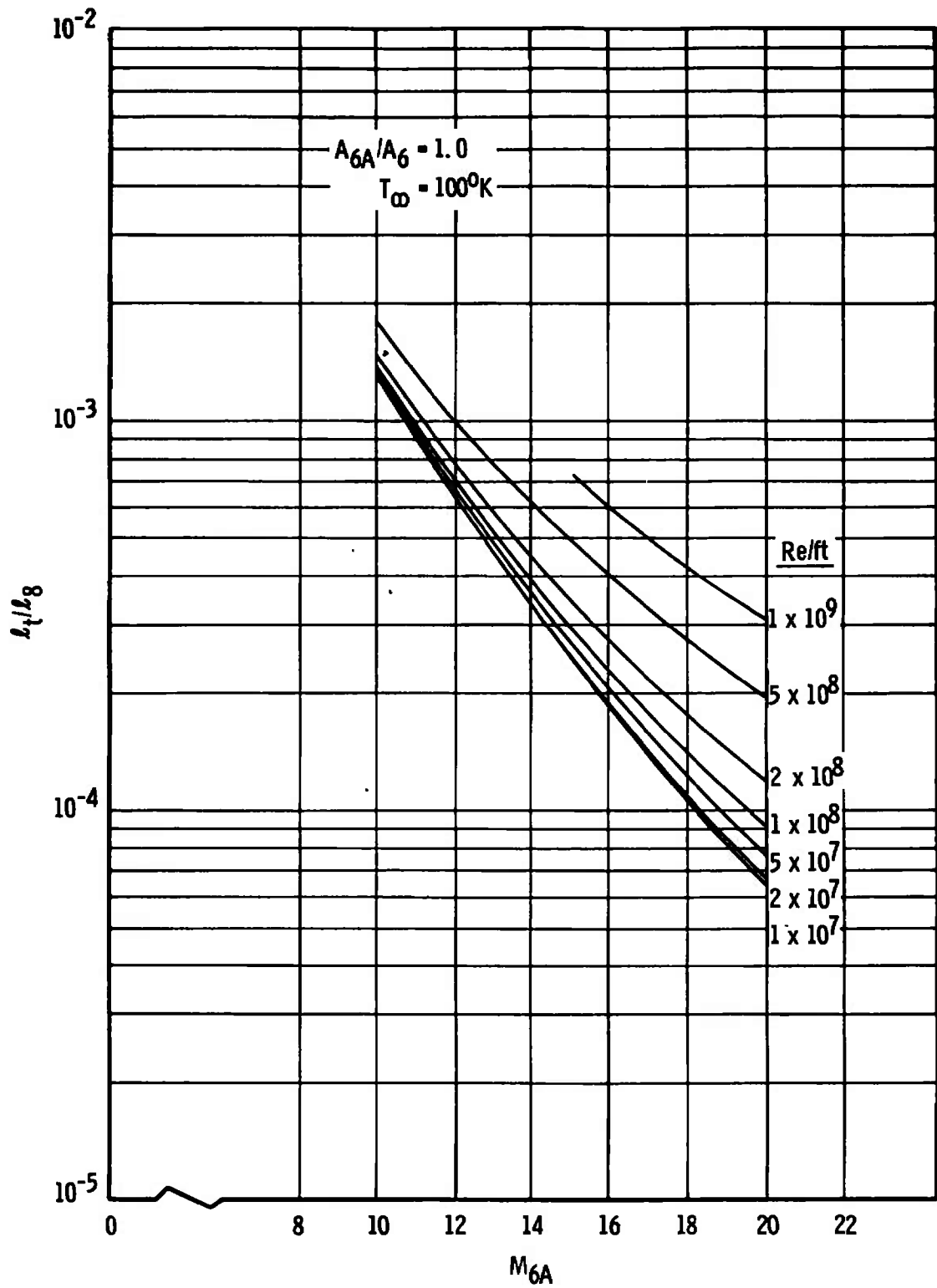
a. $A_{6A}/A_6 = 1$

Fig. II-6 Test Gas Slug Length Ratio, ℓ_t/ℓ_8, versus M_{6A}
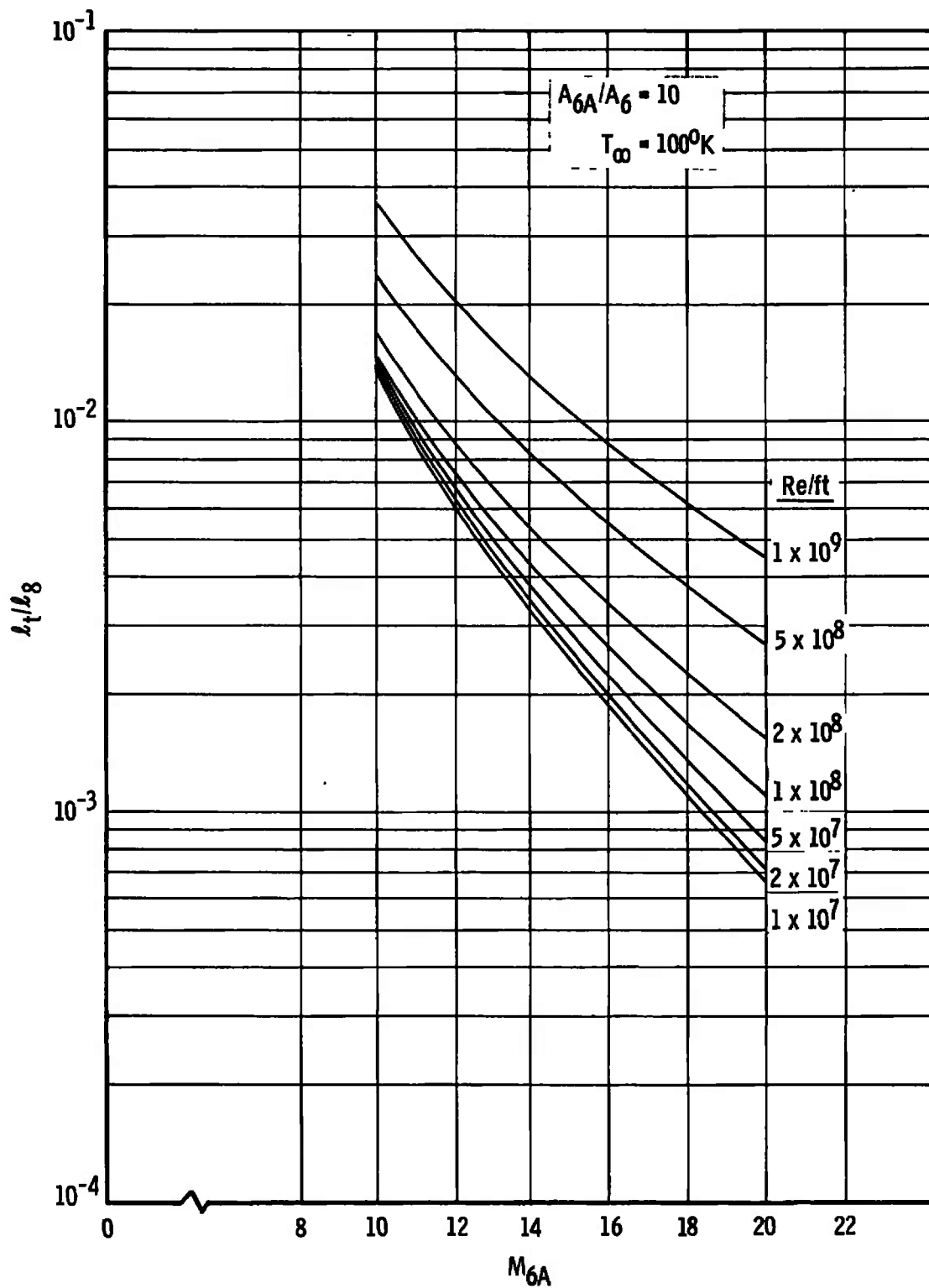
b. $A_{6A}/A_6 = 10$
Fig. II-6 Continued
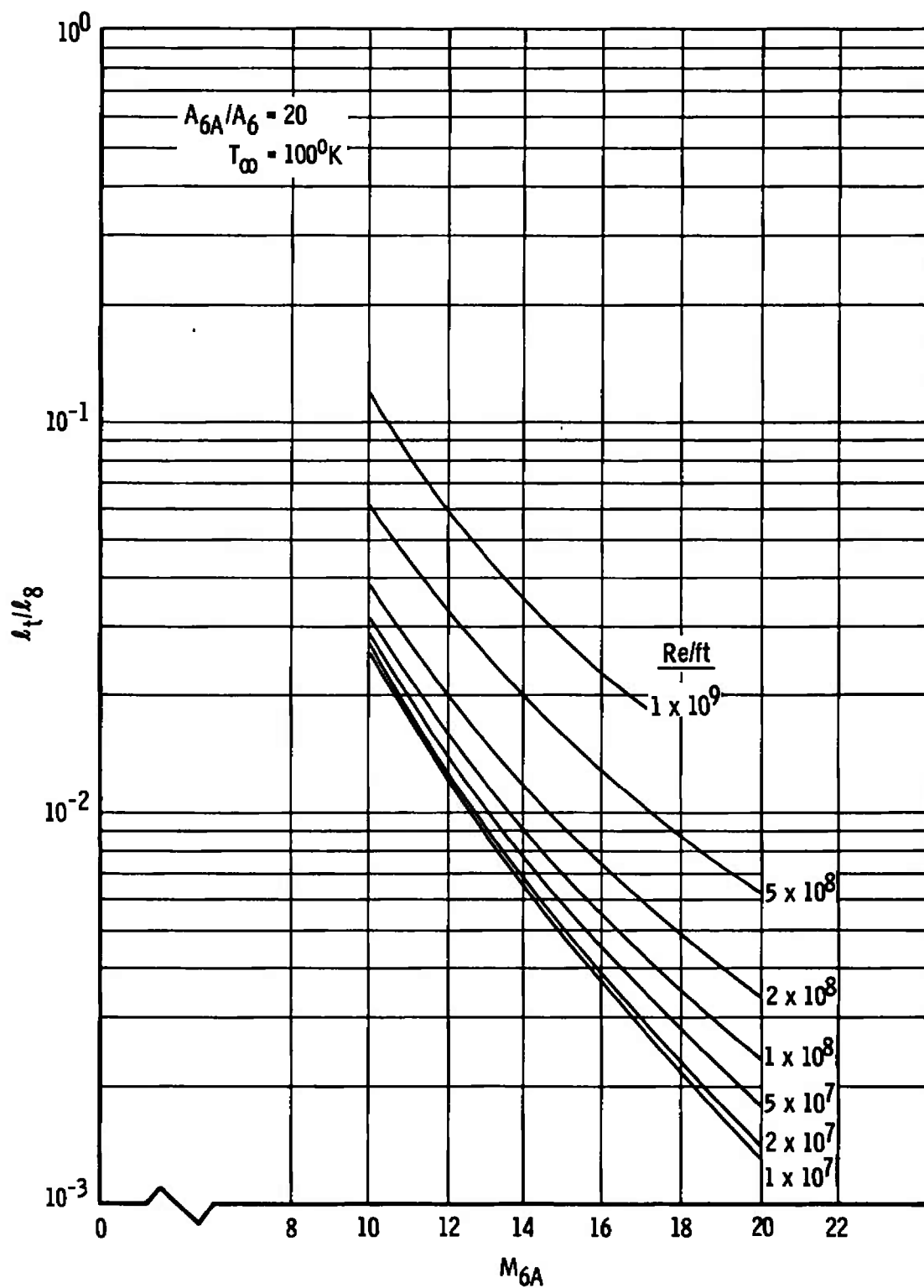
c. A_{6A}/A_6 20

Fig. II-6 Continued
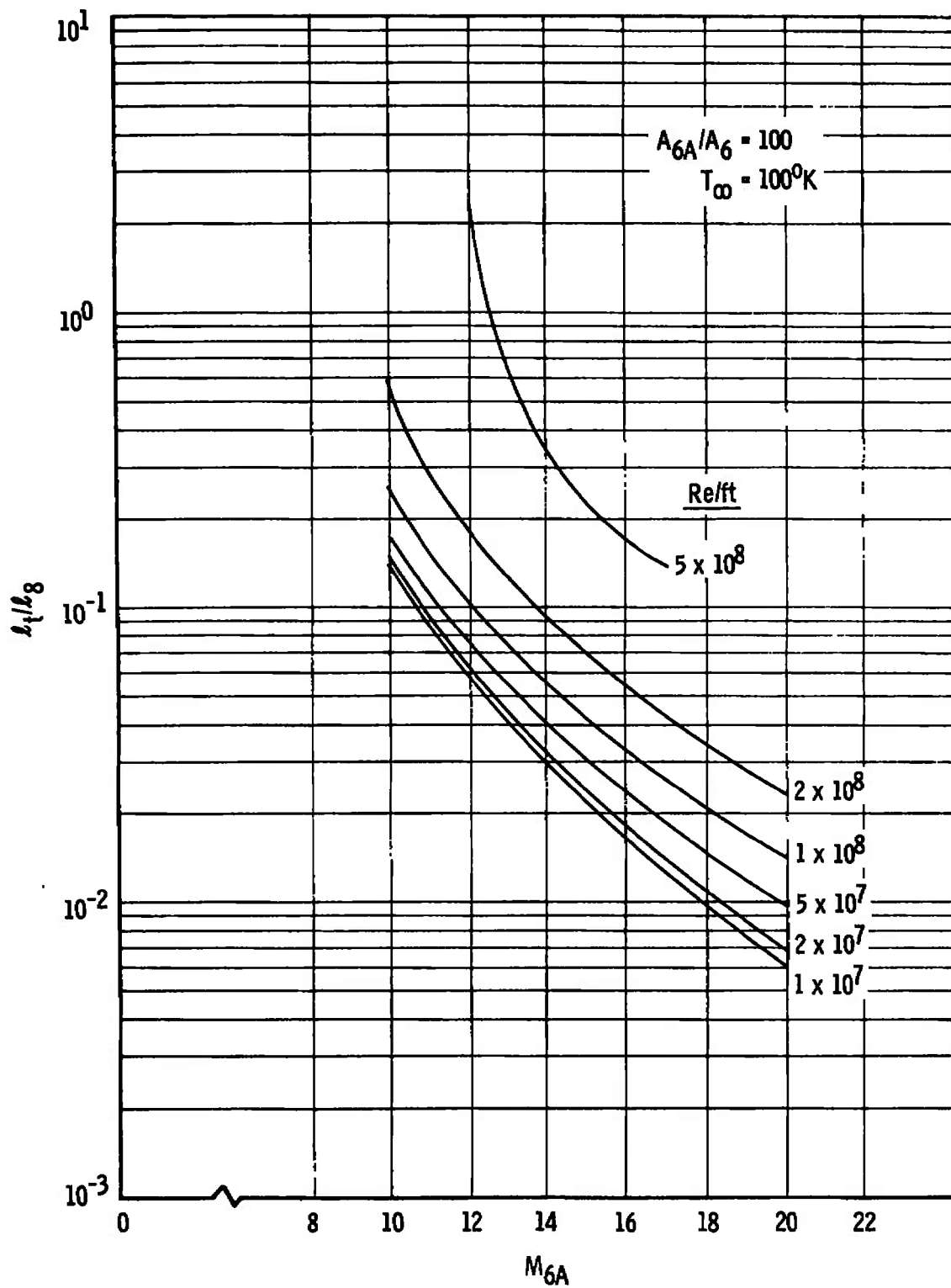
d. $A_{6A}/A_6 = 100$
Fig. II-6 Concluded
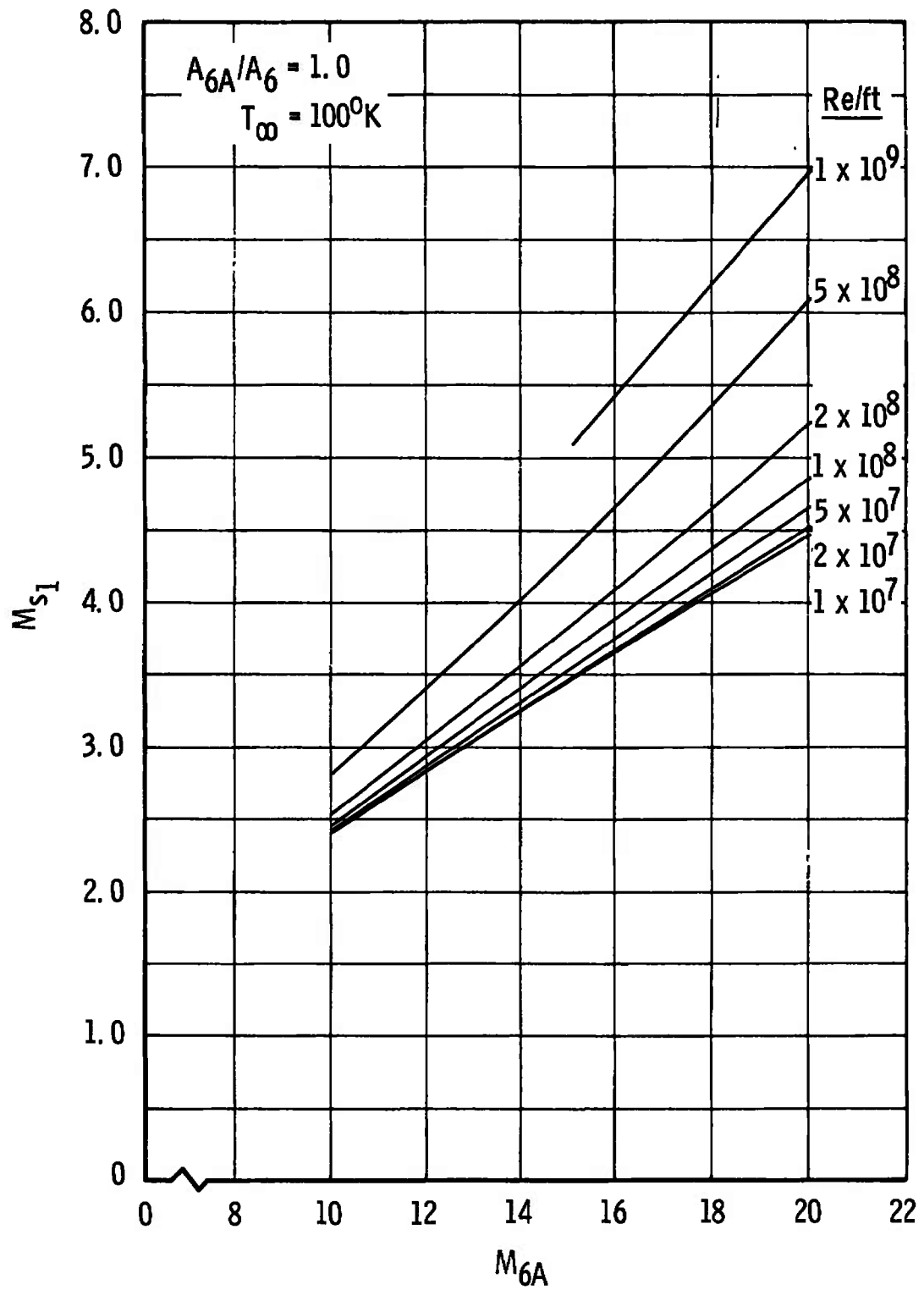
a. $A_{6A}/A_6 = 1$

Fig. II-7 Driven Tube Shock Strength, M_{s_1}, versus M_{6A}
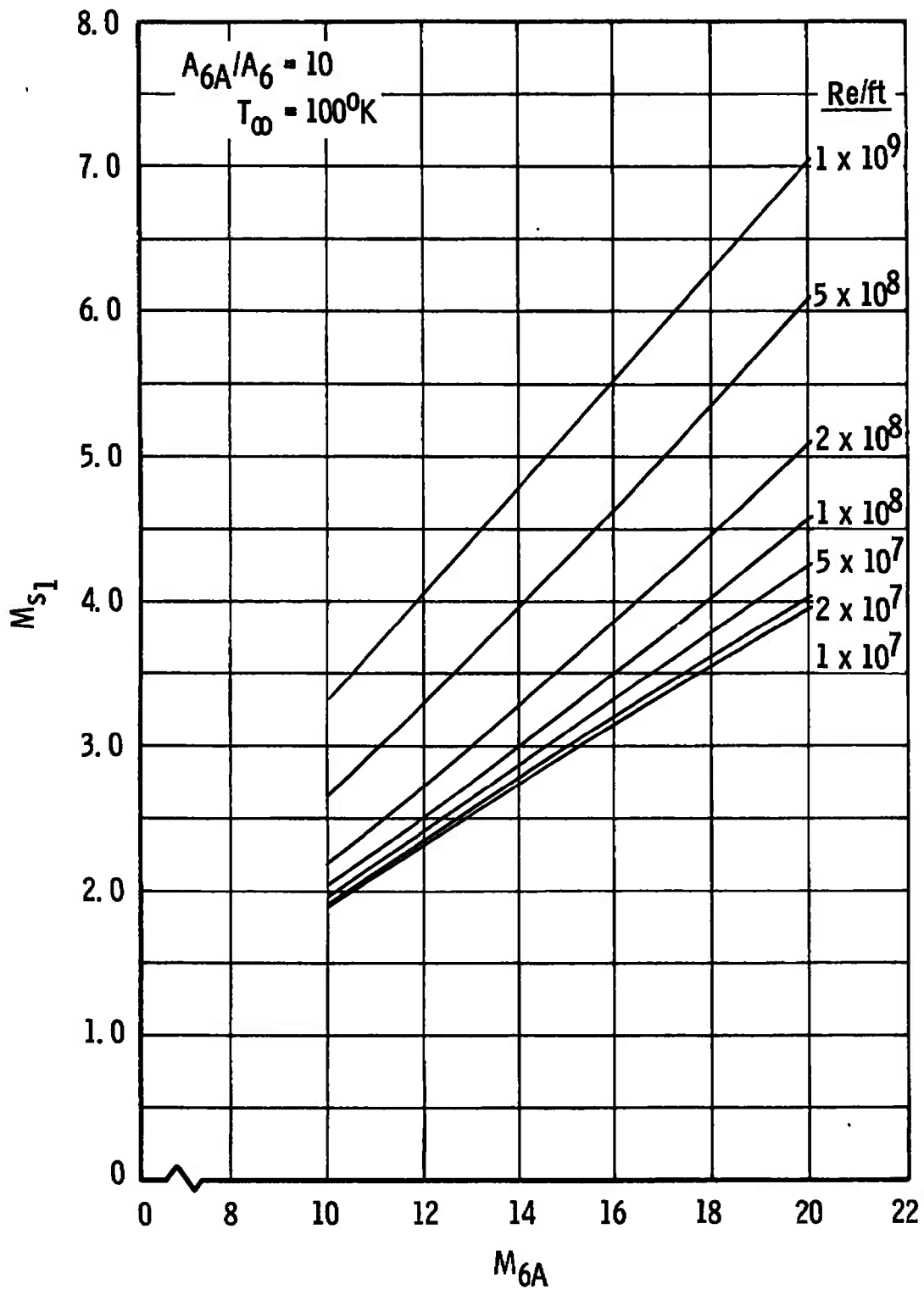
b. $A_{6A}/A_6 = 10$
Fig. II-7 Continued
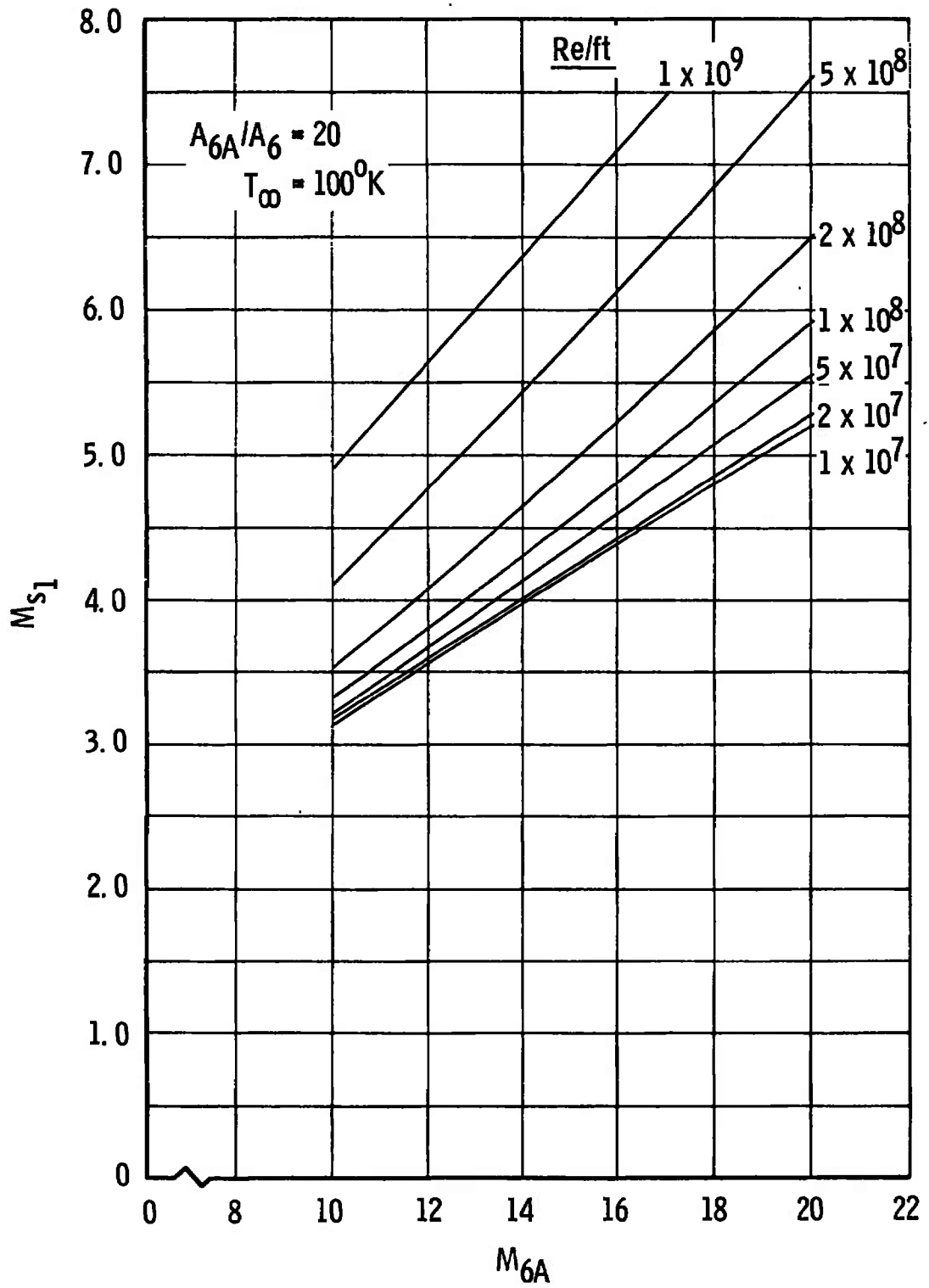
c. $A_{6A}/A_6 = 20$
Fig. II-7 Continued
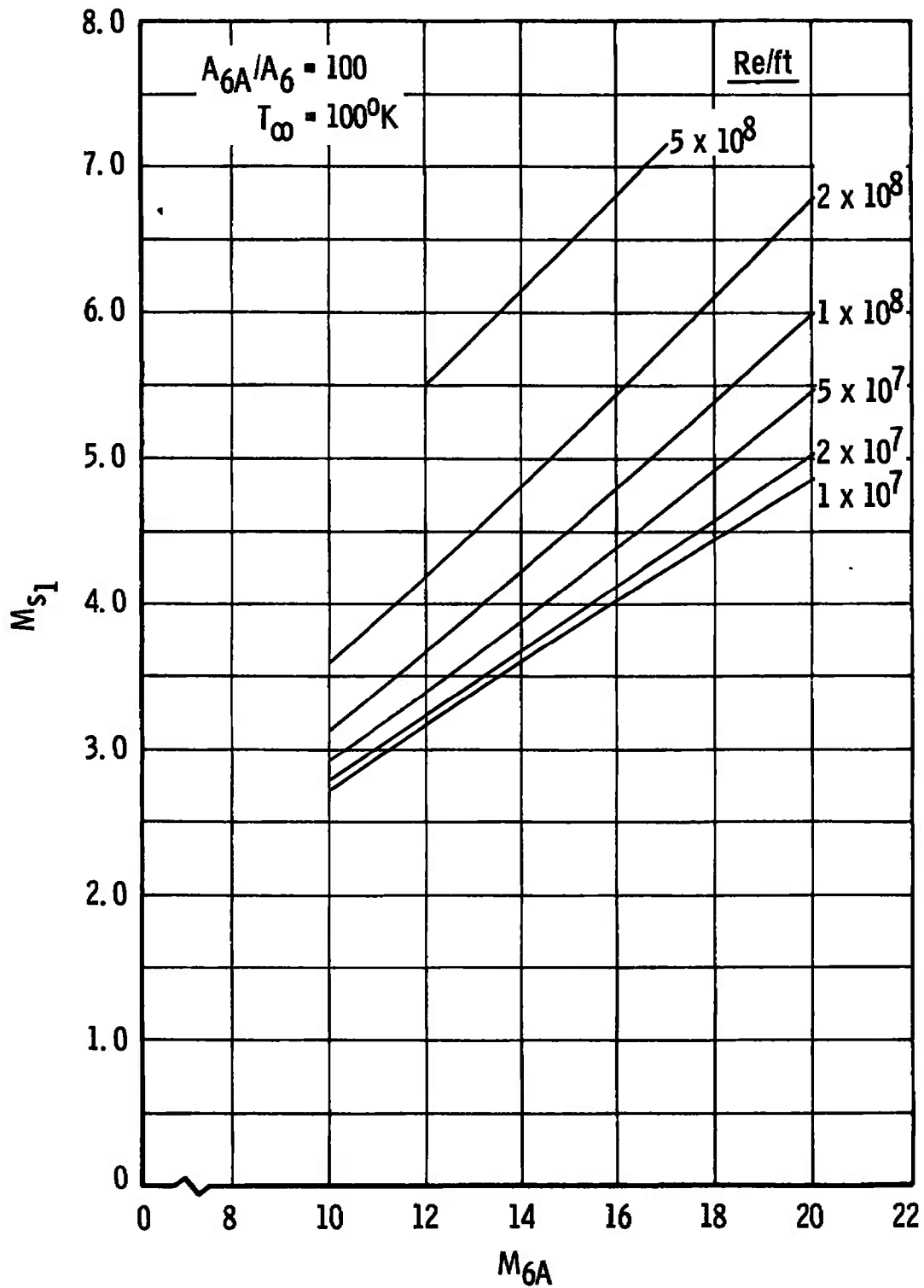
d. $A_{6A}/A_6 = 100$
Fig. II-7 Concluded
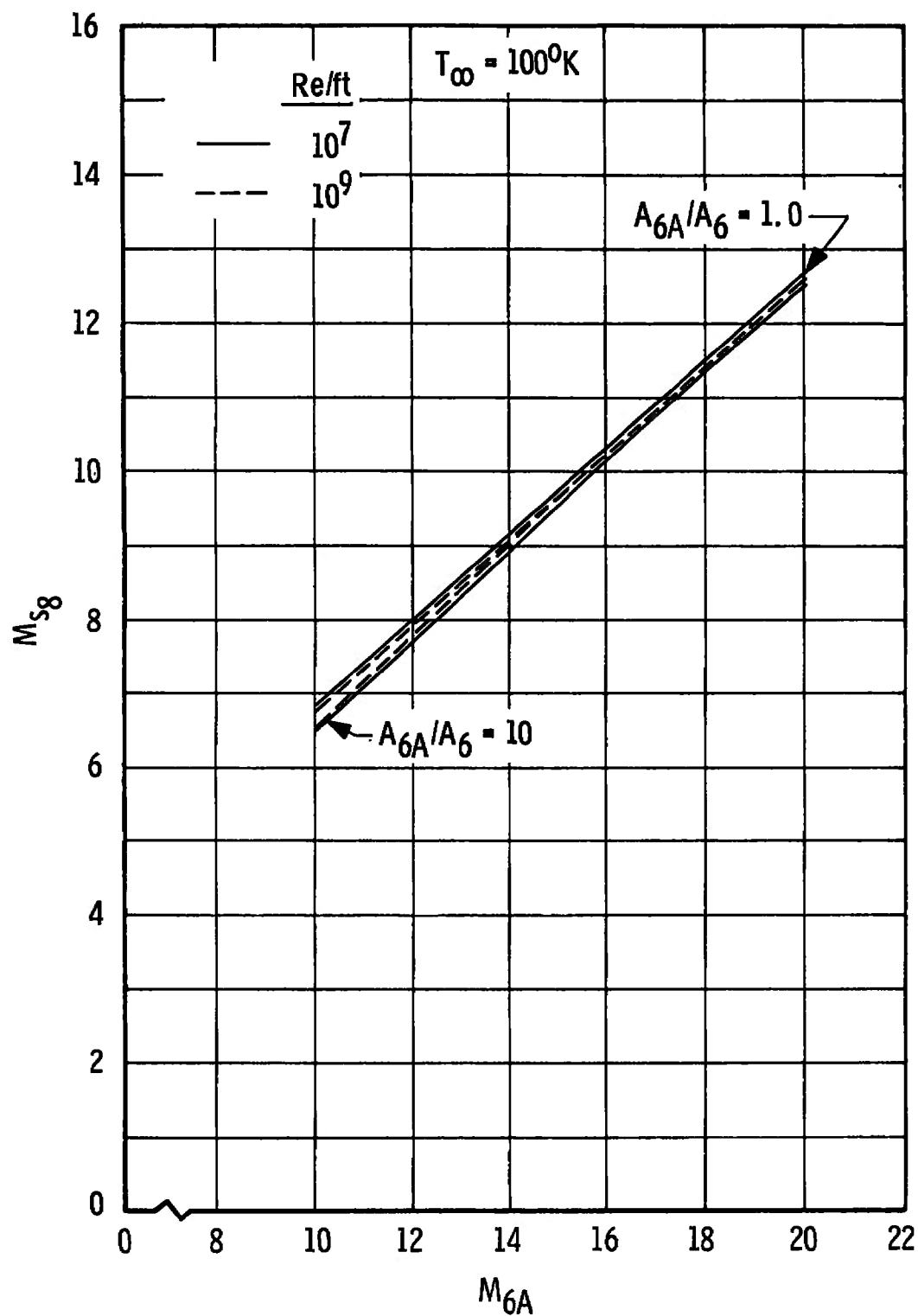
a. $A_{6A}/A_6 = 1$ and 10

Fig. II-8 Acceleration Tube Shock Strength, M_{s8}, versus M_{6A}
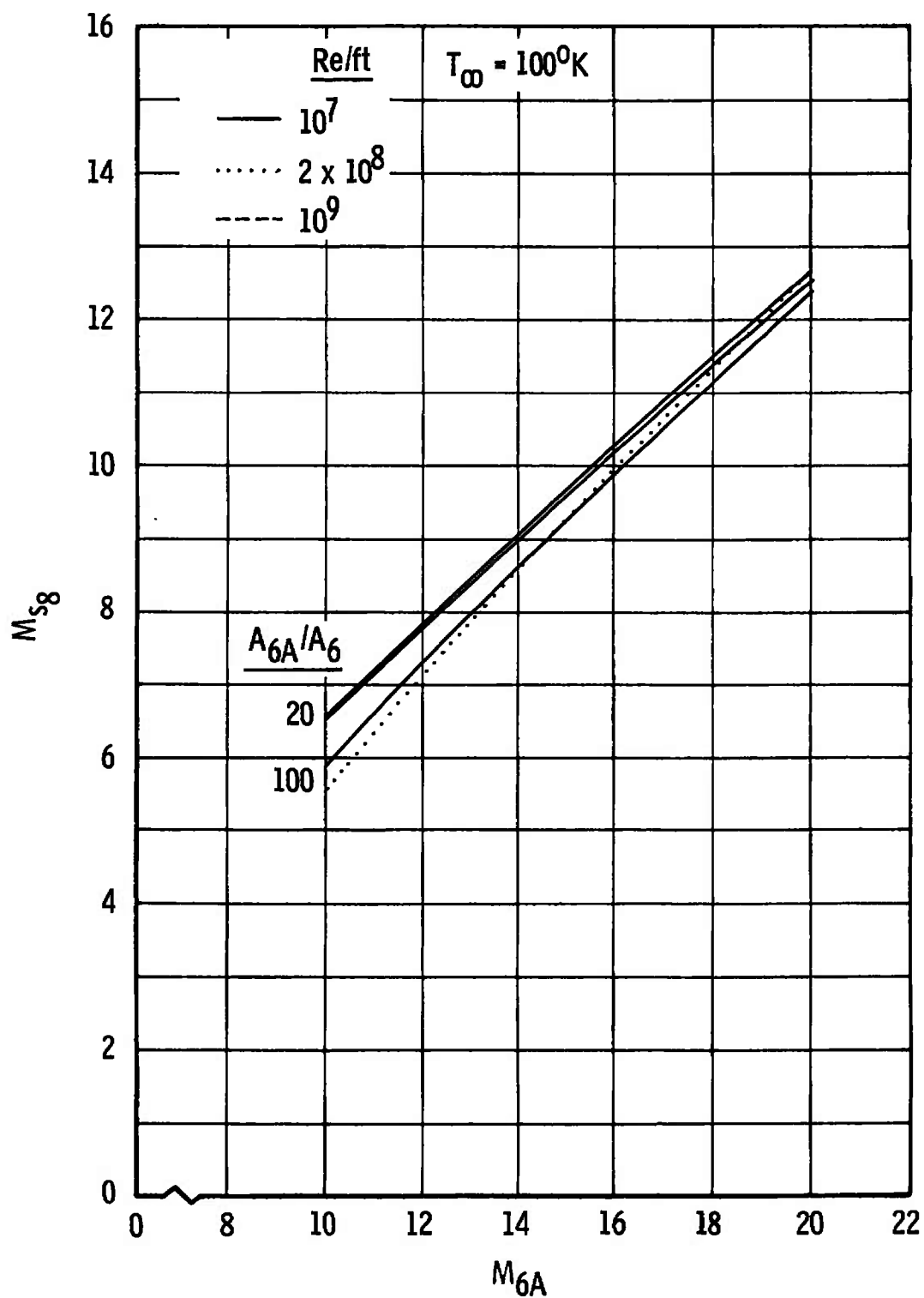
b. $A_{6A}/A_6 = 20$ and 100

Fig. II-8 Concluded

a. $A_{6A}/A_6 = 1$

Fig. II-9 Driven Tube Charge Pressure Ratio, P_1/P_{6A}, versus M_{6A}
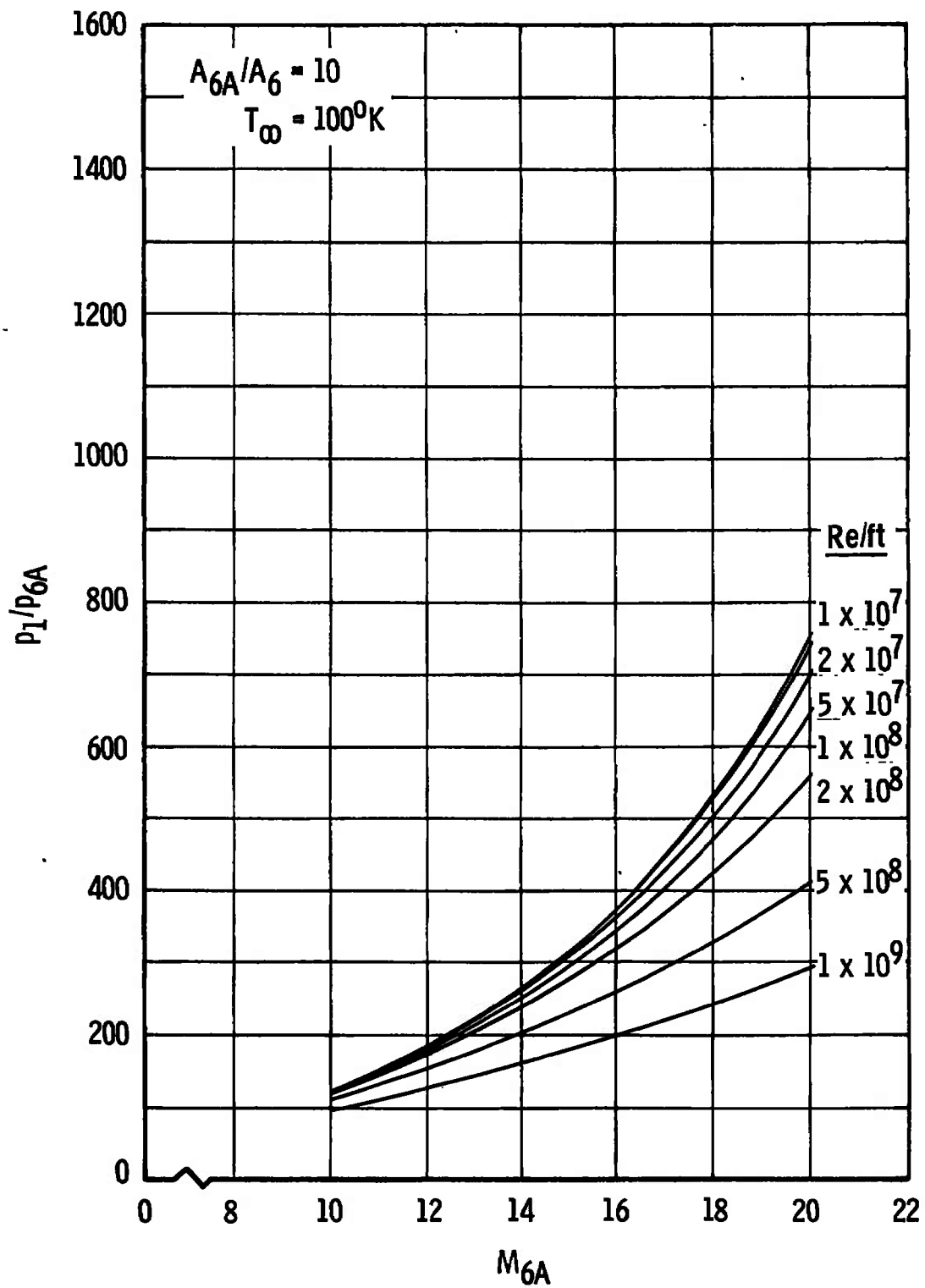
b. $A_{6A}/A_6 = 10$
Fig. II-9 Continued
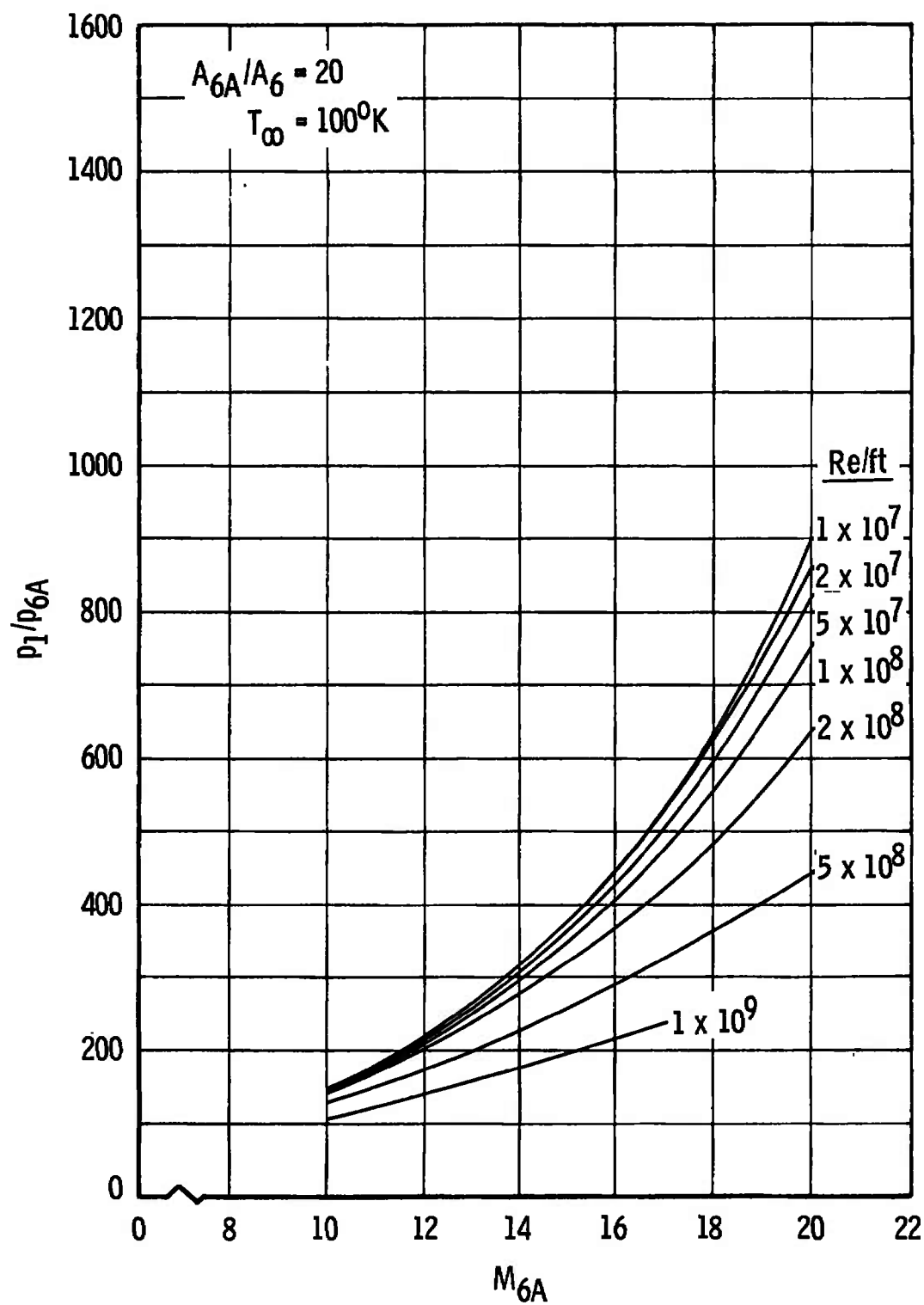
c. $A_{6A}/A_6 = 20$
Fig. II-9 Continued
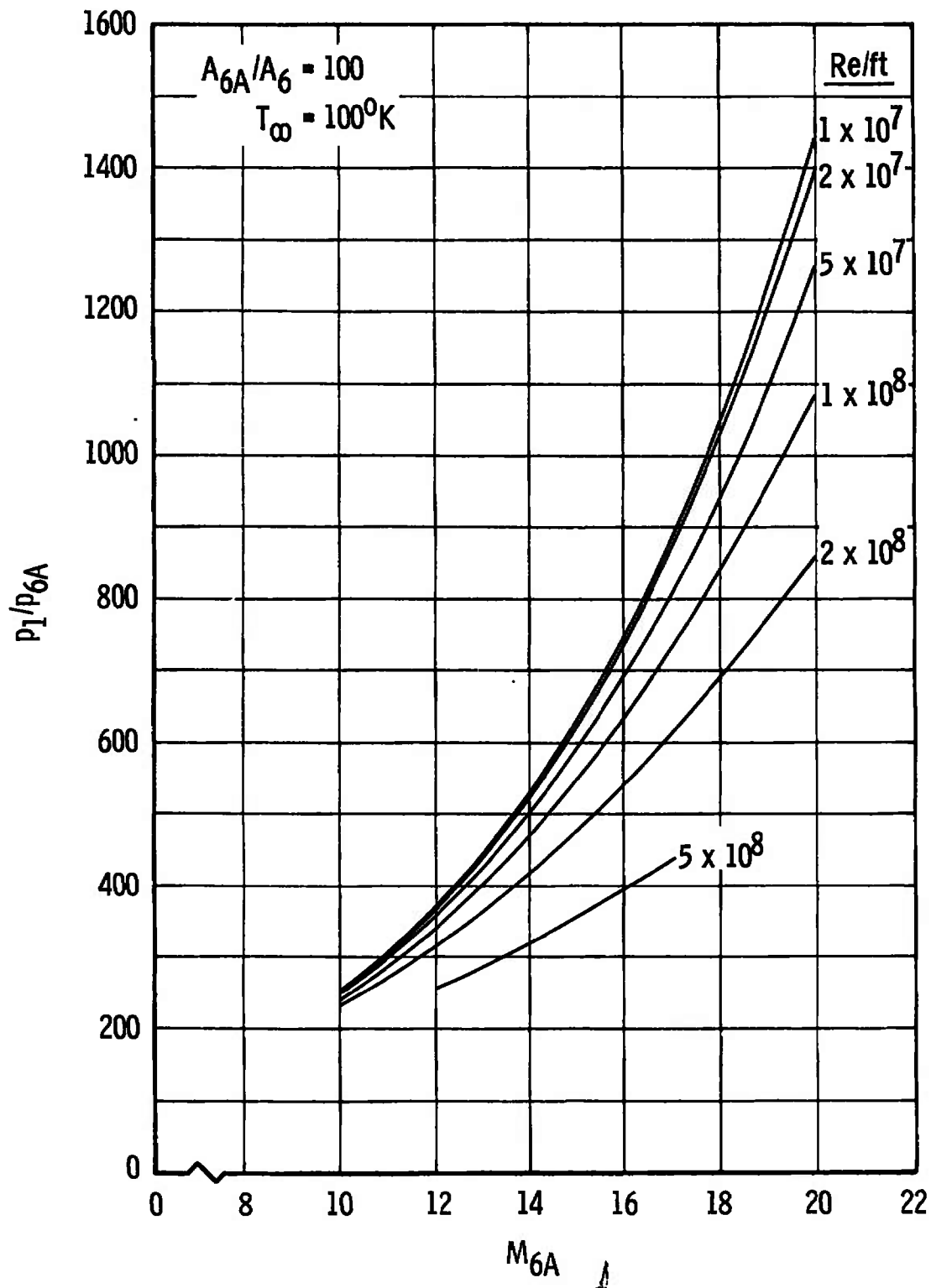
d. $A_{6A}/A_6 = 100$
Fig. II-9 Concluded
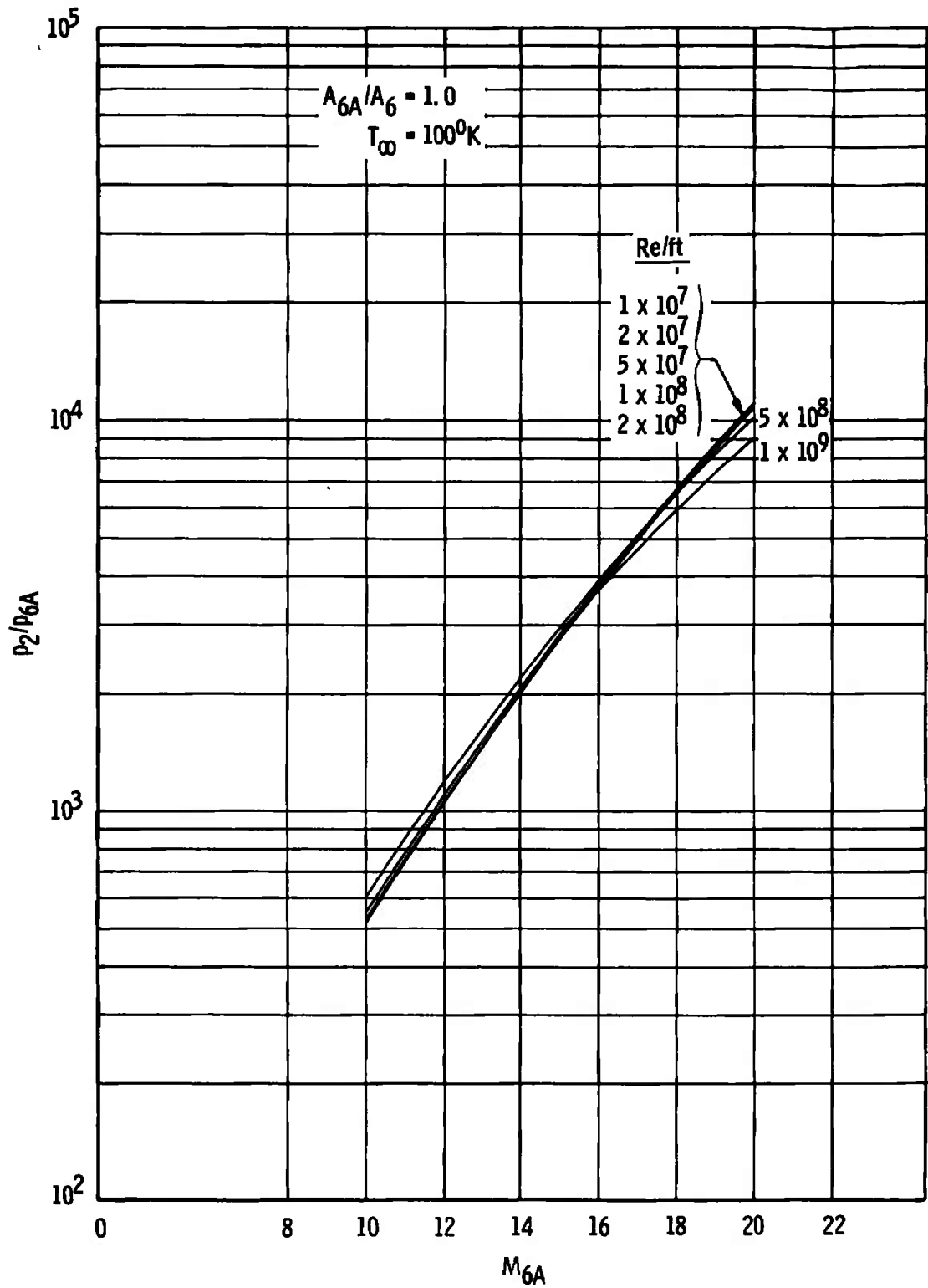
a. $A_{6A}/A_6 = 1$

Fig. II-10 Shocked Gas Pressure Ratio, P_2/P_{6A}, versus M_{6A}
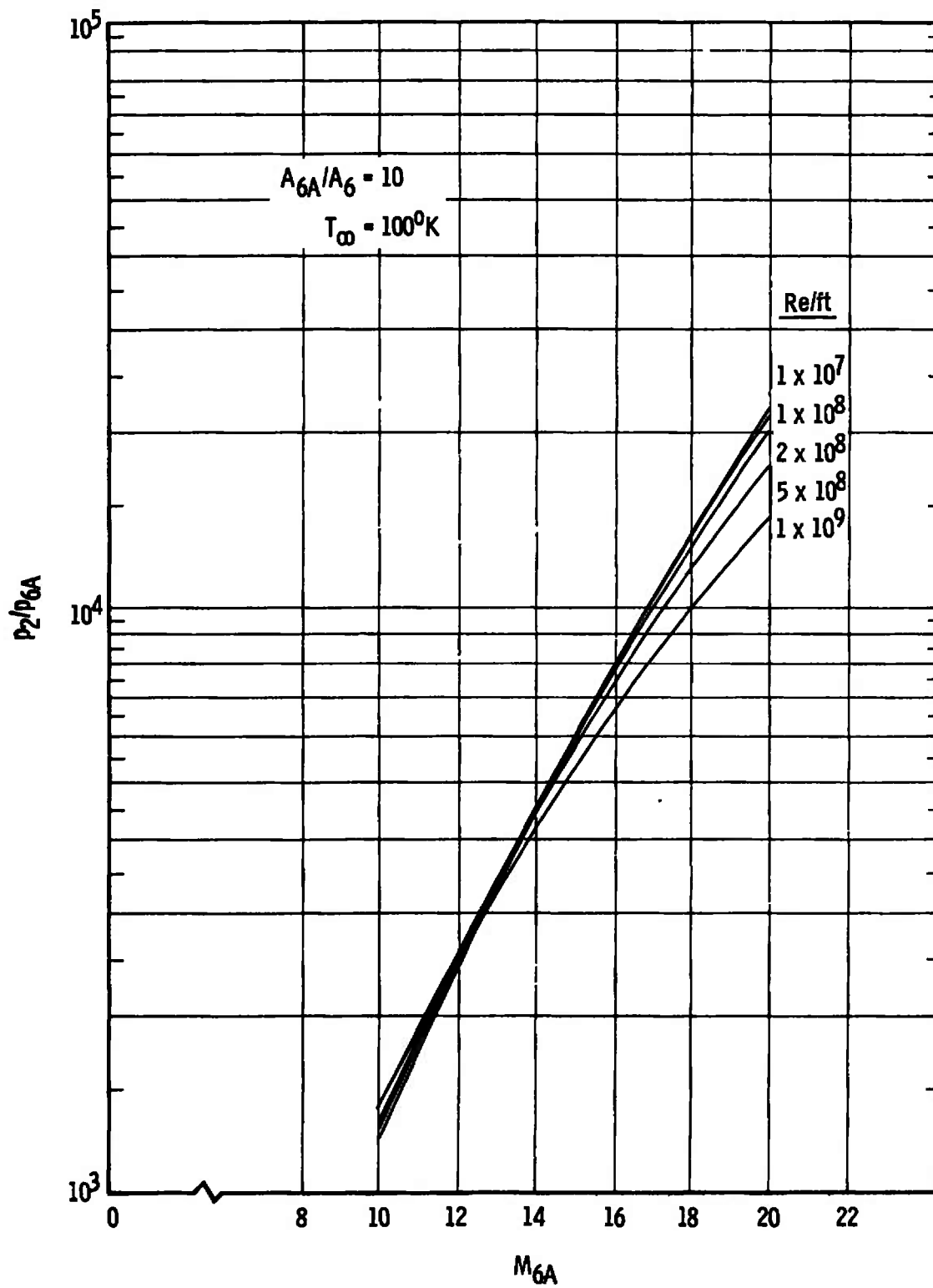
b. $A_{6A}/A_6 = 10$

Fig. II-10 Continued
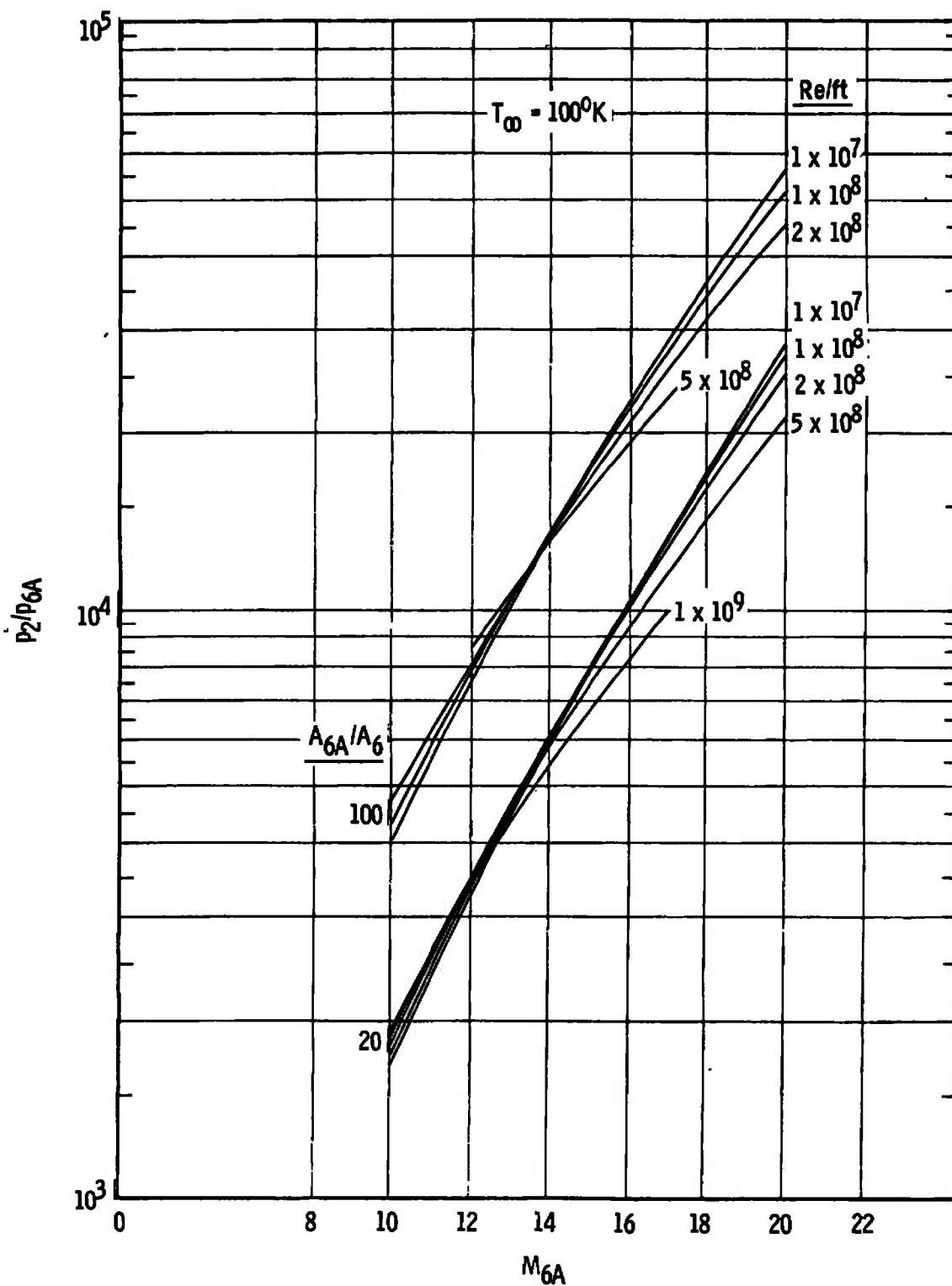
c. $A_{6A}/A_6 = 20$ and 100

Fig. II-10 Concluded
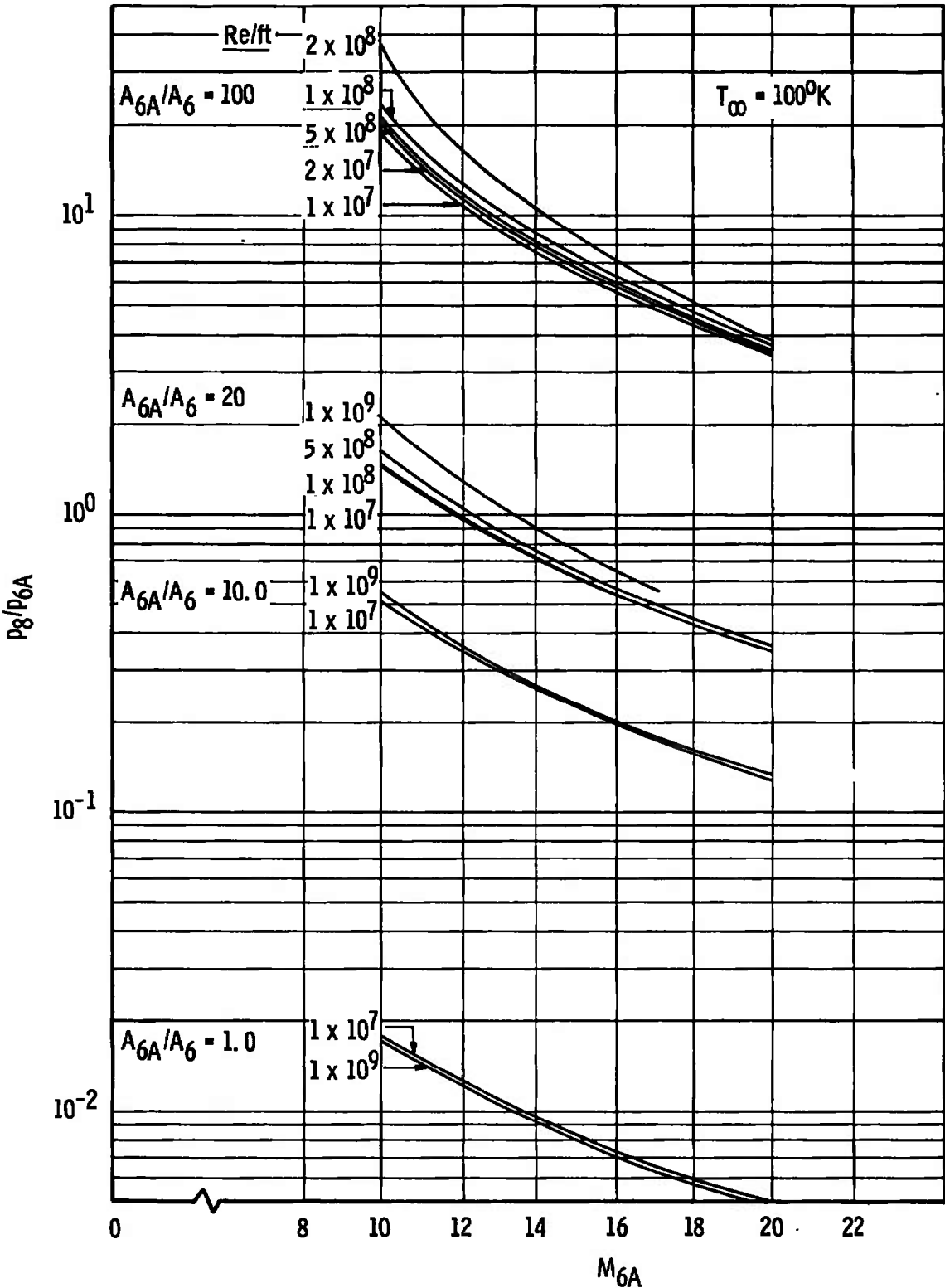
Fig. II-11 Acceleration Tube Charge Pressure Ratio, P_8/P_{6A}
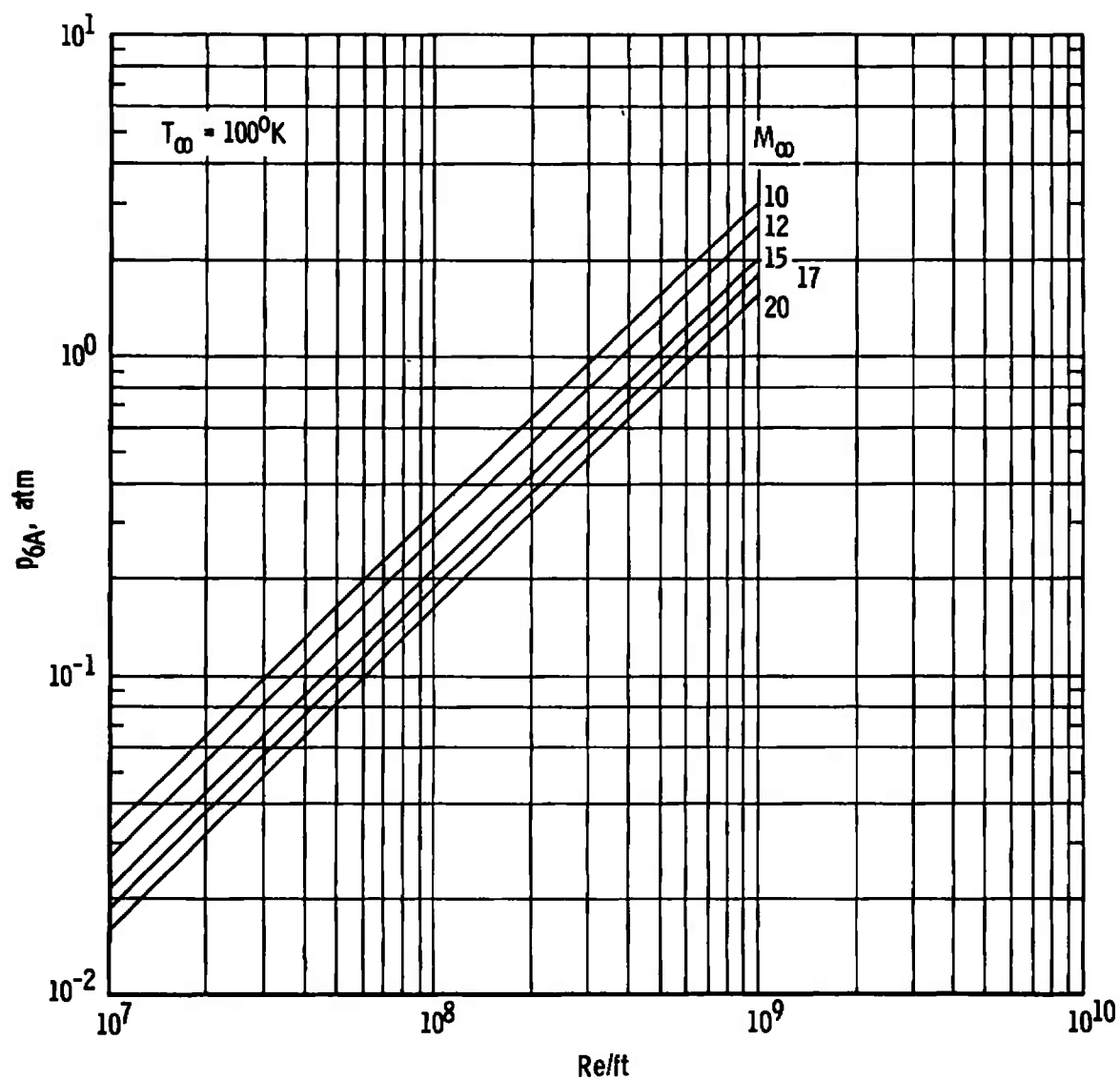
Fig. II-12 Free-Stream Pressure, $P_{6A,}$ versus Reynolds Number

APPENDIX III
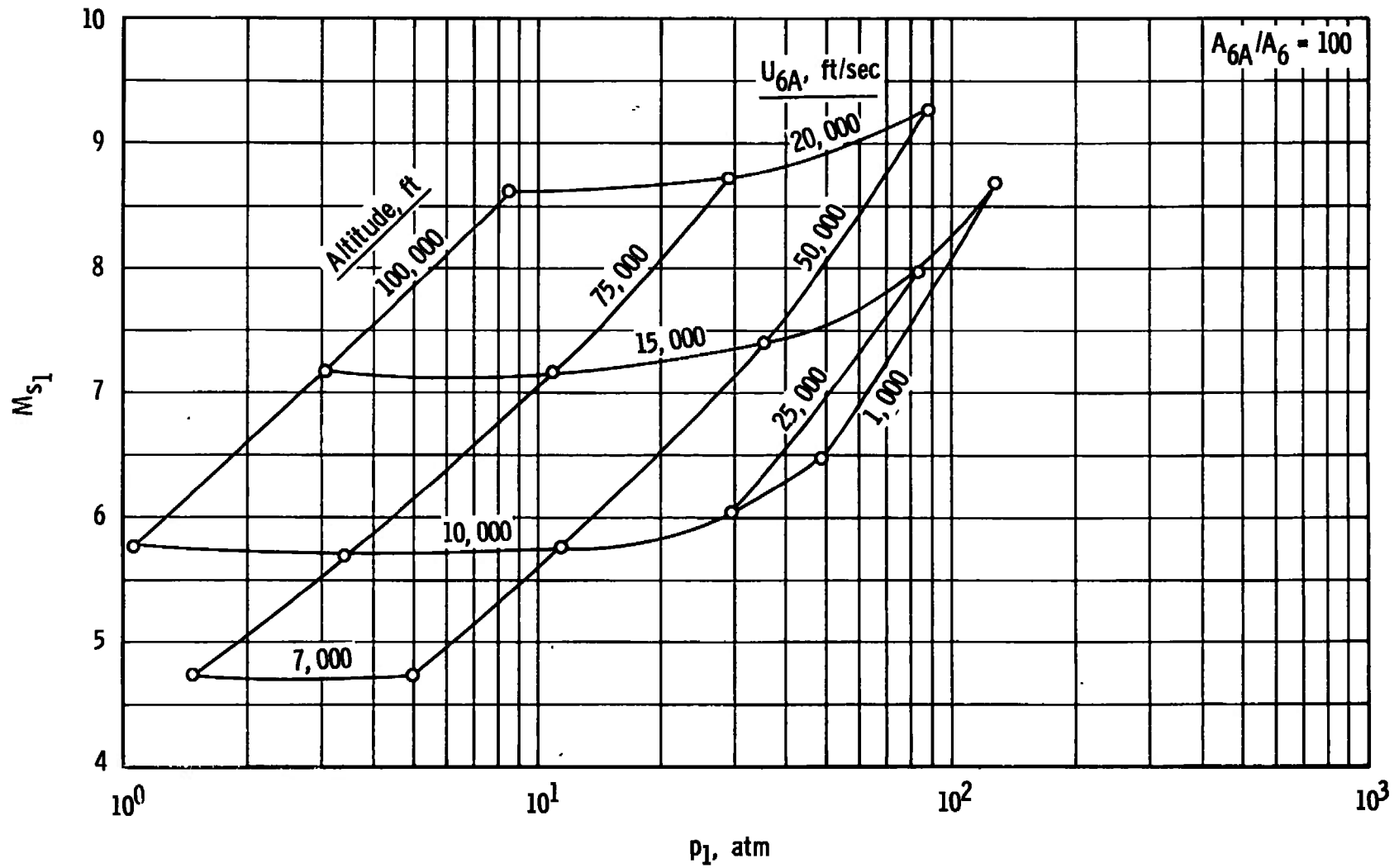## WORKING GRAPHS FOR FLOW DUPLICATION

a. $A_{6A}/A_6 = 1$

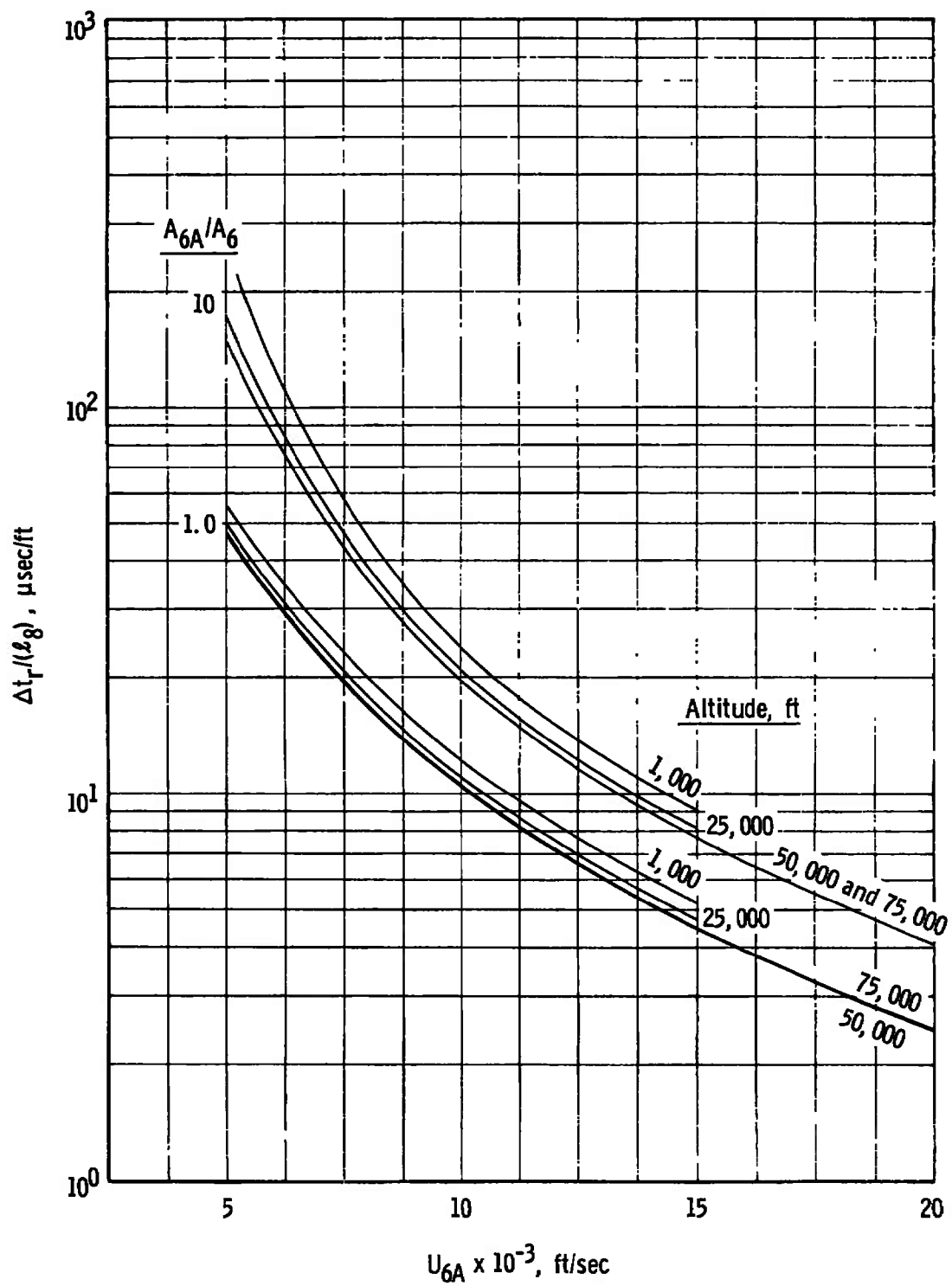Fig. III-1 Altitude and Velocity as a Function of M_{s_1} and P_1

b. A_{6A}/A_6 10
Fig. III-1 Continued
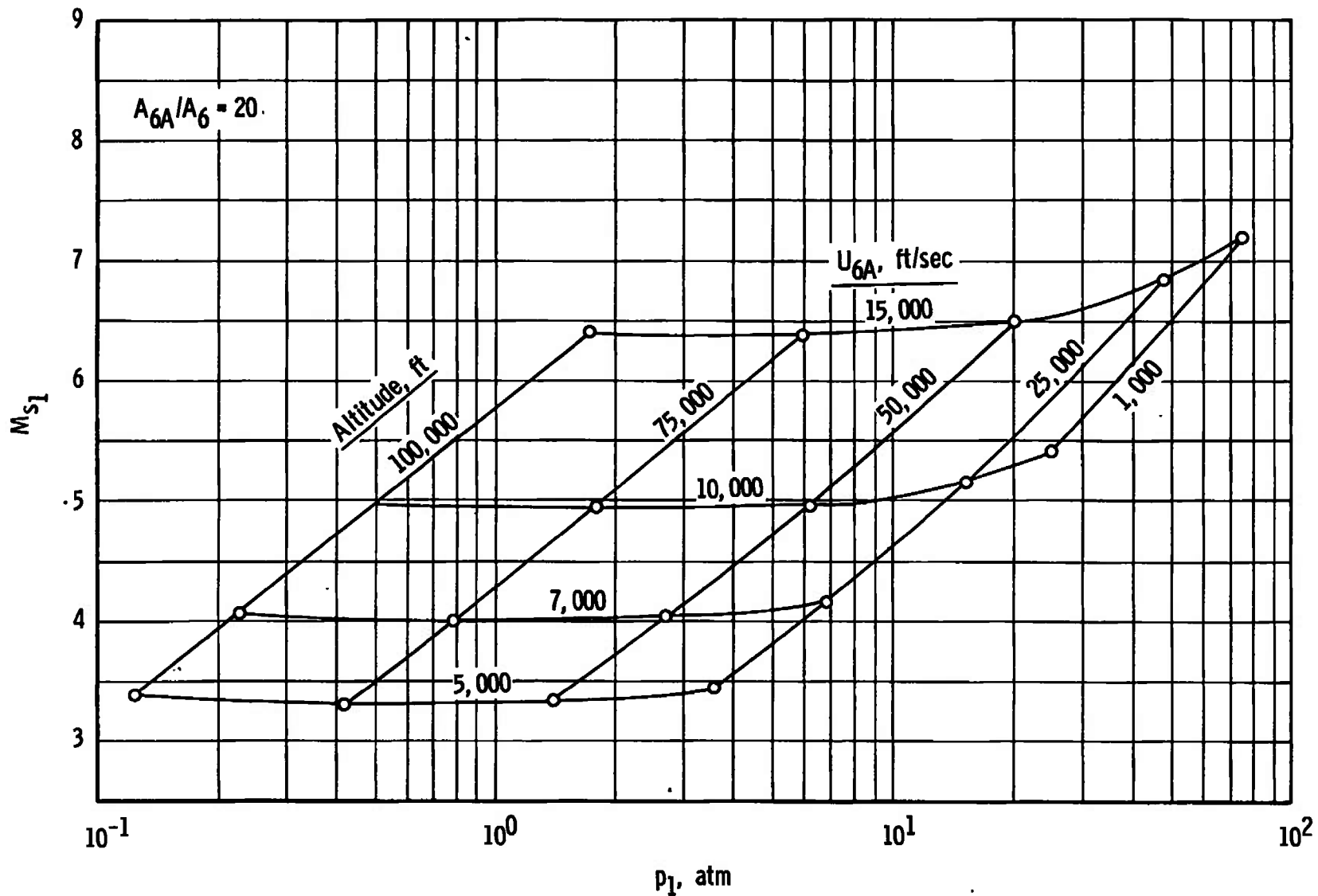
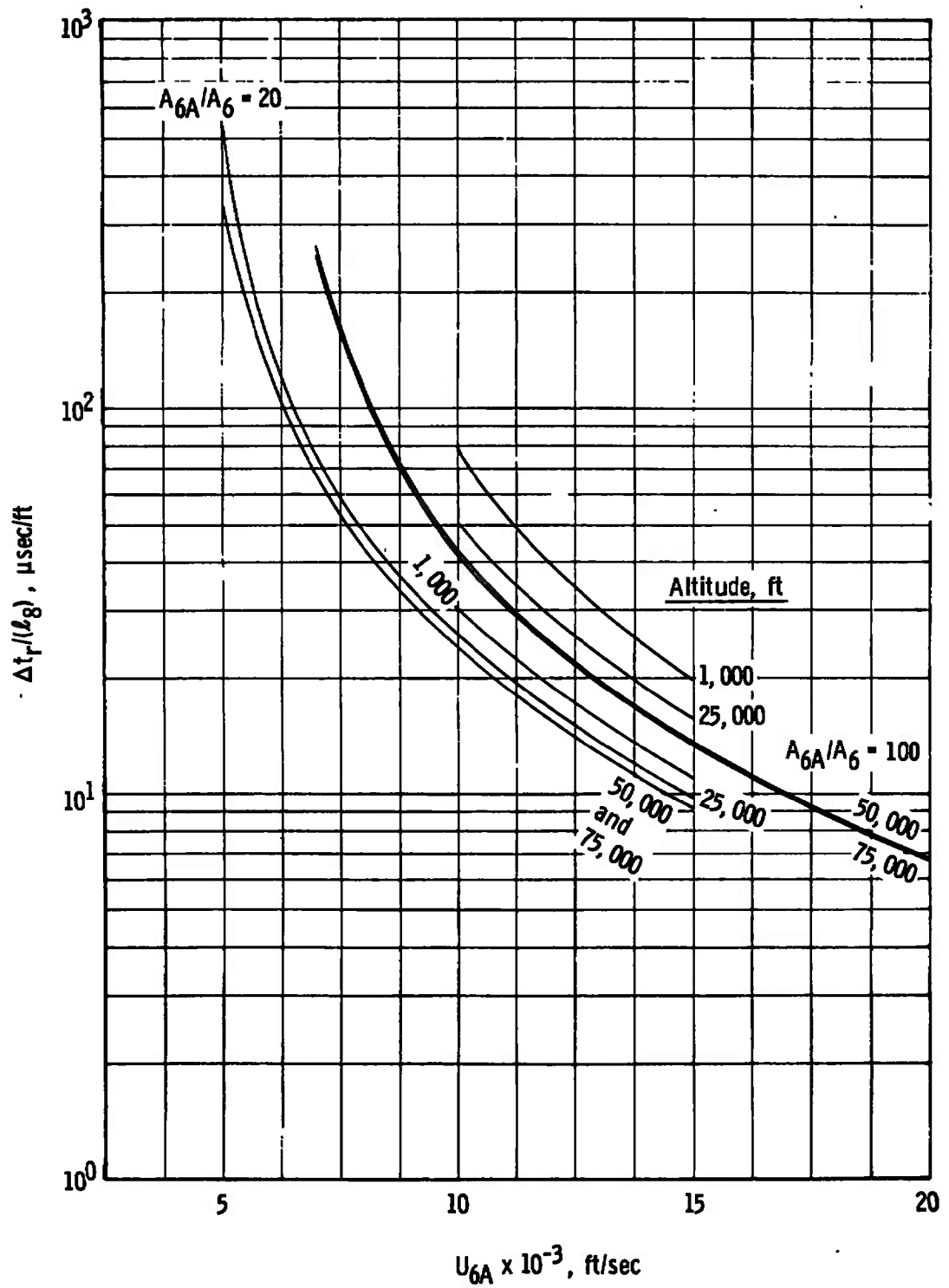c. $A_{6A}/A_6 = 20$

Fig. III-1 Continued
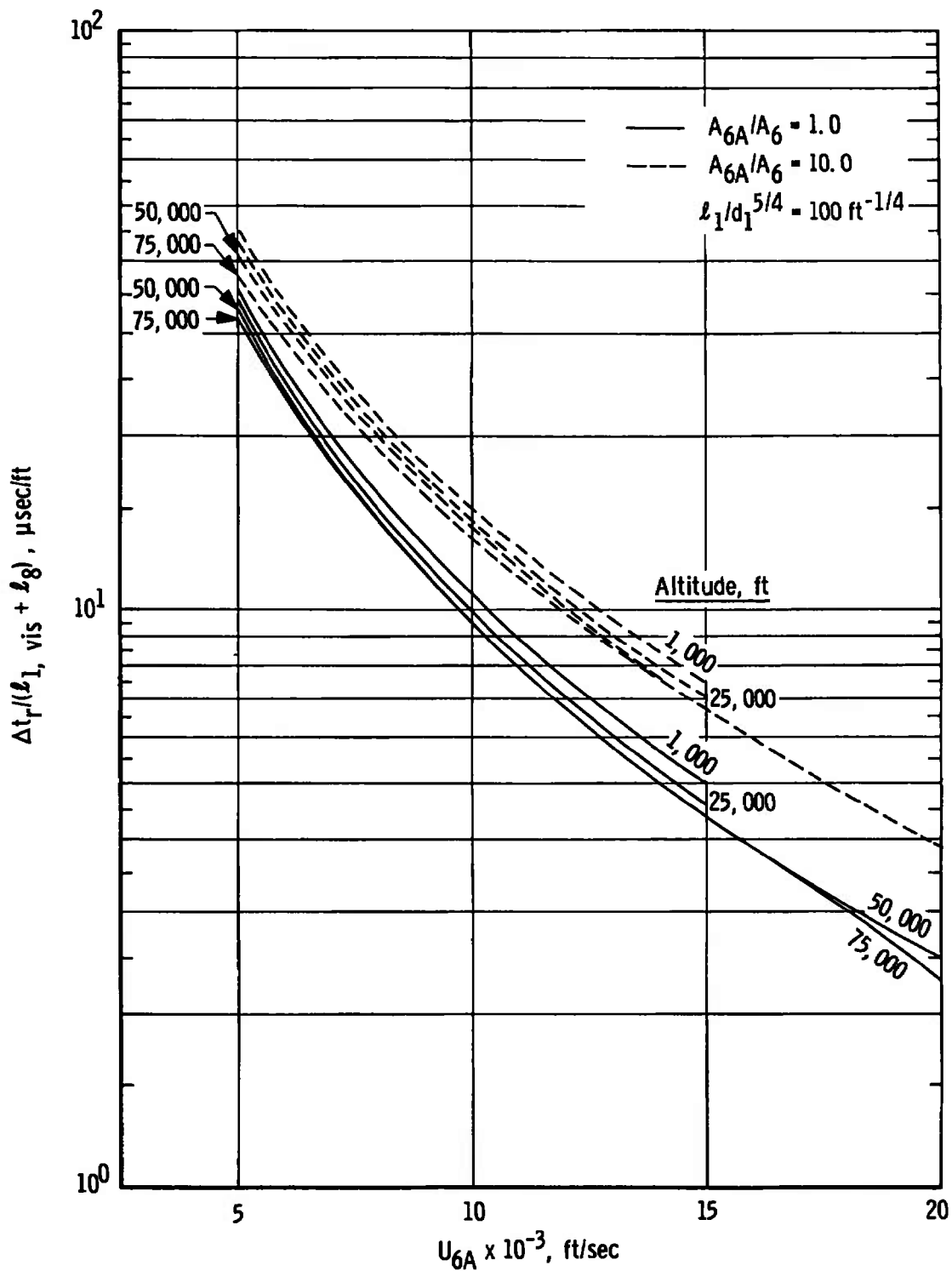
d. $A_{6A}/A_6 = 100$

Fig. III-1 Concluded

a. $A_{6A}/A_6 = 1$ and 10

Fig. III-2 Run Time per Unit Length of Acceleration
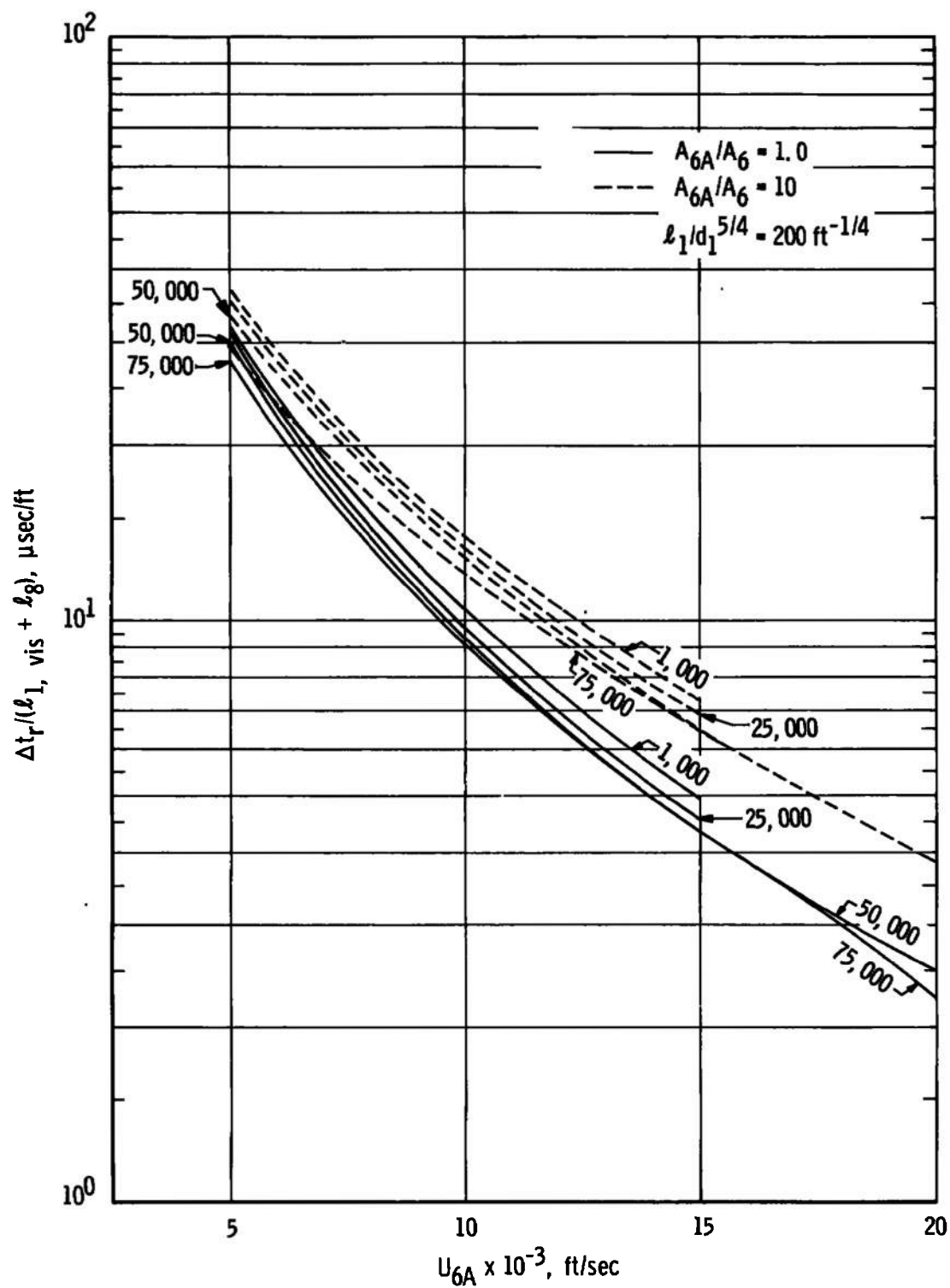Tube, $\Delta t_r / \ell_8$, versus U_{6A}

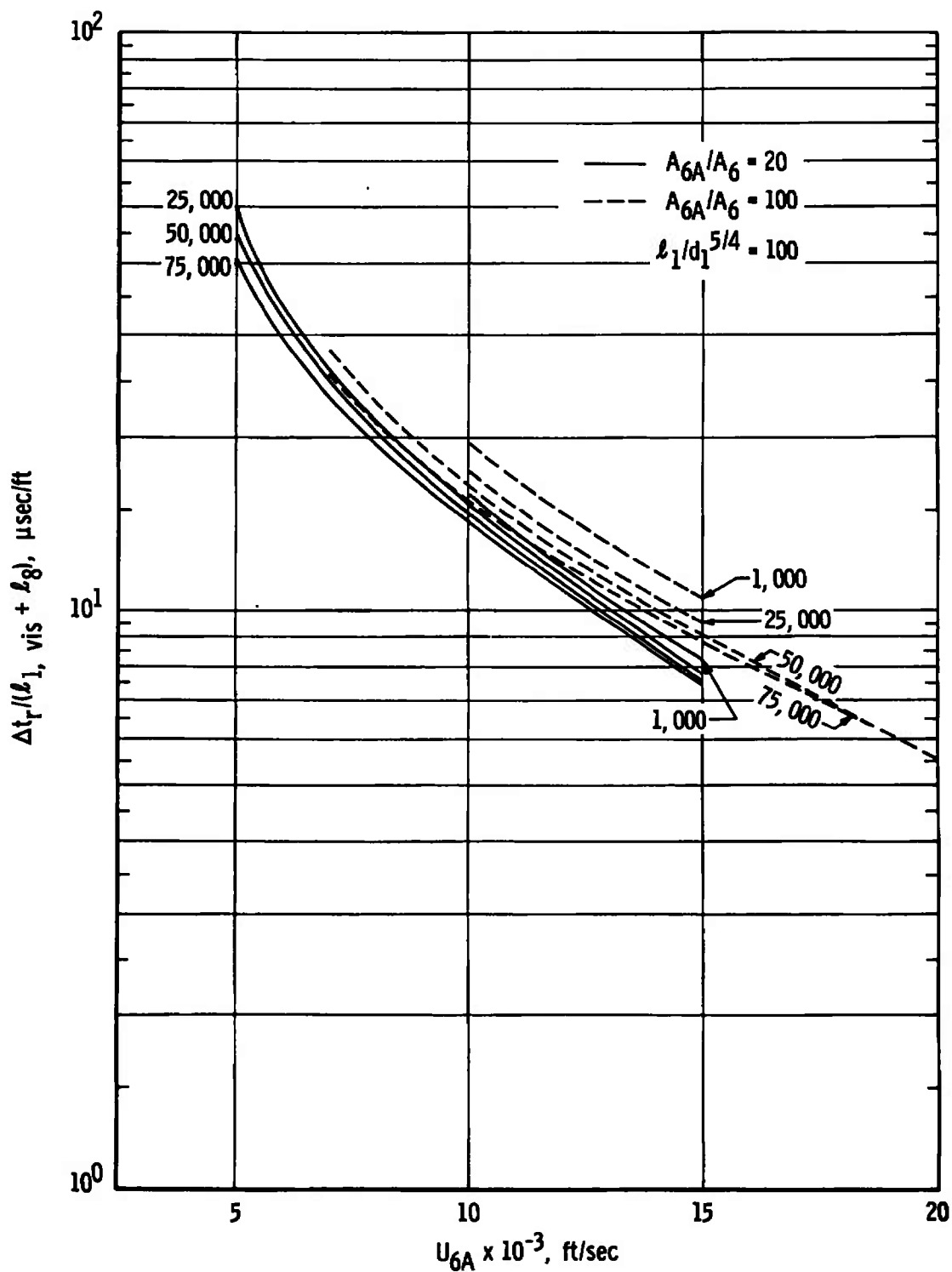b. A_{6A}/A_6 = 20 and 100
Fig. III-2 Concluded

a. $A_{6A}/A_6 = 1$ and 10, $\ell_1/d_1^{5/4} = 100$ ft$^{-1/4}$

Fig. III-3 Run Time per Unit Length of Driven and Acceleration Tubes, $\dfrac{\Delta_{tr}}{(\ell_{1,vis} + \ell_8)}$, versus U_{6A}
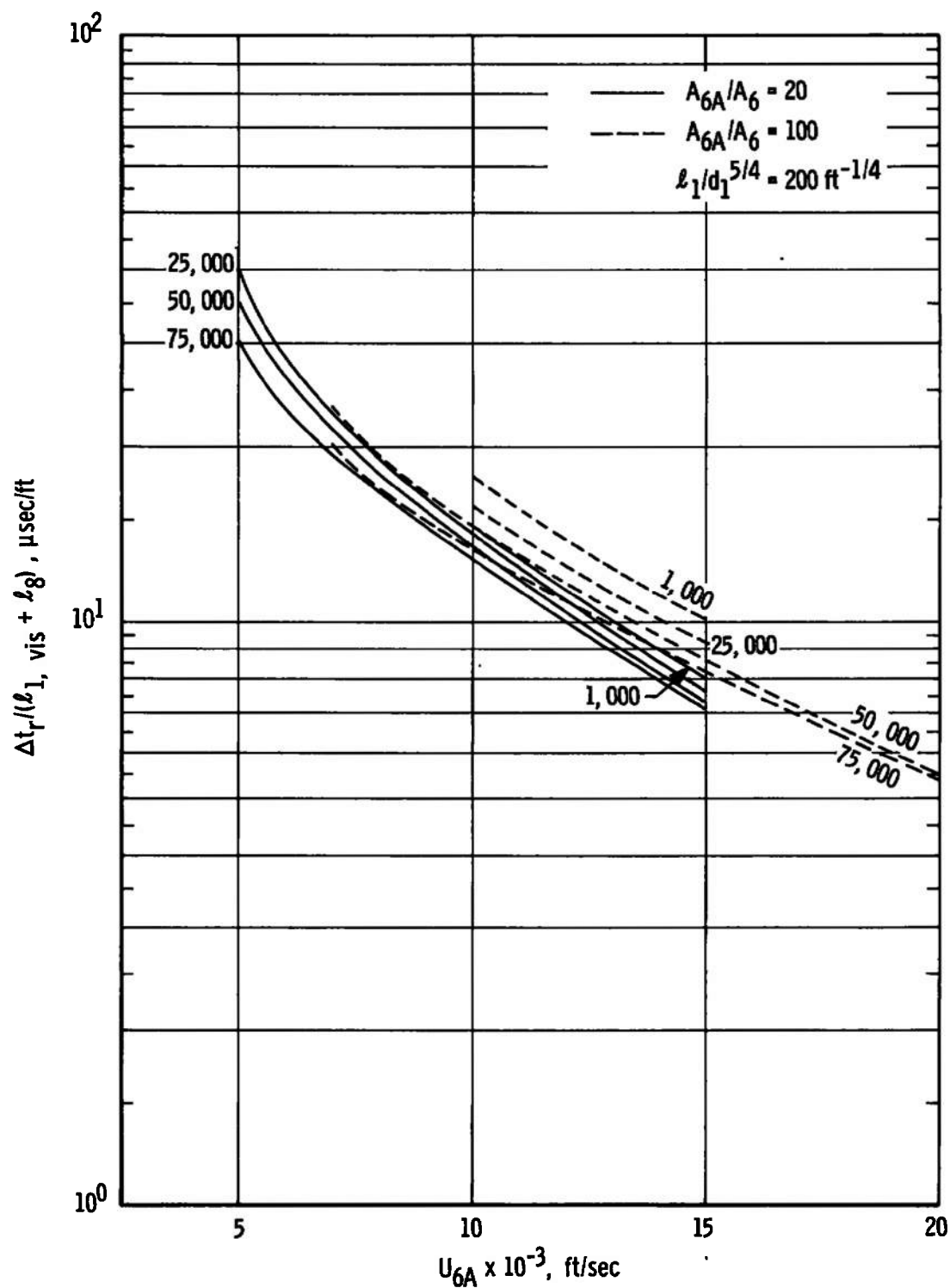
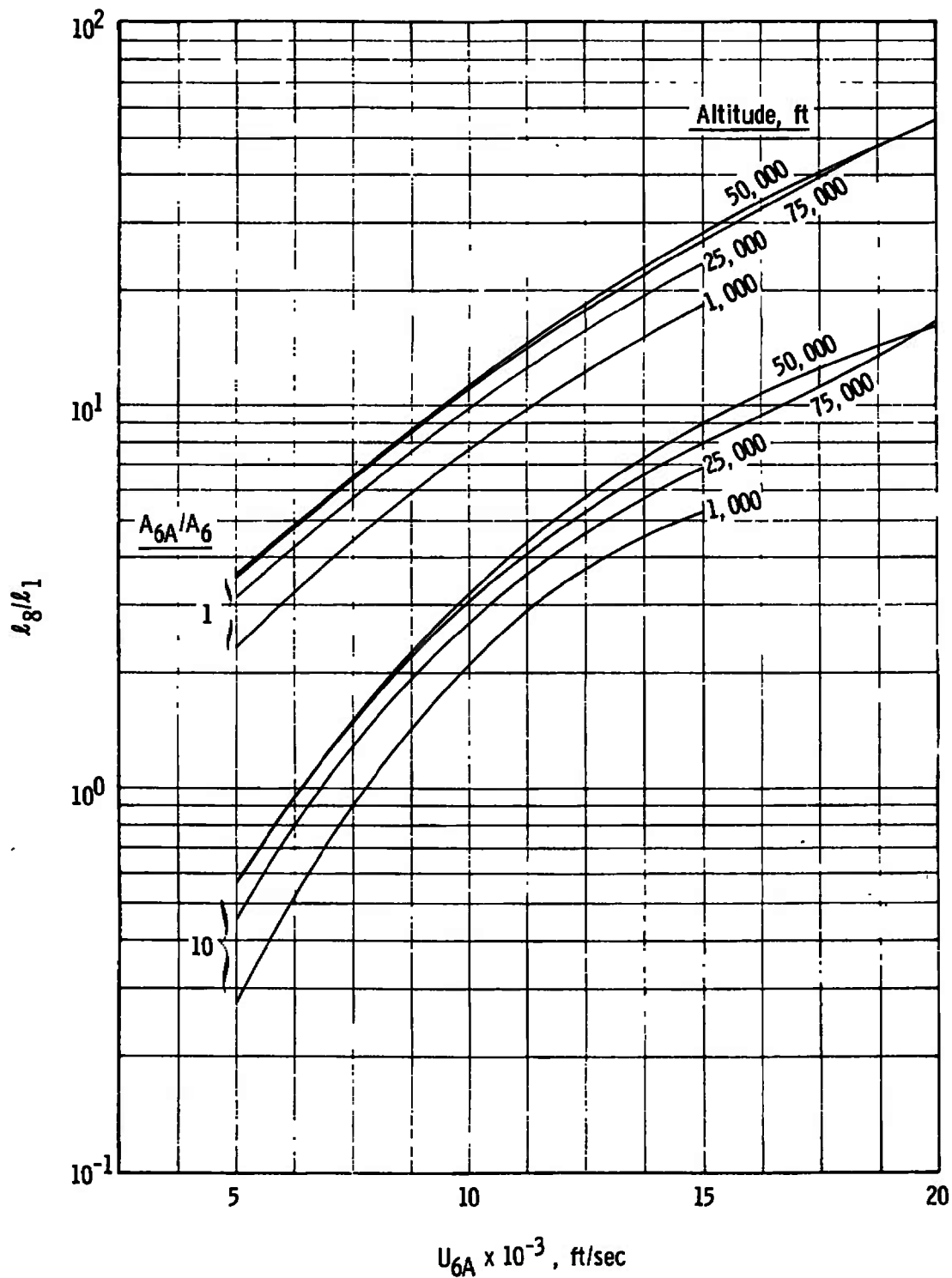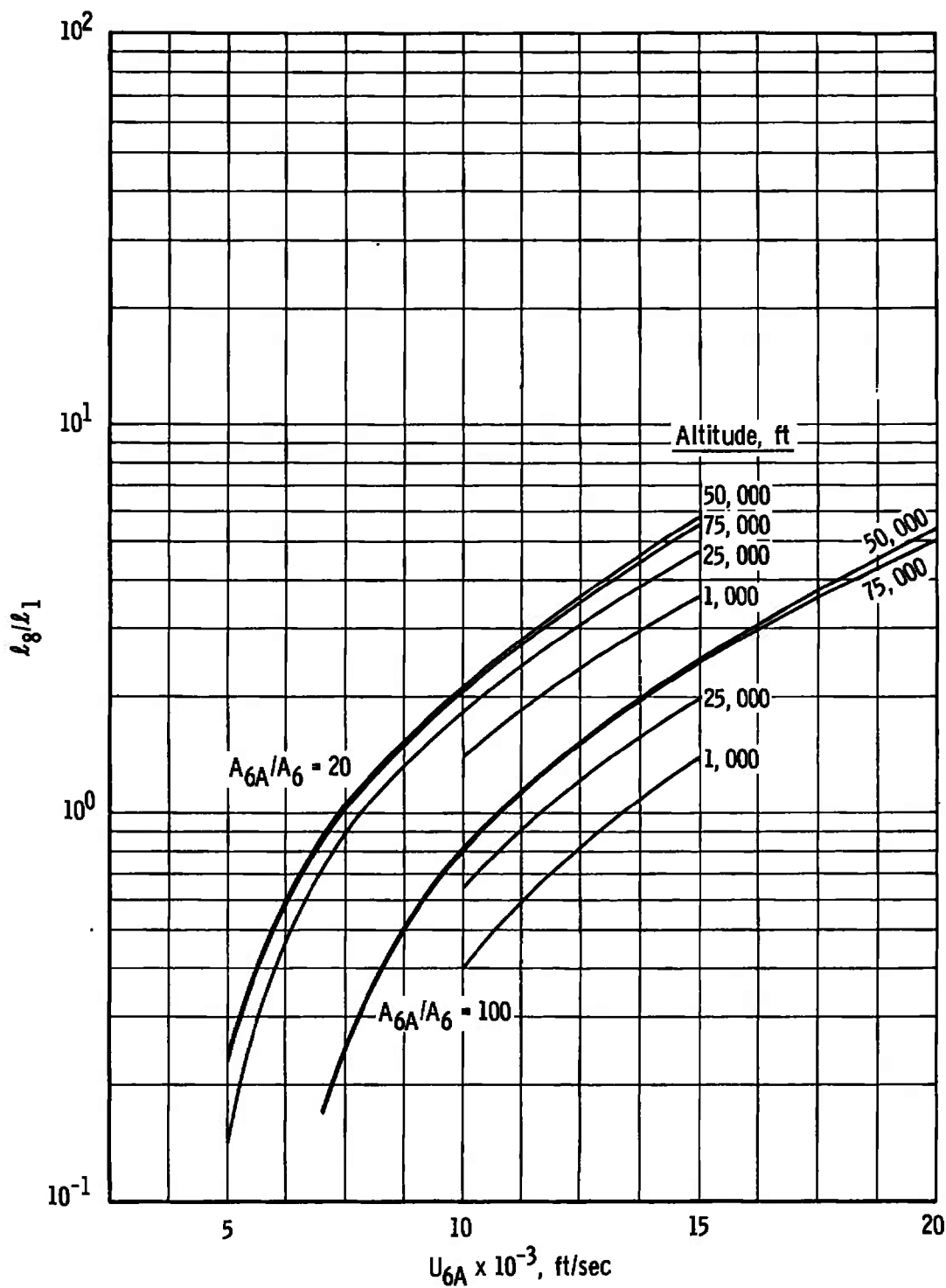b. $A_{6A}/A_6 = 1$ and 10, $\ell_1/d_1^{5/4} = 200 \text{ ft}^{-1/4}$
Fig. III-3 Continued

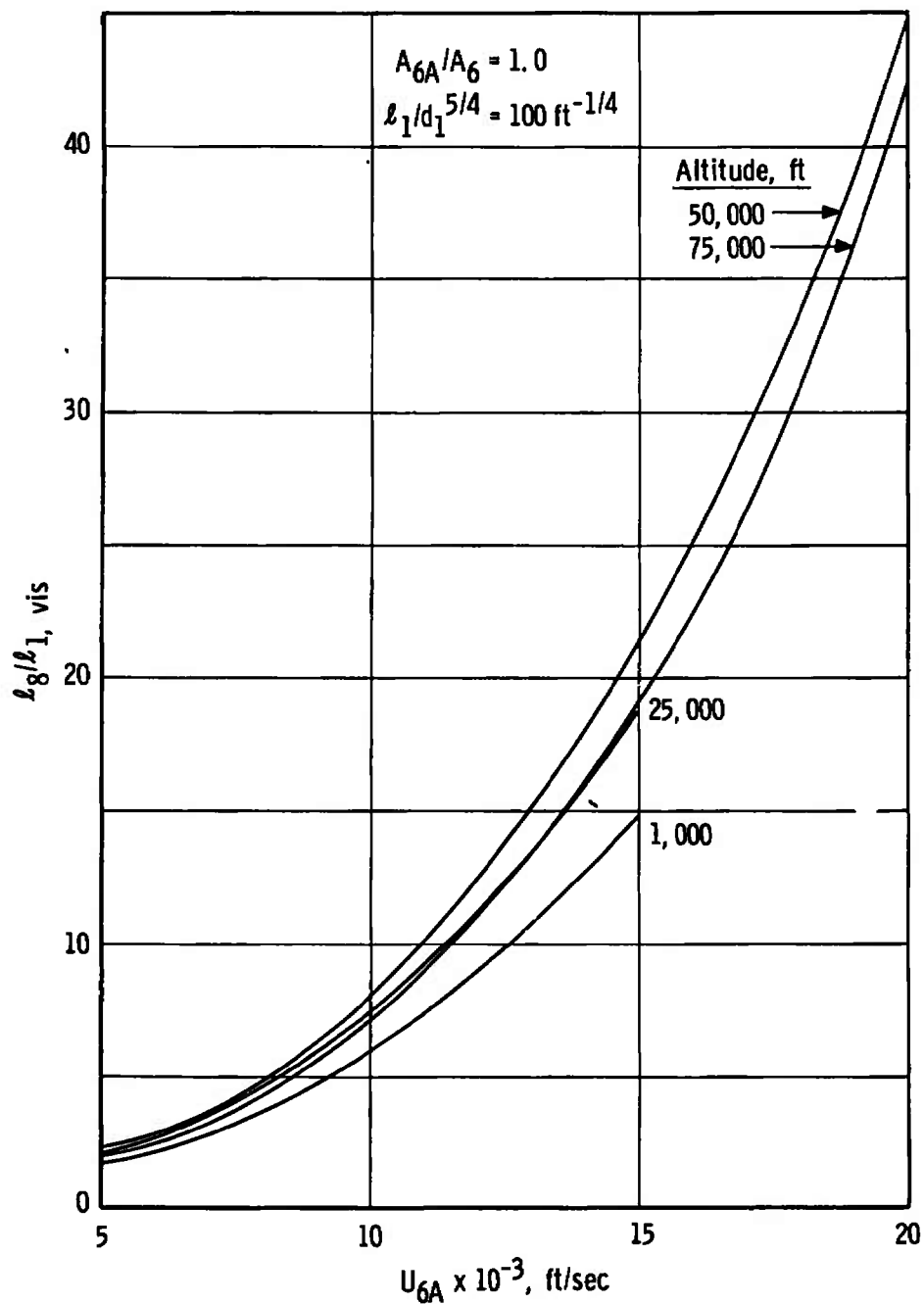c. $A_{6A}/A_6 = 20$ and 100, $\ell_1/d_1^{5/4} = 100$ ft$^{-1/4}$

Fig. III-3 Continued

d. $A_{6A}/A_6 = 20$ and 100, $\ell_1/d_1^{5/4} = 200$ ft$^{-1/4}$
Fig. III-3 Concluded

a. $A_{6A}/A_6 = 1$ and 10
Fig. III-4 Acceleration-to-Driven Tube Length Ratio
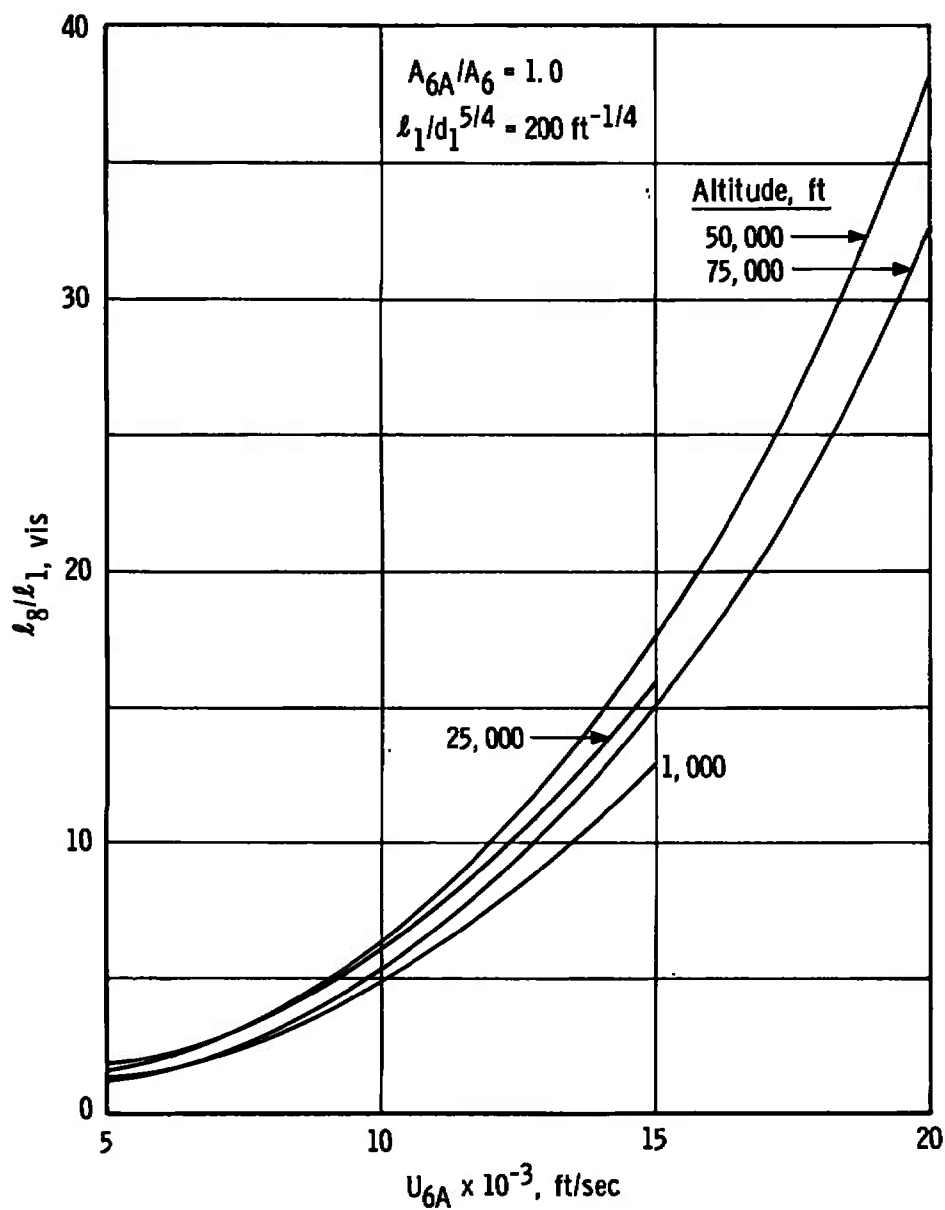(Inviscid), ℓ_8/ℓ_1, versus U_{6A}
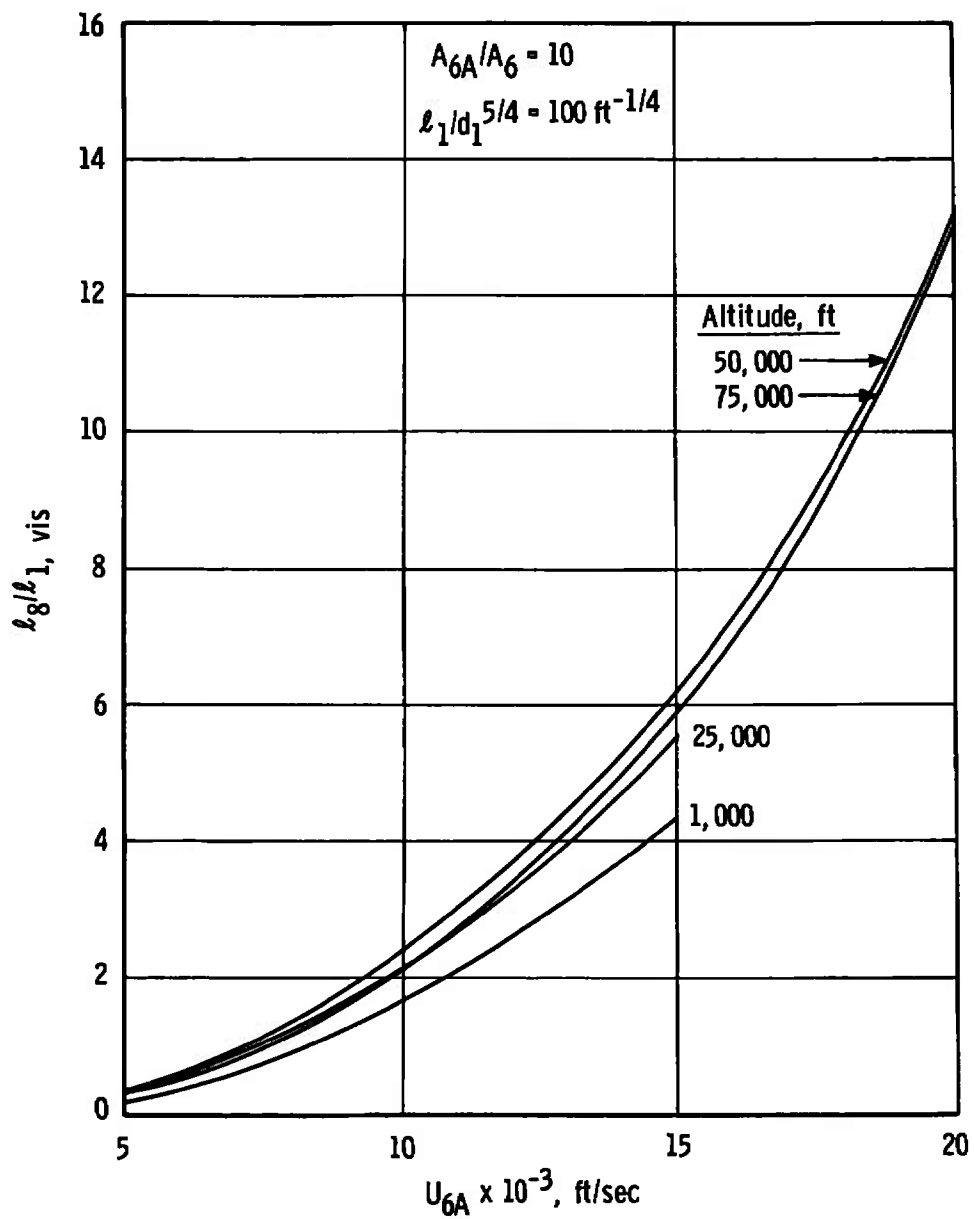
b. $A_{6A}/A_6 = 20$ and 100
Fig. III-4 Concluded

a. $A_{6A}/A_6 = 1$, $\ell_1/d_1^{5/4} = 100 \text{ ft}^{-1/4}$

Fig. III-5 Acceleration-to-Driven Tube Length Ratio
(Viscid), $\ell_8/\ell_{1,vis}$, versus U_{6A}

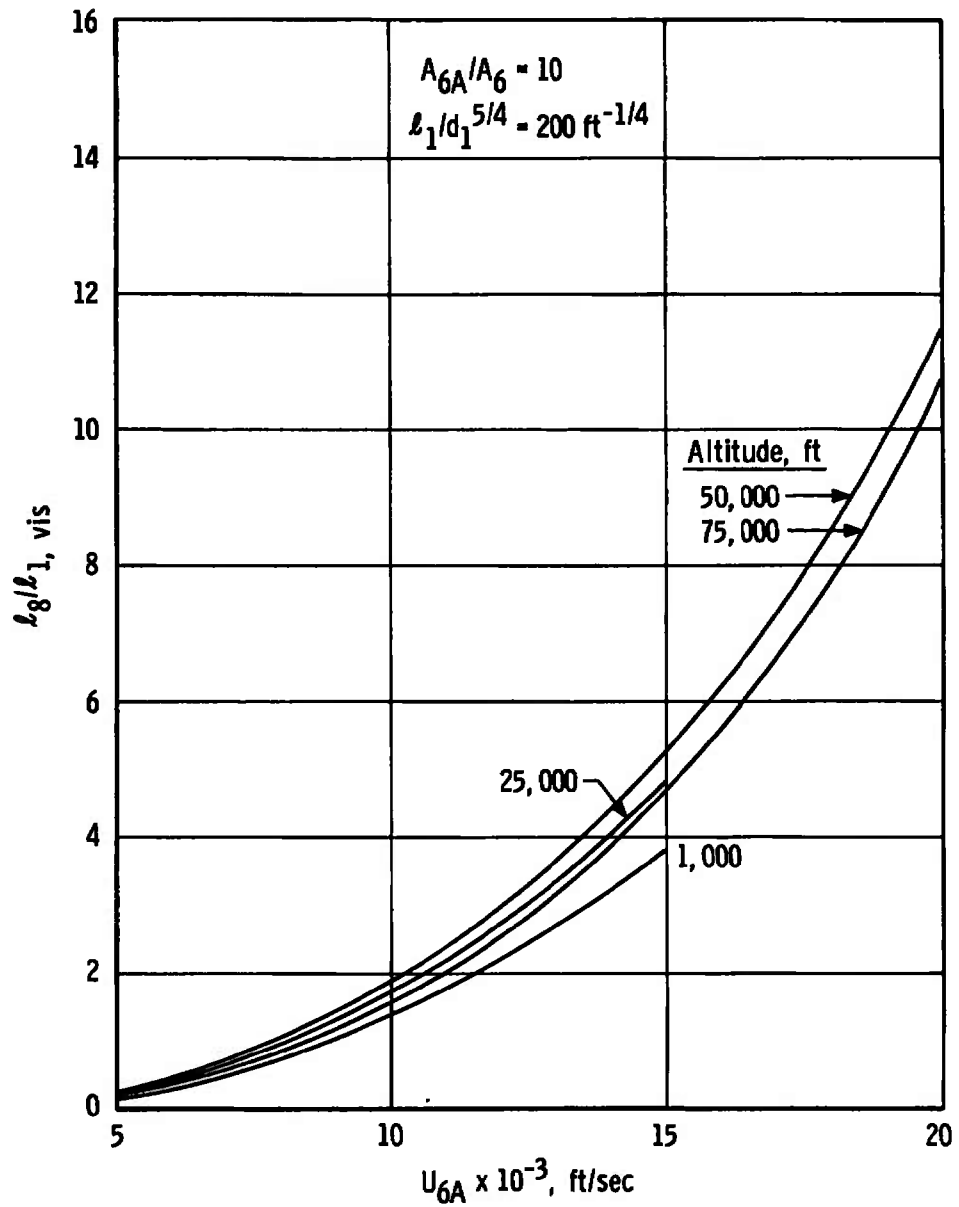b. $A_{6A}/A_6 = 1$, $\ell_1/d_1^{5/4} = 200$ ft$^{-1/4}$
Fig. III-5 Continued

c. $A_{6A}/A_6 = 10$, $\ell_1/d_1^{5/4} = 100 \text{ ft}^{-1/4}$

Fig. III-5 Continued

d. $A_{6A}/A_6 = 10$, $\ell_1/d_1^{5/4} = 200 \text{ ft}^{-1/4}$
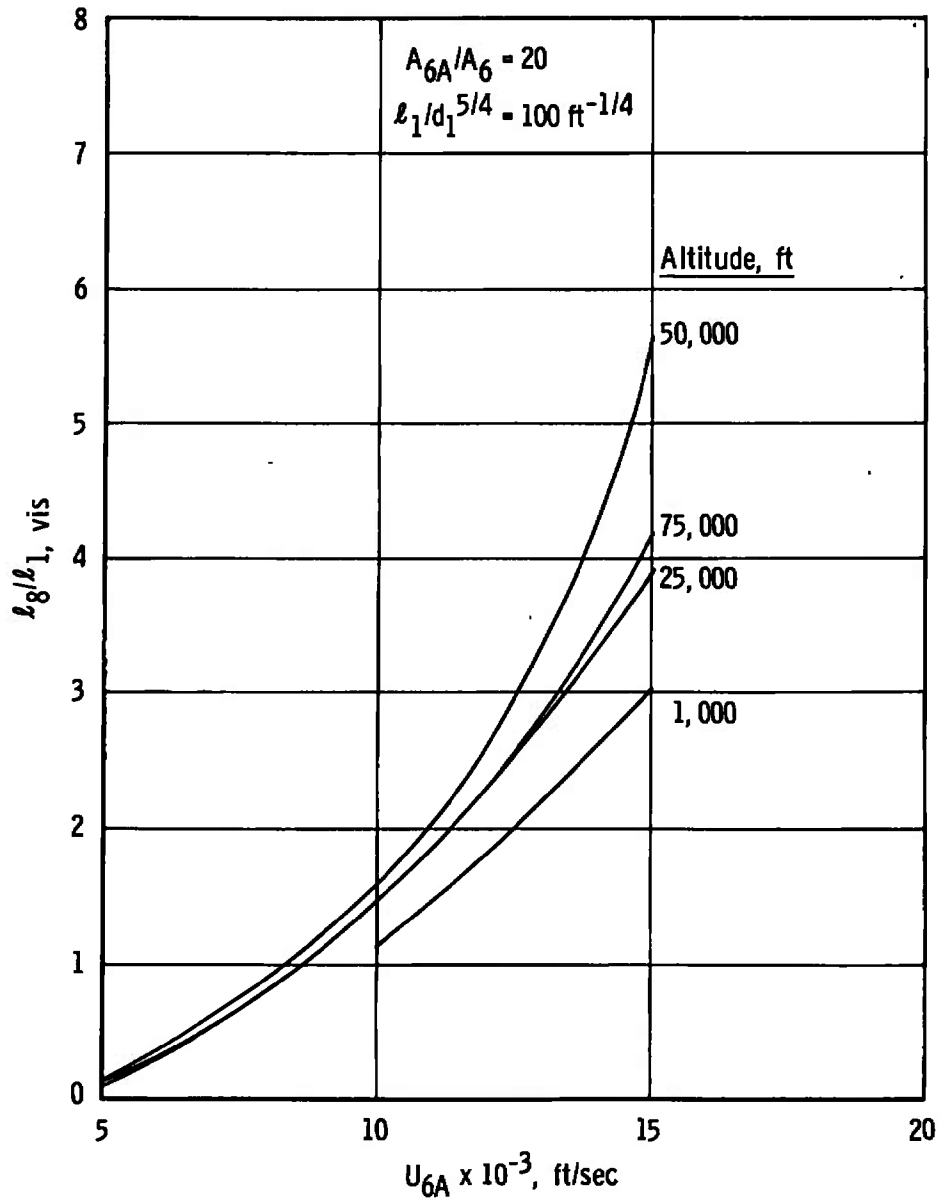Fig. III-5 Continued

e. $A_{6A}/A_6 = 20$, $\ell_1/d_1^{5/4} = 100 \text{ ft}^{-1/4}$

Fig. III-5 Continued

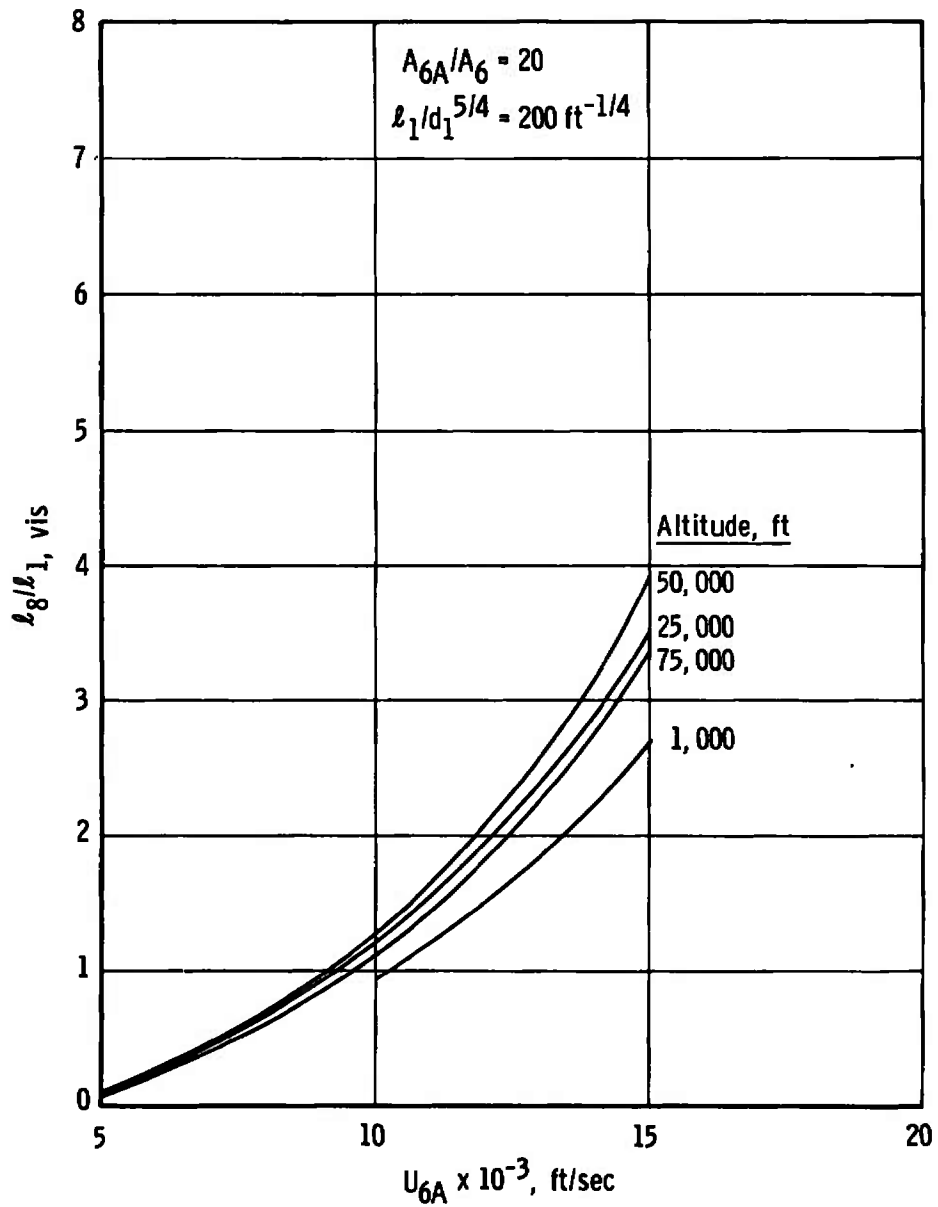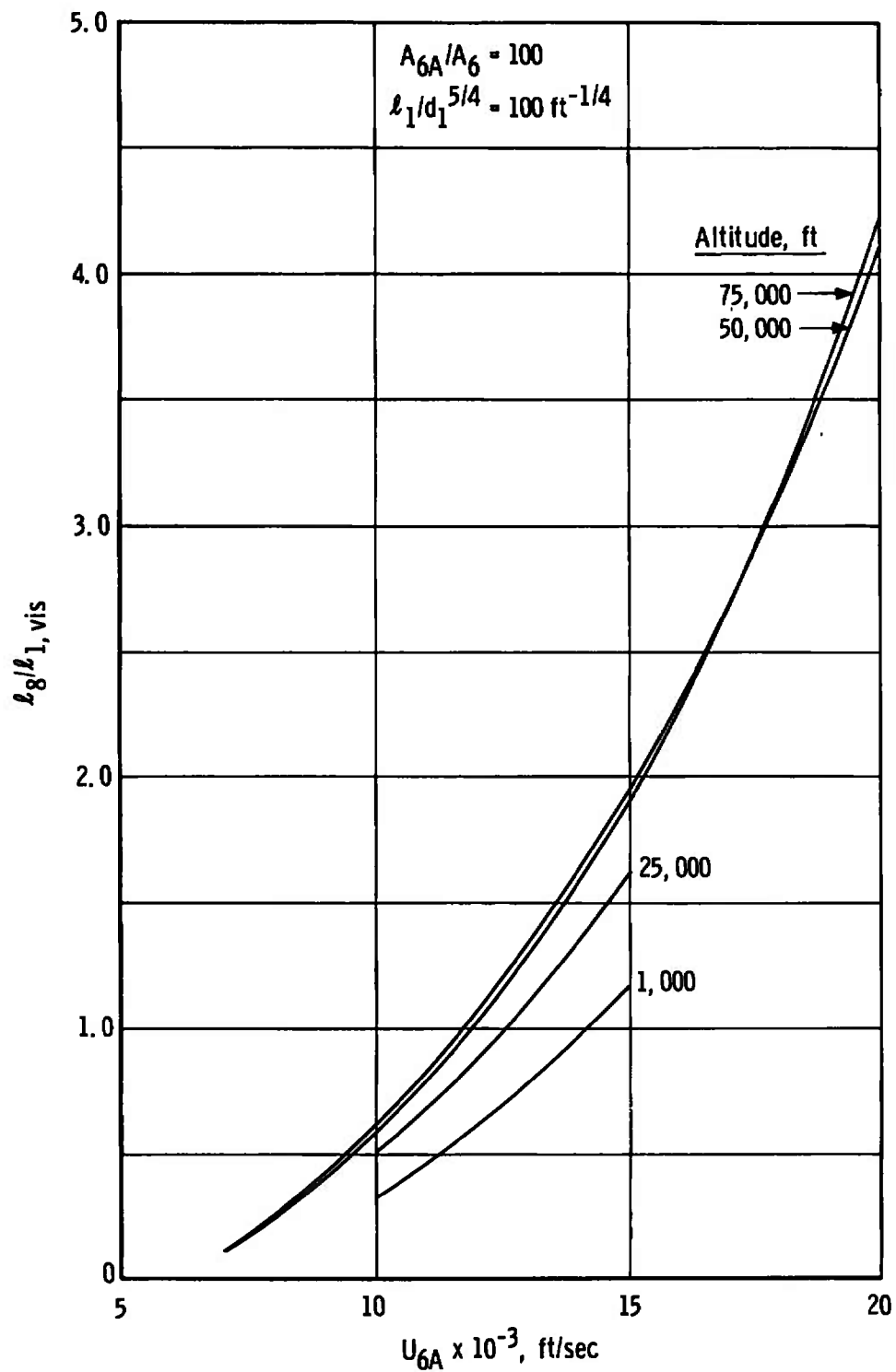f. $A_{6A}/A_6 = 20$, $\ell_1/d_1^{5/4} = 200 \text{ ft}^{-1/4}$

Fig. III-5 Continued

g. $A_{6A}/A_6 = 100$, $\ell_1/d_1^{5/4} = 100 \ ft^{-1/4}$
Fig. III-5 Continued
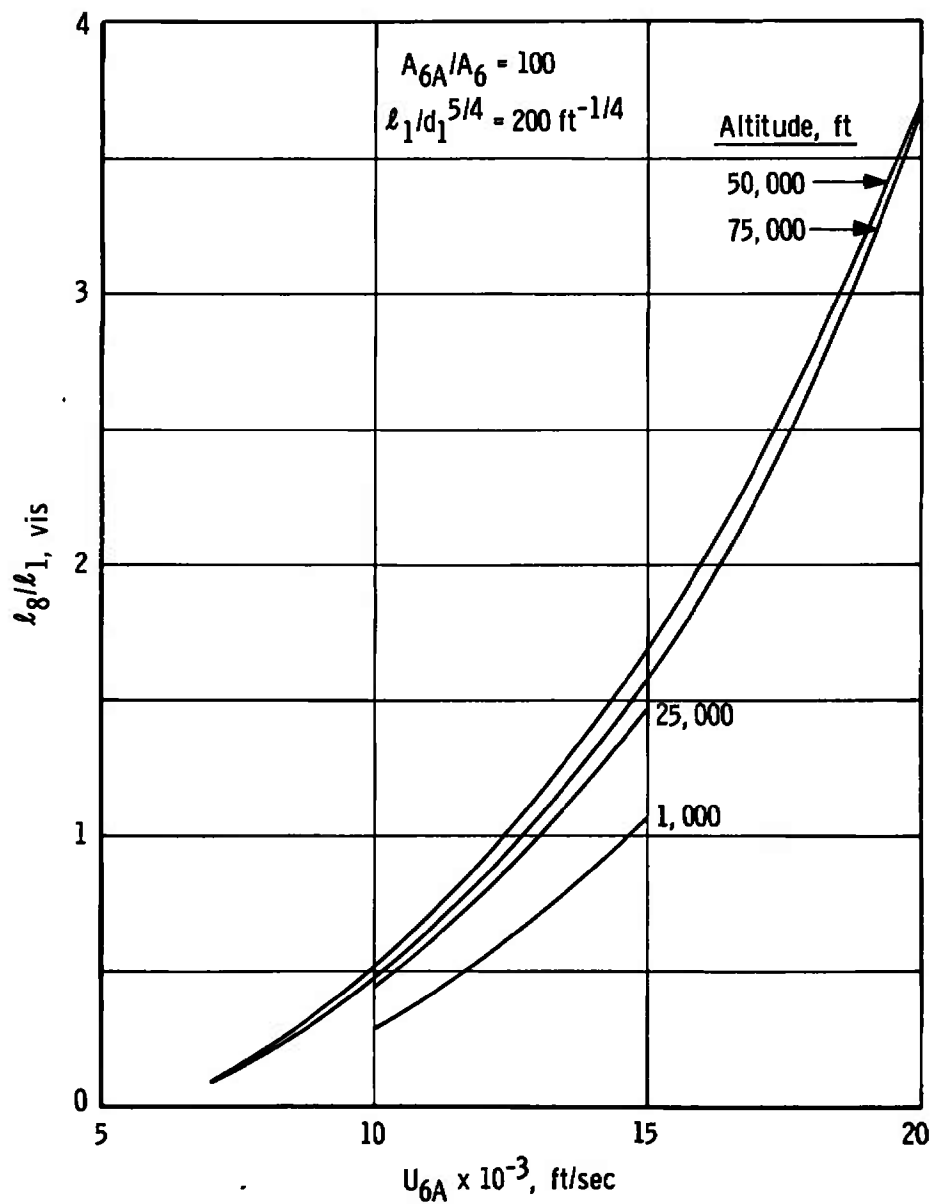
h. $A_{6A}/A_6 = 100$, $\ell_1/d_1^{5/4} = 200$ ft$^{-1/4}$

Fig. III-5 Concluded
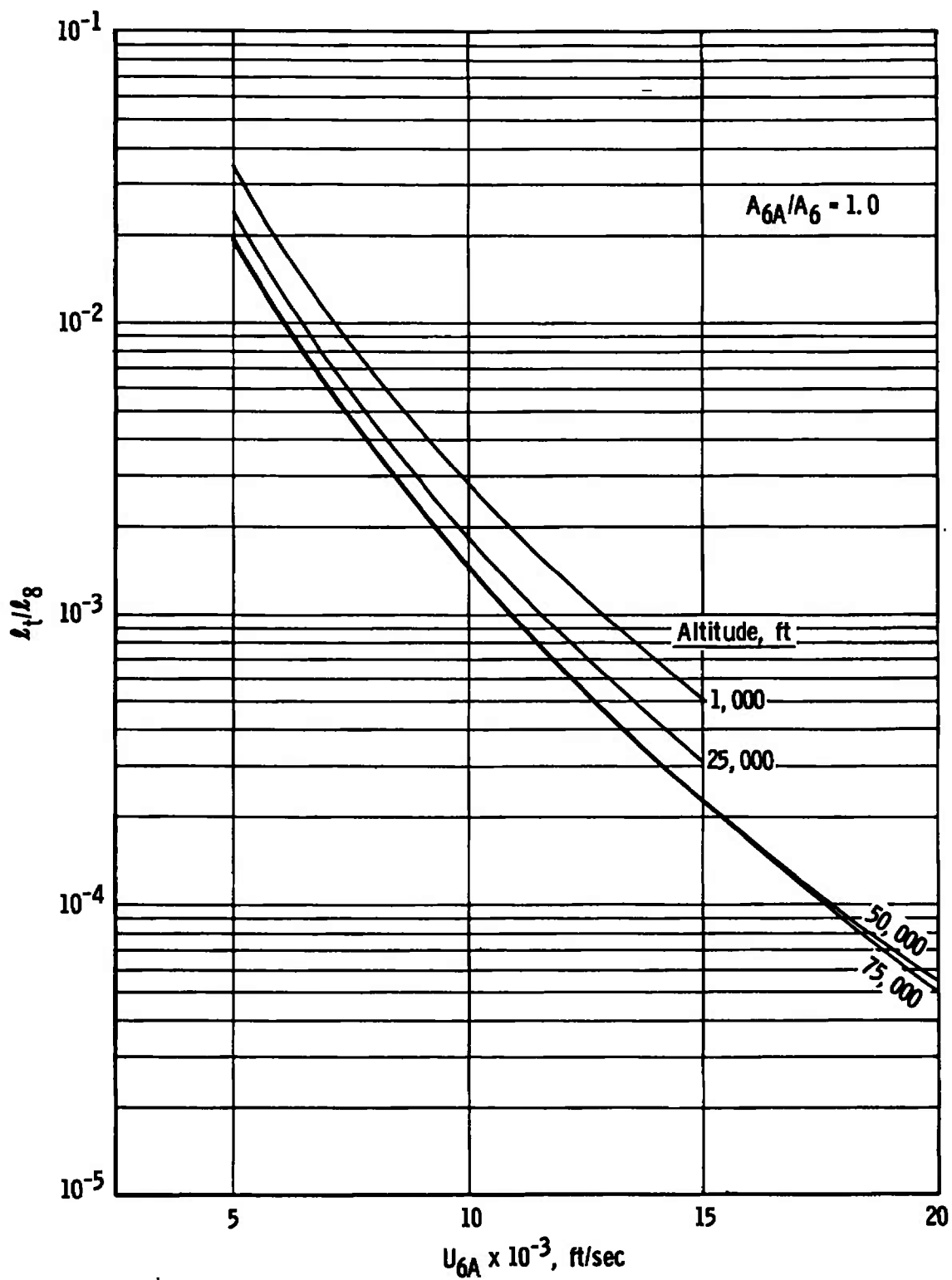
a. $A_{6A}/A_6 = 1$

Fig. III-6 Test Gas Slug Length Ratio, ℓ_t/ℓ_8, versus U_{6A}
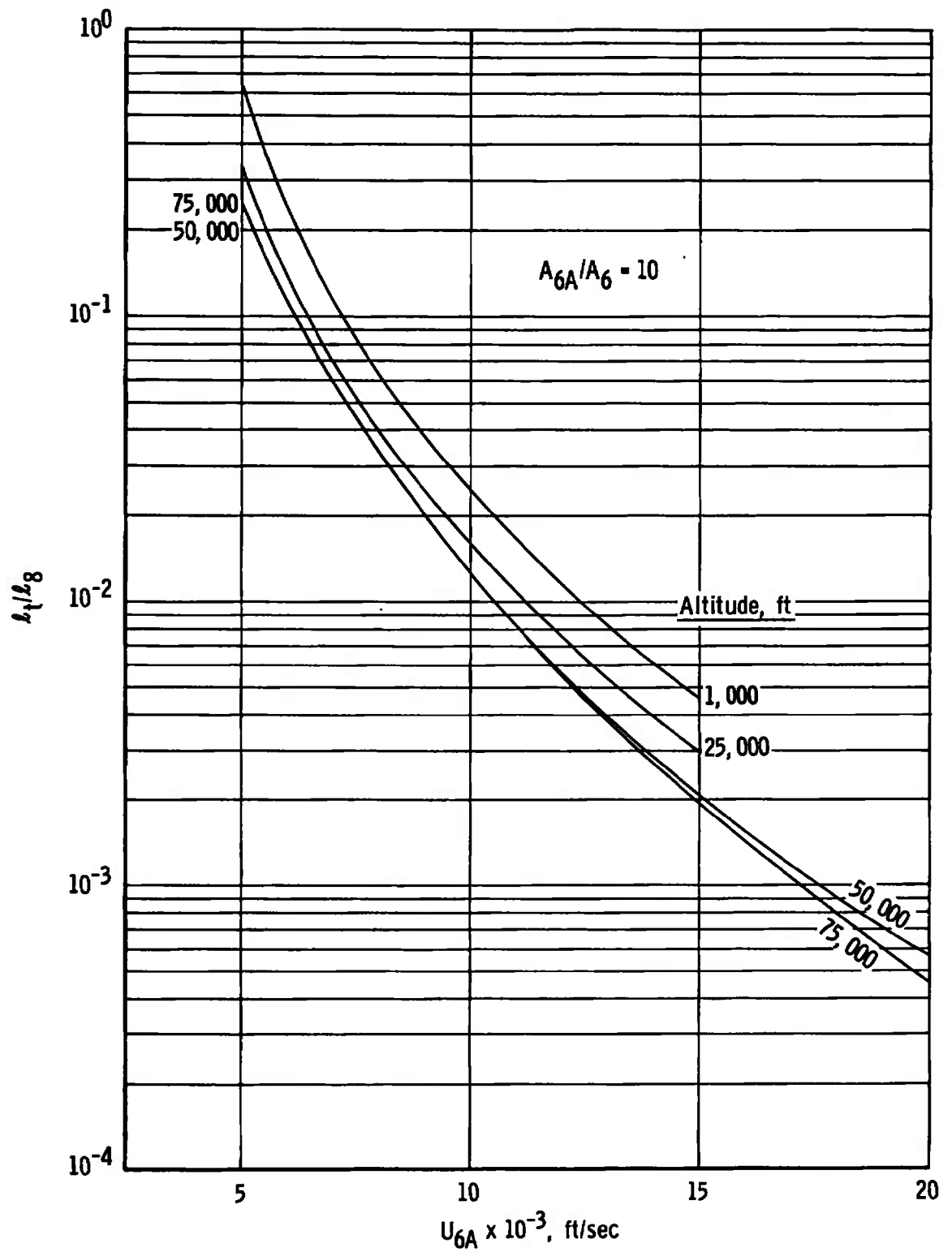
b. $A_{6A}/A_6 = 10$

Fig. III-6 Continued
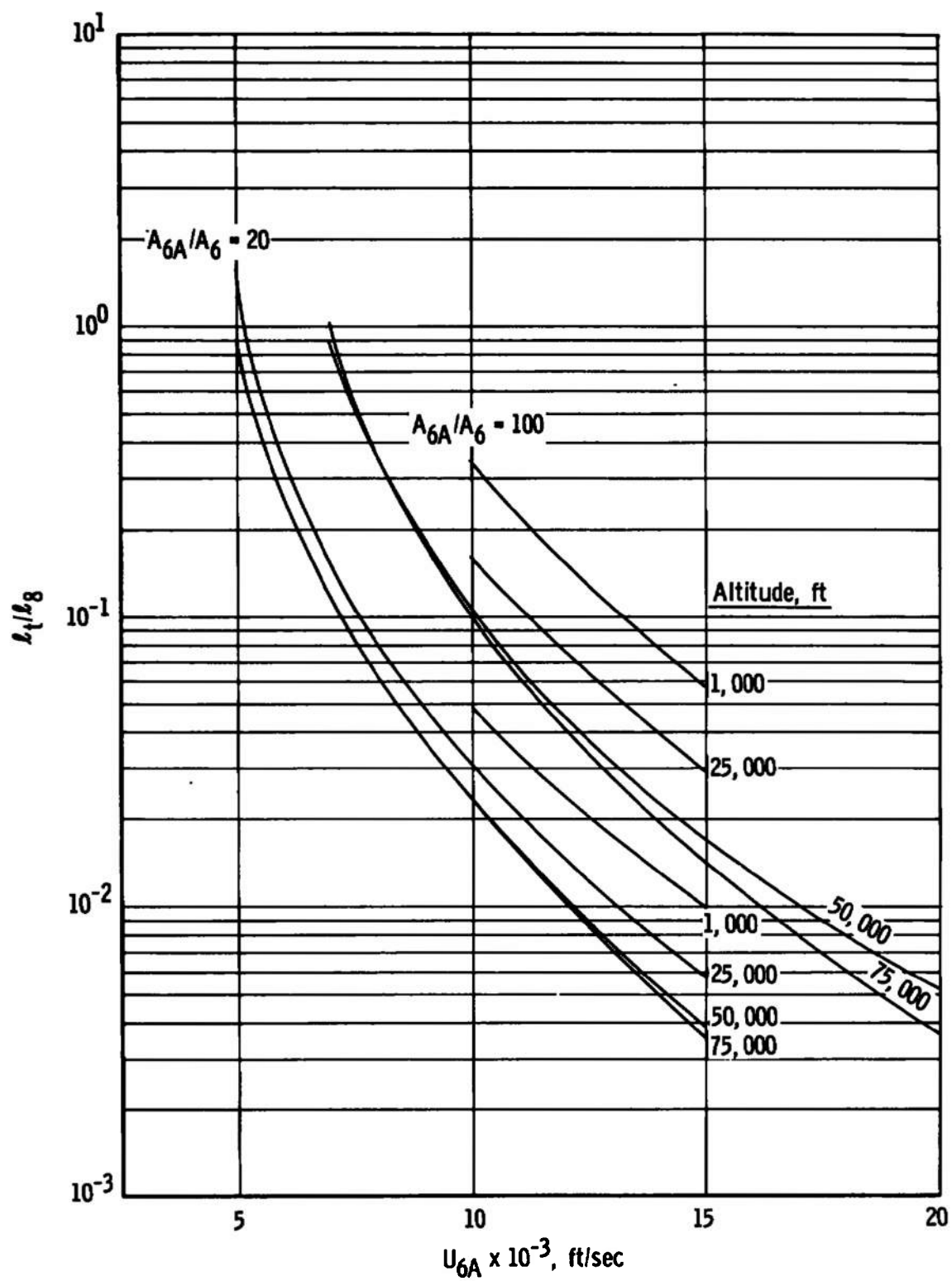
c. $A_{6A}/A_6 = 20$ and 100
Fig. III-6 Concluded
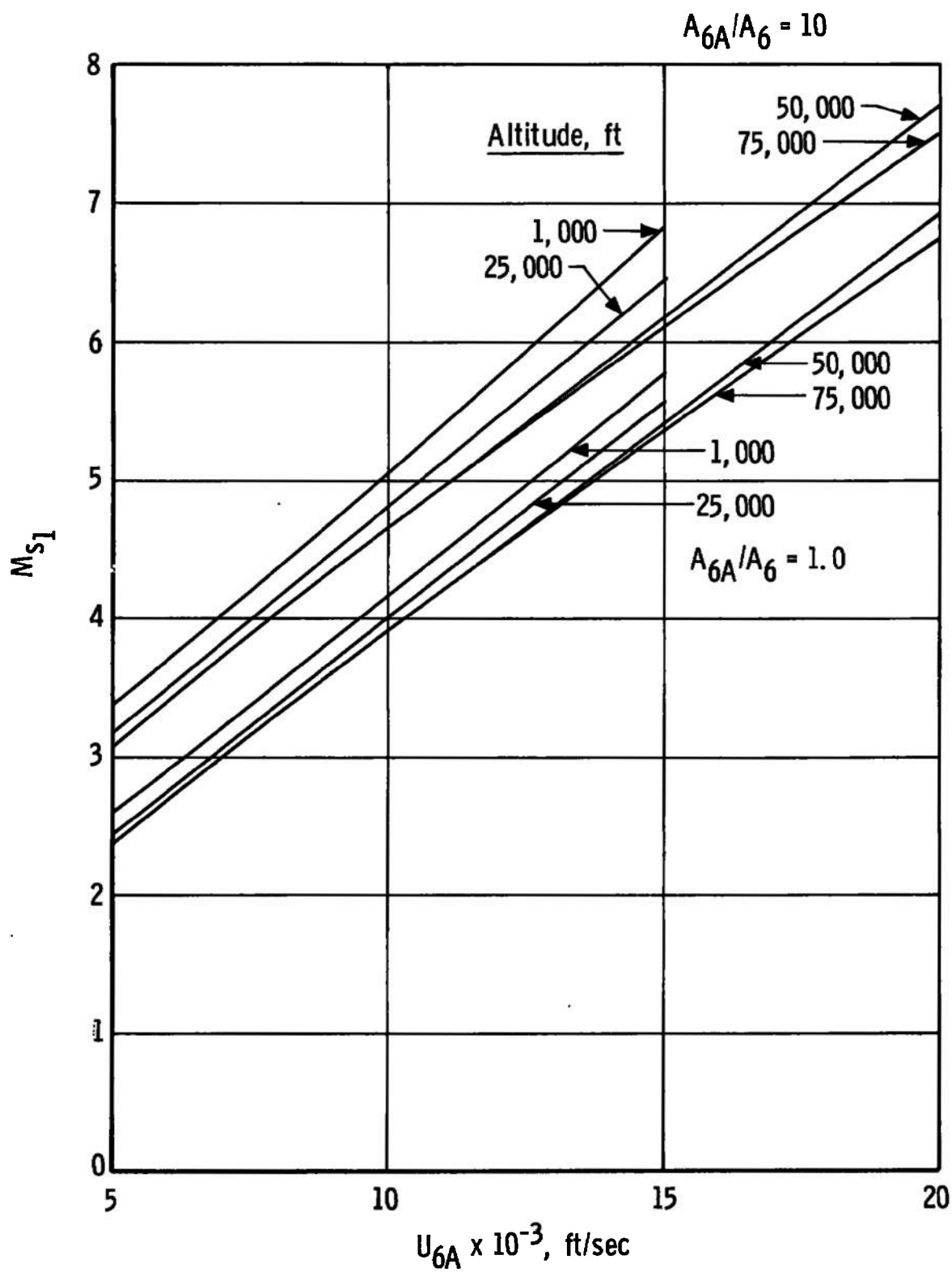
a. $A_{6A}/A_6 = 1$ and 10

Fig. III-7 Driven Tube Shock Strength, M_{s_1}, versus U_{6A}
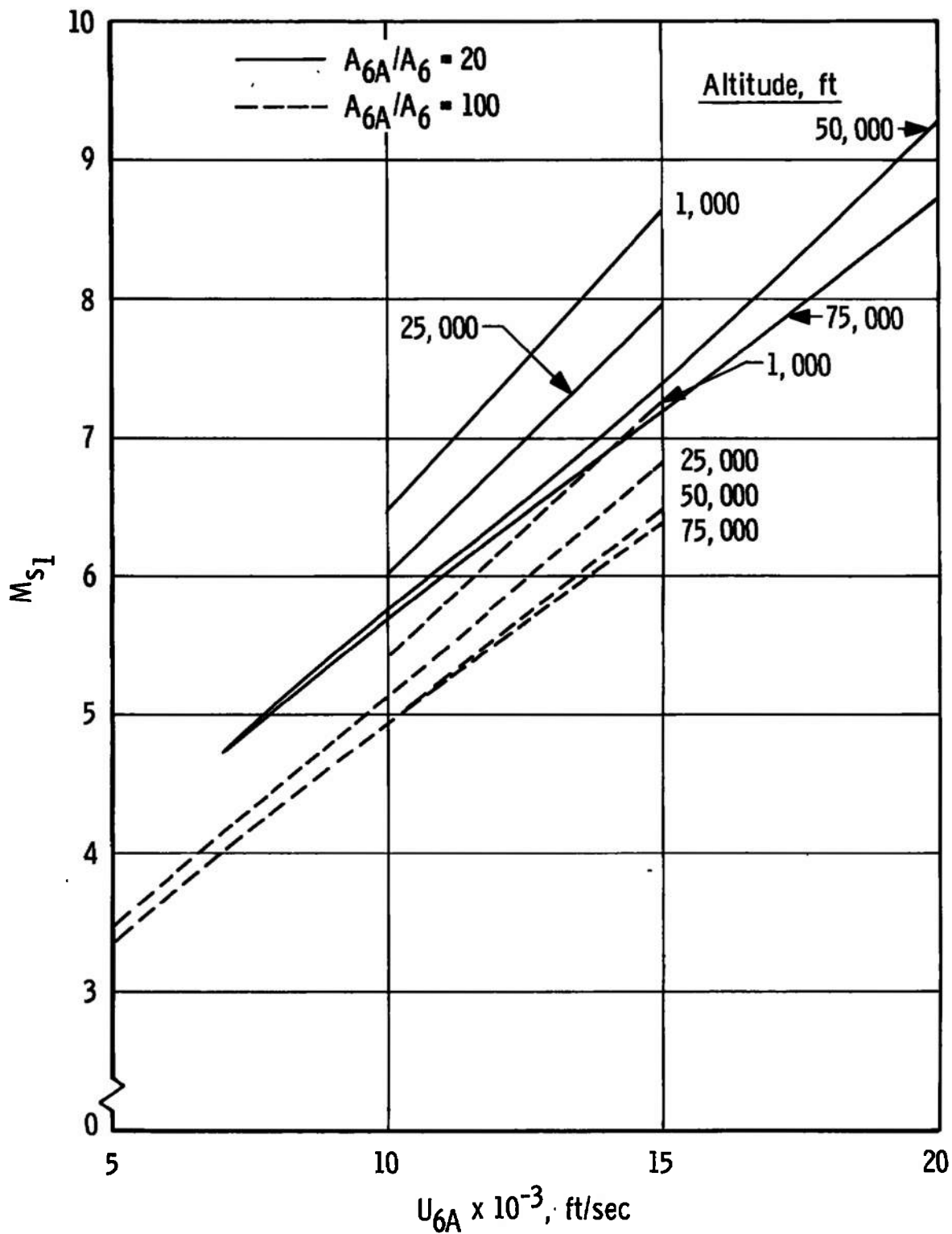
b. $A_{6A}/A_6 = 20$ and 100
Fig. III-7 Concluded
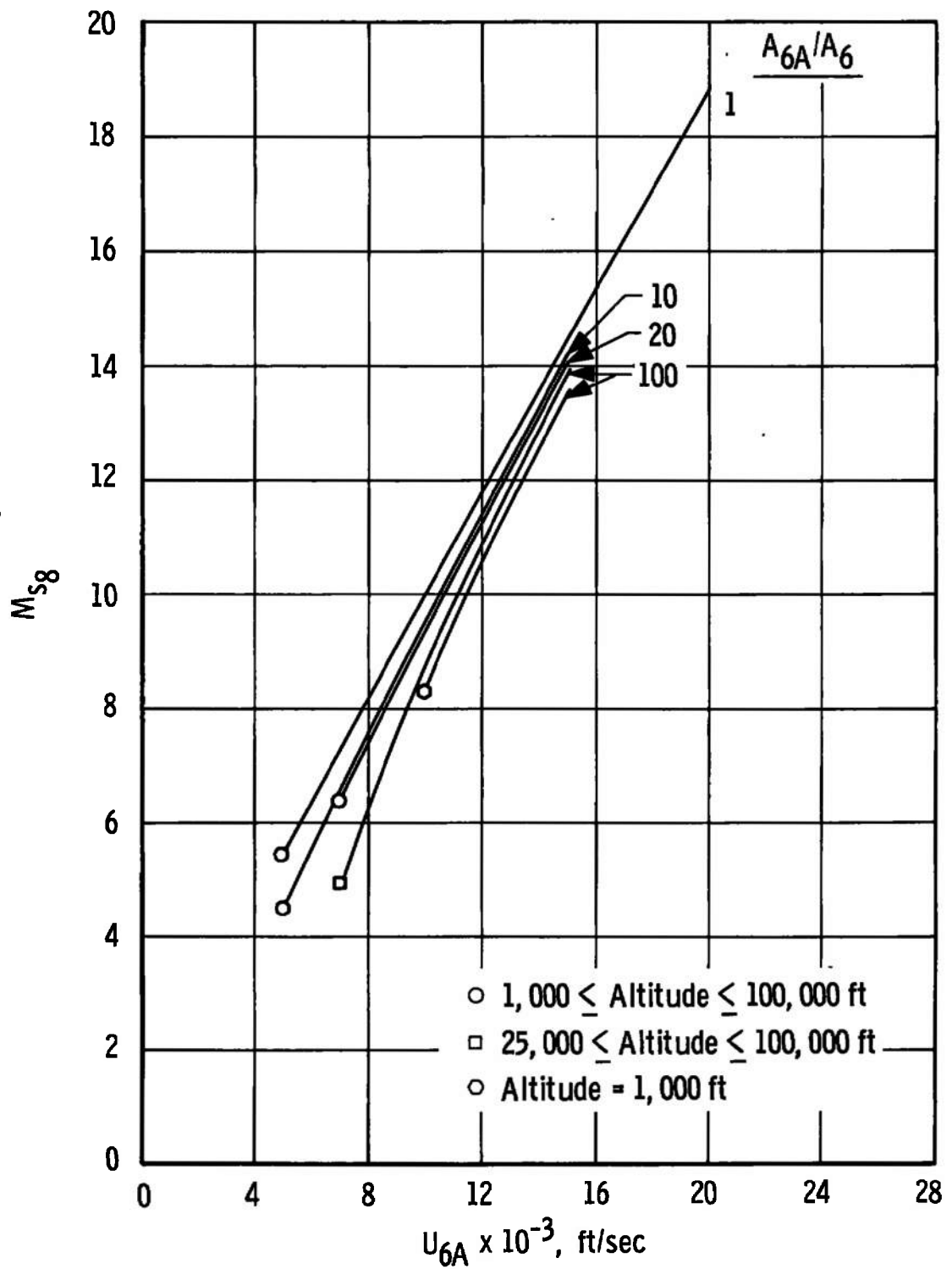
Fig. III-8 Acceleration Tube Shock Strength, M_{s8}, versus U_{6A}
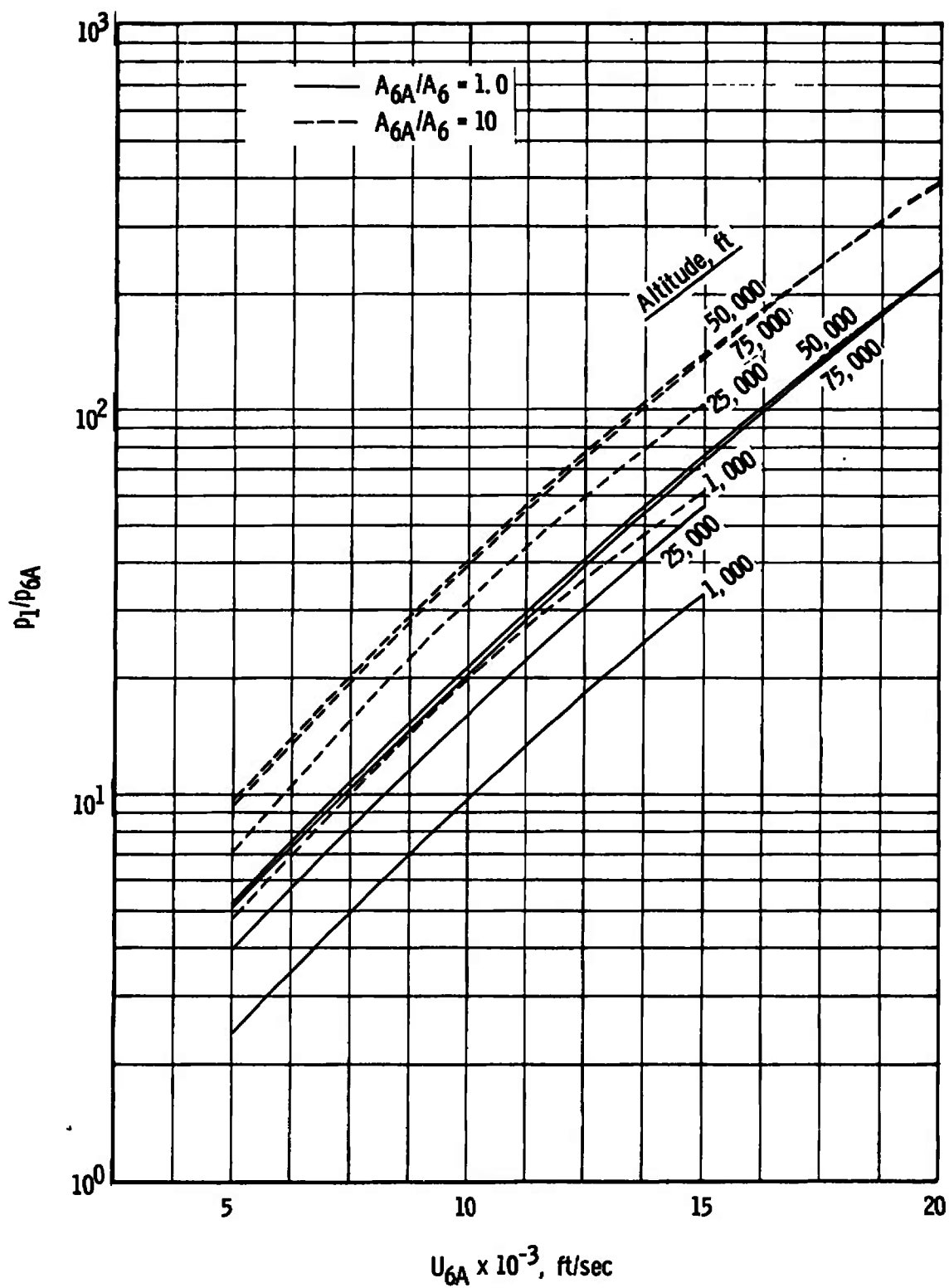
a. $A_{6A}/A_6 = 1$ and 10

Fig. III-9 Driven Tube Charge Pressure Ratio, P_1/P_{6A}, versus U_{6A}
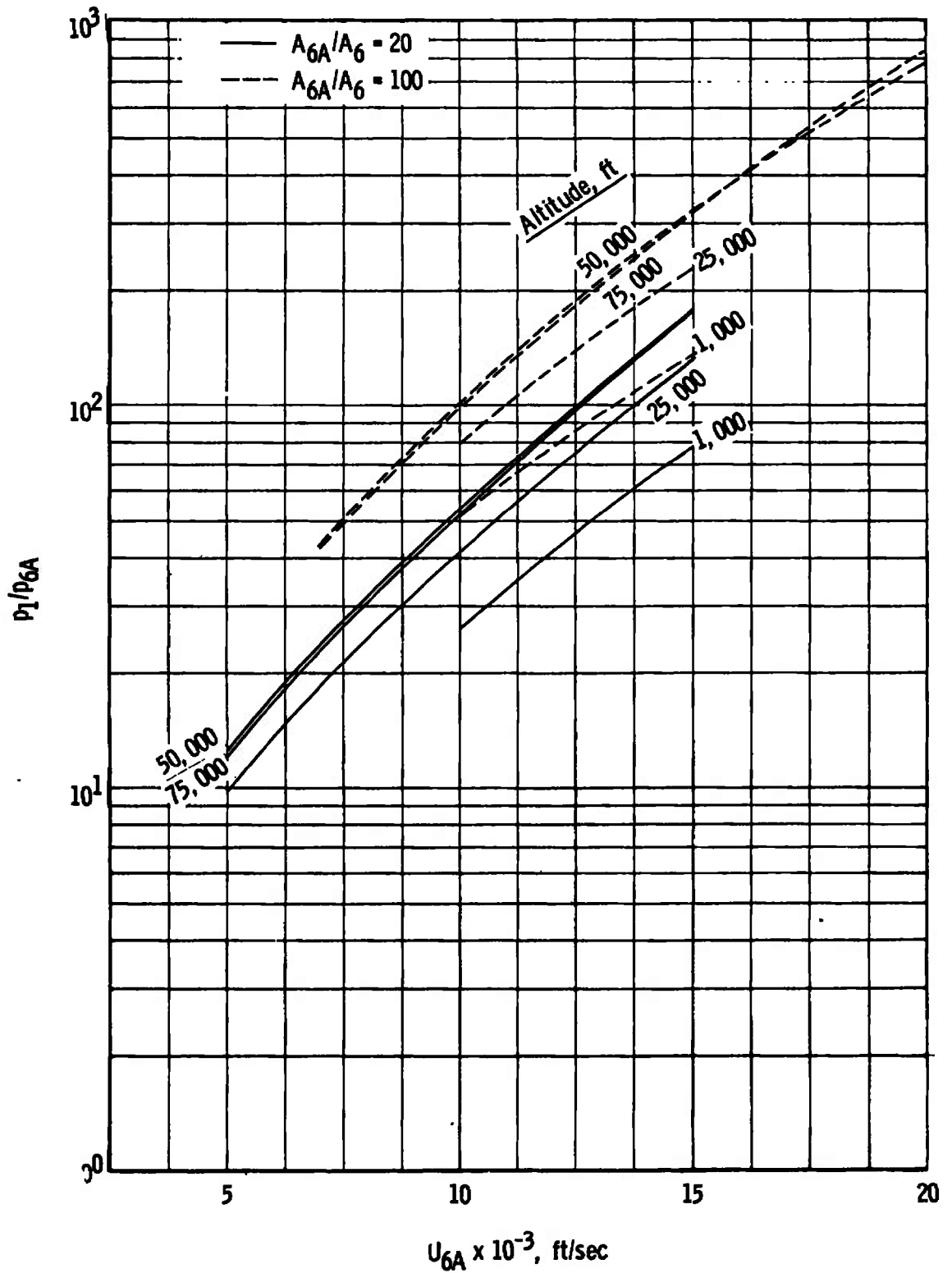
b. $A_{6A}/A_6 = 20$ and 100

Fig. III-9 Concluded

a. $A_{6A}/A_6 = 1$ and 10

Fig. III-10 Driven Tube Shocked Gas Pressure Ratio, P_2/P_{6A}, versus U_{6A}
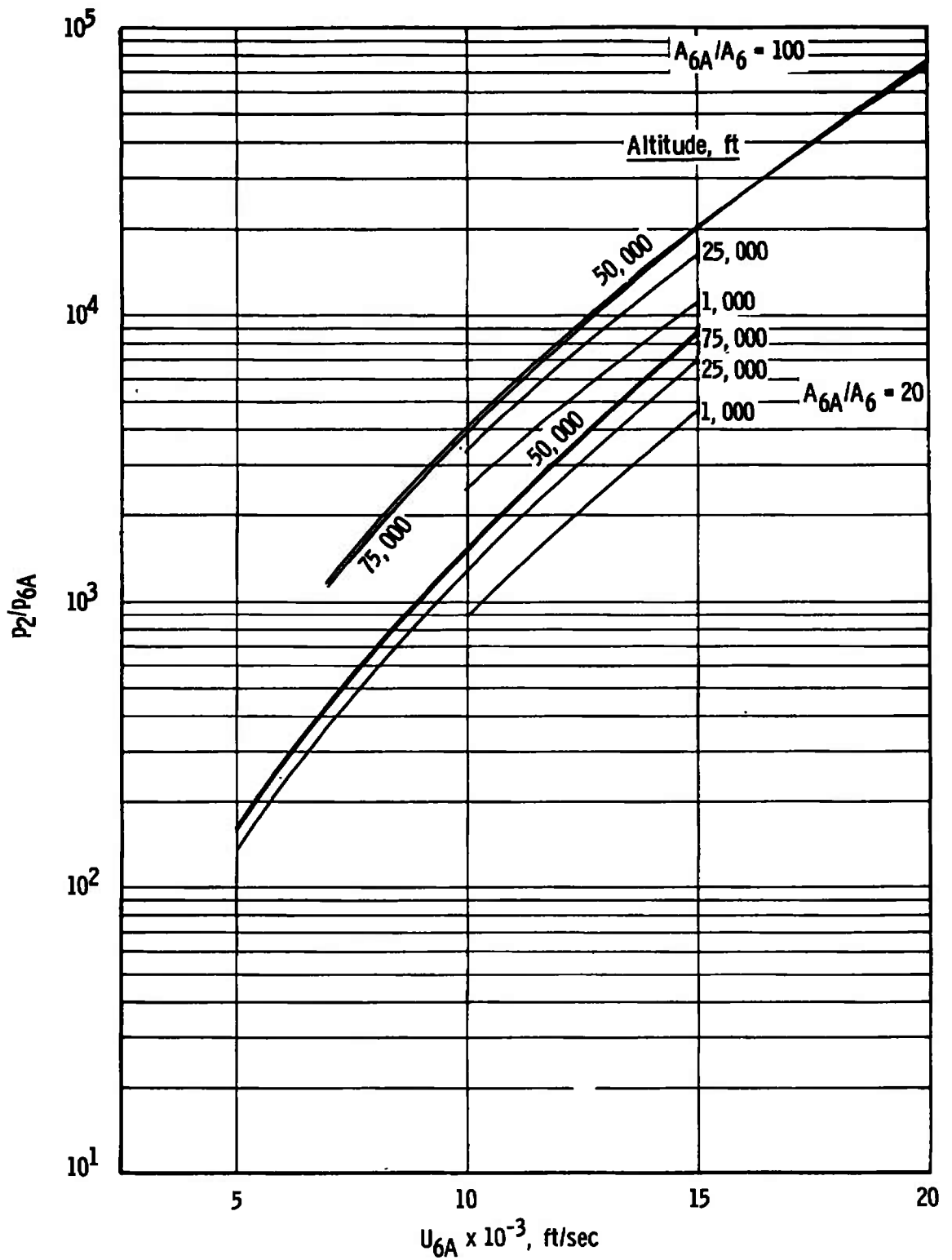
b. $A_{6A}/A_6 = 20$ and 100
Fig. III-10 Concluded

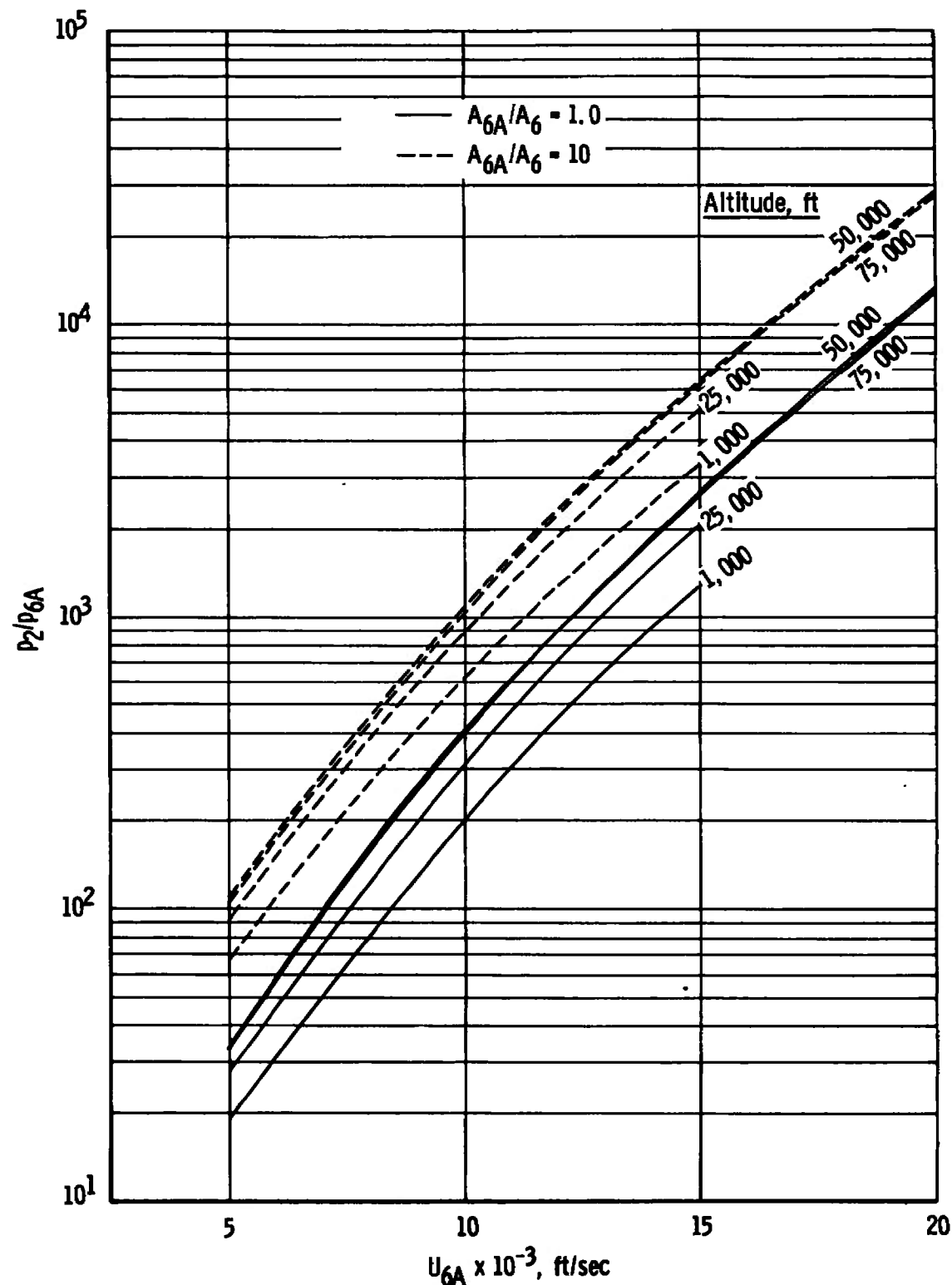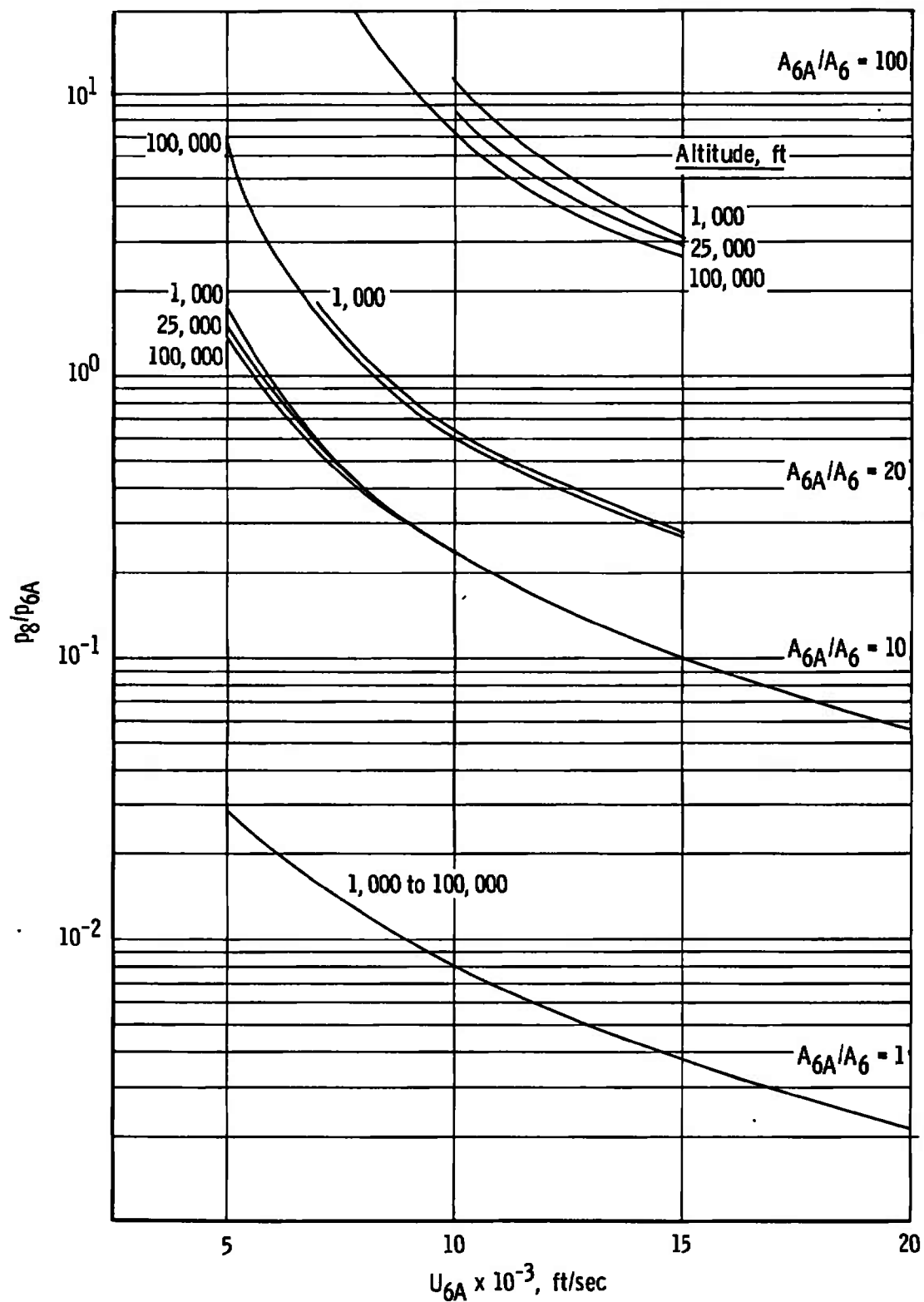Fig. III-11 Acceleration Tube Charge Pressure Ratio, P_8/P_{6A}, versus U_{6A}
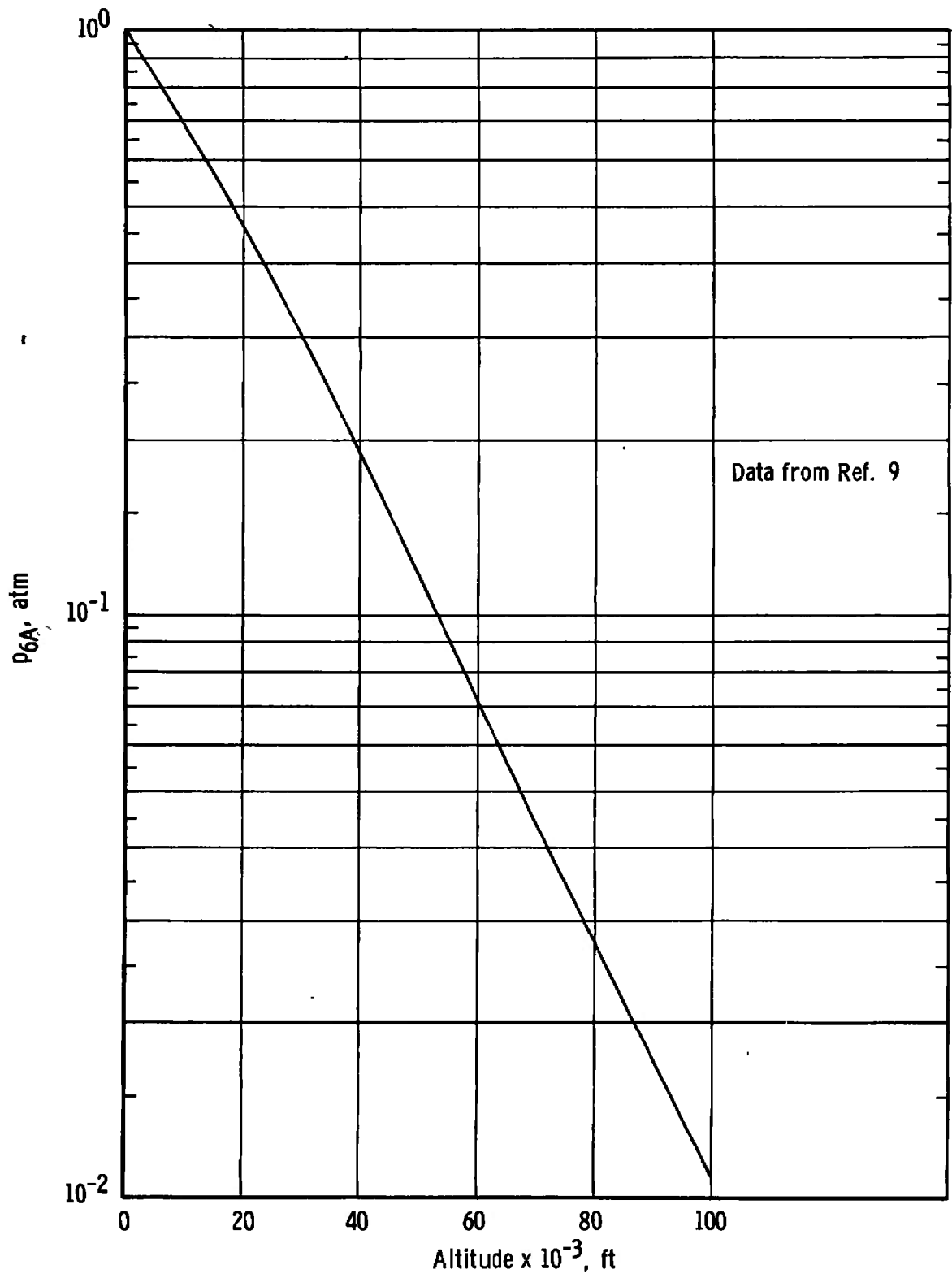
Fig. III-12 Free-stream Pressure, P_{6A}, versus Altitude

TABLE I
EXPANSION TUNNEL PROGRAM INPUT AND OUTPUT DATA

INPUT DATA

Full Duplication Option

U_{6A} Altitude $\qquad$ A_{6A}/A_6 $\qquad$ T_1

Reynolds Number Simulation Option

U_{6A}	P_{6A}	T_{6A}	ρ_{6A}	h_{6A}
a_{6A}	Z_{6A}	A_{6A}/A_6	T_1	

OUTPUT DATA

P_1	U_{s_1}	M_{s_1}	ℓ_1/ℓ_8		$\ell_8/\Delta t_r$*	
P_2	U_2	T_2	ρ_2	h_2	a_2	Z_2
P_6	U_6	T_6	ρ_6	h_6	a_6	Z_6
P_{6A}	U_{6A}	T_{6A}	ρ_{6A}	h_{6A}	a_{6A}	Z_{6A}

*This Δt_r assumes no loss in the nozzle starting-stopping process.

DOCUMENT CONTROL DATA · R & D

(Security classification of title, body of abstract and indexing annotation must be entered when the overall report is classified)

1. ORIGINATING ACTIVITY *(Corporate author)*	2a. REPORT SECURITY CLASSIFICATION
Arnold Engineering Development Center ARO, Inc., Operating Contractor Arnold Air Force Station, Tenn. 37389	UNCLASSIFIED
	2b. GROUP N/A

3. REPORT TITLE

THEORETICAL PERFORMANCE OF THE EXPANSION TUNNEL OPERATING IN THE HIGH DENSITY TEST REGIME

4. DESCRIPTIVE NOTES *(Type of report and inclusive dates)*

Final Report   September 1967 to January 1968

5. AUTHOR(S) *(First name, middle initial, last name)*

Glenn D. Norfleet, ARO, Inc.

6. REPORT DATE	7a. TOTAL NO. OF PAGES	7b. NO. OF REFS
July 1968	100	13

8a. CONTRACT OR GRANT NO. F40600-69-C-0001	9a. ORIGINATOR'S REPORT NUMBER(S)
b. PROJECT NO. 7778	AEDC-TR-68-104
c. Program Element 6241003F	9b. OTHER REPORT NO(S) *(Any other numbers that may be assigned this report)*
d. Task 777807	N/A

10 DISTRIBUTION STATEMENT

This document has been approved for public release and sale; its distribution is unlimited.

11. SUPPLEMENTARY NOTES	12. SPONSORING MILITARY ACTIVITY
Available in DDC.	Arnold Engineering Development Center, Air Force Systems Command, Arnold AF Station, Tenn. 37389

13. ABSTRACT

Theoretical real gas performance calculations have been made for the expansion tunnel operating in a high density regime at modest velocity. Both Mach number-Reynolds number simulation and flow duplication were considered. Typical results and detailed working graphs are presented. To illustrate the potential of the expansion tunnel, the performance was calculated for the case of a $1000^{\circ}K$, 5000-atm helium driver. This example illustrates that the expansion tunnel does show promise for testing in the high density regime at modest velocity.

DD FORM 1 NOV 65 **1473**

14. KEY WORDS	LINK A		LINK B		LINK C	
	ROLE	WT	ROLE	WT	ROLE	WT
wind tunnel, expansion						
high density						
real gas						
theoretical calculations						